Volume 53
Number 24
21 December 2024
Pages 11695–12100

Chem Soc Rev

Chemical Society Reviews

rsc.li/chem-soc-rev

ISSN 0306-0012

ROYAL SOCIETY OF CHEMISTRY

REVIEW ARTICLE

Bert F. Sels *et al.*

From sugars to aliphatic amines: as sweet as it sounds? Production and applications of bio-based aliphatic amines

Chem Soc Rev

REVIEW ARTICLE

View Article Online
View Journal | View Issue

Cite this: *Chem. Soc. Rev.*, 2024, **53**, 11804

From sugars to aliphatic amines: as sweet as it sounds? Production and applications of bio-based aliphatic amines†

Benjamin Vermeeren,[a] Sofie Van Praet,[a] Wouter Arts,[a] Thomas Narmon,[a] Yingtuan Zhang,[a] Cheng Zhou,[a] Hans P. Steenackers[b] and Bert F. Sels *[a]

Aliphatic amines encompass a diverse group of amines that include alkylamines, alkyl polyamines, alkanolamines and aliphatic heterocyclic amines. Their structural diversity and distinctive characteristics position them as indispensable components across multiple industrial domains, ranging from chemistry and technology to agriculture and medicine. Currently, the industrial production of aliphatic amines is facing pressing sustainability, health and safety issues which all arise due to the strong dependency on fossil feedstock. Interestingly, these issues can be fundamentally resolved by shifting toward biomass as the feedstock. In this regard, cellulose and hemicellulose, the carbohydrate fraction of lignocellulose, emerge as promising feedstock for the production of aliphatic amines as they are available in abundance, safe to use and their aliphatic backbone is susceptible to chemical transformations. Consequently, the academic interest in bio-based aliphatic amines *via* the catalytic reductive amination of (hemi)cellulose-derived substrates has systematically increased over the past years. From an industrial perspective, however, the production of bio-based aliphatic amines will only be the middle part of a larger, ideally circular, value chain. This value chain additionally includes, as the first part, the refinery of the biomass feedstock to suitable substrates and, as the final part, the implementation of these aliphatic amines in various applications. Each part of the bio-based aliphatic amine value chain will be covered in this Review. Applying a holistic perspective enables one to acknowledge the requirements and limitations of each part and to efficiently spot and potentially bridge knowledge gaps between the different parts.

Received 29th March 2024

DOI: 10.1039/d4cs00244j

rsc.li/chem-soc-rev

[a] *Center for Sustainable Catalysis and Engineering (CSCE), KU Leuven, Belgium. E-mail: bert.sels@kuleuven.be*

[b] *Centre of Microbial and Plant Genetics (CMPG), KU Leuven, Belgium*

† Electronic supplementary information (ESI) available. See DOI: https://doi.org/10.1039/d4cs00244j

1. Introduction

Amines are defined as compounds in which at least one of the hydrogen atoms of ammonia (NH_3) is replaced by an organic substituent, making them a versatile class of chemicals. In

Benjamin Vermeeren

Benjamin Vermeeren earned his PhD in 2024 from KU Leuven, where he conducted his research under the supervision of Professor Bert F. Sels within the CSCE research group. His doctoral work focused on the selective production of bio-based aliphatic amines, specifically through the catalytic reductive amination of α-hydroxy carbonyl oxygenates. Before pursuing his PhD, Benjamin completed his MSc in Bioscience Engineering, specializing in Catalytic Technology, at KU Leuven in 2019.

Sofie Van Praet

Sofie Van Praet completed her PhD in 2023 at KU Leuven, working under the supervision of Professor Bert F. Sels in the CSCE research group. Her research centered on developing sustainable catalytic pathways for the production of amines from carbohydrates, conducted in close collaboration with Eastman Chemical Company. Prior to her doctoral studies, Sofie earned her MSc in Bioscience Engineering, with a specialization in Catalytic Technology, from KU Leuven in 2019.

aliphatic amines, these substituents comprise (functionalized) alkyl groups. Alkylamines, alkyl polyamines, aliphatic heterocyclic amines, and alkanolamines are all different types of aliphatic amines. Alkylamines contain up to three alkyl substituents while in alkyl polyamines two or more amino groups are present, and in aliphatic heterocyclic amines at least one amino group is part of a saturated cyclic structure. As bifunctional aliphatic amines, alkanolamines contain at least both one amino and one hydroxyl group. This structural diversity makes aliphatic amines of great industrial importance as they are used in a wide range of applications in almost every field of chemistry, technology, agriculture, and medicine.[1,2] As an introduction, all elementary steps in today's aliphatic amine industry will be concisely discussed (Fig. 1).

Wouter Arts

Wouter Arts is a postdoctoral researcher in the CSCE research group at KU Leuven, where he also earned his PhD in 2024 under the supervision of Professor Bert F. Sels. His research focuses on biorefinery processes, combining process modeling with laboratory experiments. Before pursuing his PhD, Wouter completed an MSc in Bioscience Engineering, specializing in Catalytic Technologies, at KU Leuven in 2018, followed by a postgraduate degree in Chemical Engineering from Imperial College London in 2019.

1.1. Overview of the traditional aliphatic amine industry

Nearly all nitrogen-containing chemicals, including amines, originate from ammonia (NH_3), the second most produced chemical worldwide.[3,4] Since natural ammonia sources are scarce, NH_3 is predominantly produced *via* the Haber–Bosch process where hydrogen (H_2) and nitrogen (N_2) are converted into NH_3 using an iron catalyst at an elevated temperature (400–500 °C) and pressure (>10 MPa). N_2 and H_2 are typically sourced from air and syngas, respectively.[5,6] Methylamines, the simplest and industrially most relevant alkylamines, are produced through an exothermic reaction of NH_3 with methanol (MeOH) over amorphous silica-alumina catalysts (*i.e.*, solid acid catalysts or shape-selective zeolites) at 350–450 °C. This process yields a mixture of monomethylamine (MMA), dimethylamine (DMA) and trimethylamine (TMA), with product selectivity controlled by reaction conditions and catalyst choice.[7–10] NH_3, MMA and DMA are the indispensable nitrogen sources for all larger aliphatic amines.

The primary carbon sources in today's aliphatic amine industry are derived from fossil feedstock. For instance, industrially important aliphatic C2 amines (*i.e.*, ethanolamines, ethylene polyamines and piperazine derivatives) originate from ethylene, a key petrochemical produced by steam cracking petroleum hydrocarbons.[11–13] From ethylene, two substrates of our interest can be derived, namely ethylene oxide (EO) and ethylene dichloride (EDC), which after amination lead to ethanolamines and ethylene polyamines, respectively. The former, EO, is produced *via* partial oxidation of ethylene with oxygen in the presence of a silver catalyst at 200–300 °C. Ethylene conversion rates are intentionally kept low (<10%) to minimize complete combustion of CO_2.[14,15] The latter, EDC, is produced by gas- or liquid-phase oxychlorination of ethylene. In the gas-phase process, ethylene and HCl are reacted with oxygen in the presence of a supported $CuCl_2$ catalyst at

Hans P. Steenackers

Hans P. Steenackers received his PhD from KU Leuven in 2011, where his research focused on the structure–activity relationship and mode of action of small inhibitors of biofilm formation. He is currently an associate professor at KU Leuven and leads the MICA laboratory, which is part of the Center of Microbial and Plant Genetics. His research group investigates microbial community behavior and develops antimicrobial strategies targeting these communities, with the aim of advancing the understanding of social interactions within microbial communities, resistance development, and in situ monitoring methodologies. He has published over 50 peer-reviewed papers in this field.

Bert F. Sels

Bert F. Sels, currently a full professor at KU Leuven and head of the CSCE research group, earned his PhD in 2000 in the field of heterogeneous oxidation catalysis. His research focuses on heterogeneous catalysis, addressing future challenges in industrial organic and environmental catalysis. A key area of his work is advancing carbon circularity through the use of renewable carbon sources such as biomass, carbon dioxide, and plastic waste. His group has published over 400 peer-reviewed articles and holds more than 40 patents. Professor Sels is the co-chair of the Catalysis Commission of the International Zeolite Association (IZA), a co-founder of the European Research Institute of Catalysis (ERIC), and a member of the European Academy of Sciences and Arts.

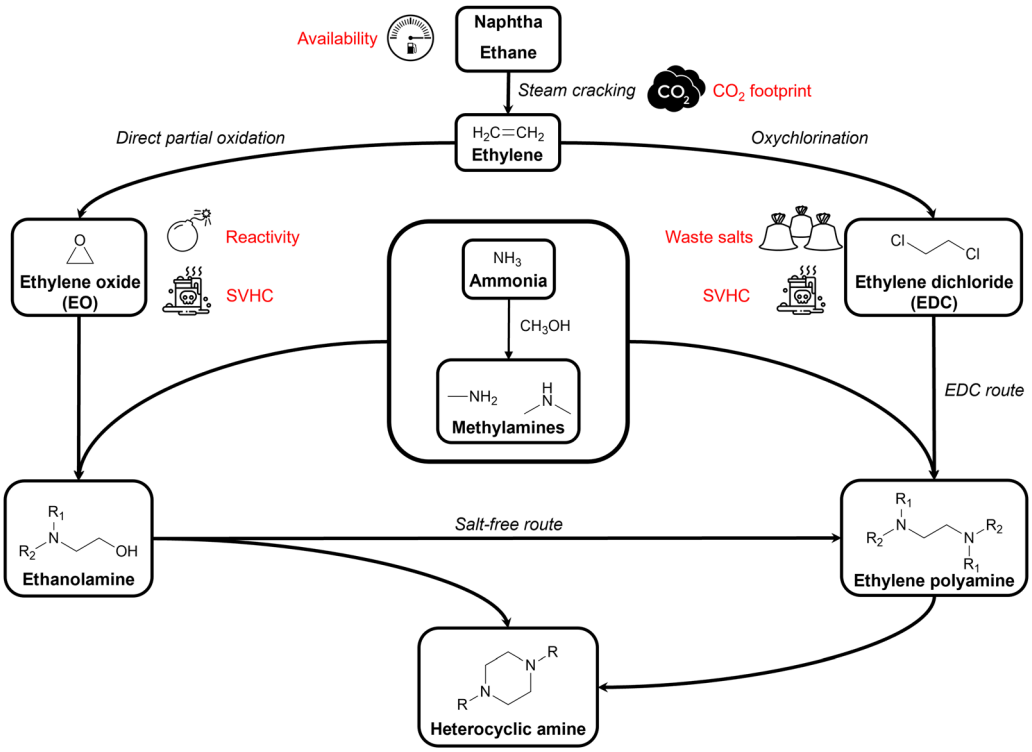

Fig. 1 Schematic overview of the traditional aliphatic amine industry and its shortcomings.

220–250 °C, while in the liquid-phase an aqueous $CuCl_2$ solution is used at 170–185 °C.[16]

By reacting these nitrogen and carbon sources, aliphatic amine products are formed. Ethanolamines are formed by reacting EO with NH_3, MMA or DMA at an elevated temperature (50–200 °C) and pressure (up to 16 MPa) producing monoethanolamine (MMA), diethanolamine (DEA), and triethanolamine (TriEA). Product distribution primarily depends on the amine-to-EO molar ratio.[17,18] Propanolamines are similarly formed by reacting NH_3 or an alkylamine with propylene oxide (PO).[19] Ethylene polyamines are currently manufactured *via* two production methods: the EDC process and the salt-free process.[1,2] The EDC process involves reacting EDC with an amine reactant at ~100 °C, producing ethylene polyamines and HCl. This process is unselective, yielding various polyamines such as ethylenediamine (EDA) and higher analogs including diethylenetriamine (DETriA), and triethylenetetramine (TriETA). The salt-free process avoids the use of EDC by reacting an ethanolamine with an amine reactant under catalytic hydrogenation conditions (150–250 °C, up to 20 MPa H_2 pressure) using modified Ni, Co, or Ru catalysts. Propylene amines, such as 1,2-propylenediamine (1,2PDA), are exclusively formed *via* this salt-free route.[2,20] Additionally, piperazine (PZ) and other heterocyclic derivatives are produced as by-products in both the EDC and salt-free processes by optimizing the reaction conditions to favor their formation.[2,21]

1.2. The aliphatic amine industry in numbers

From an economic perspective, the aliphatic amine industry represents a multibillion-dollar market that steadily increases

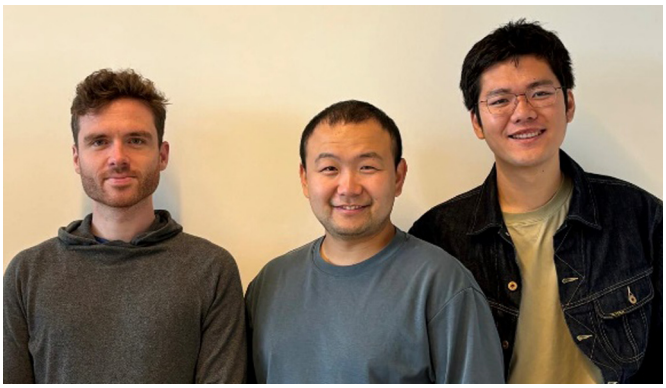

Thomas Narmon, Yingtuan Zhang, and Cheng Zhou

Thomas Narmon, Yingtuan Zhang, and Cheng Zhou are currently conducting their PhD research under the supervision of Professor Bert F. Sels in the CSCE research group at KU Leuven. Thomas Narmon's research focuses on the synthesis of lignin-derived amines for applications in functionalized polymers. He obtained his MSc in Chemistry from KU Leuven in 2019 and subsequently worked for two years as a Research and Teaching Assistant in Pharmaceutical (Neuro)sciences at the University of Brussels. Yingtuan Zhang is focused on the valorization of lignin oligomers and the synthesis of novel bio-based polymers. He earned his MSc in Polymer Chemistry and Physics from the Guangzhou Institute of Chemistry in 2019. Cheng Zhou's research is centered on CO2 capture and utilization. He received his MSc in Chemistry from Xiamen University in 2019.

with a compound annual growth rate (CAGR) of 5–6% per year.[22] In today's industry, the demand for alkanolamines is significantly higher than that for alkyl polyamines. In 2022, the global demand for alkanolamines and alkyl polyamines approximately amounted to 2 and 0.5 million tons, respectively.[23,24] Notable alkanolamines include ethanolamines such as MEA, DEA and TriEA, as well as *N*-substituted ethanolamines such as *N*,*N*-dimethylethanolamine (DMEA), and propanolamines such as 1-amino-2-propanol (1A2P). These alkanolamines play an essential role as precursors or final products in surfactants, cosmetics, pharmaceuticals, polymers and coatings, agrochemicals, water treatment applications, gas purification, *etc.*[17,19] The most prominent alkyl polyamines encompass the ethylene polyamines EDA, DETriA, and TriETA, and the propylene polyamines 1,2PDA and 1,3-propylenediamine (1,3PDA). These alkyl polyamines are crucial components in polymer synthesis, surfactants, agrochemicals, gas purification applications, corrosion inhibitors, lubricant oils, *etc.*[2,20]

1.3. Shortcomings of the current aliphatic amine industry

Not only the amine industry, but the entire chemical industry currently is a petrochemical industry, as it heavily relies on fossil fuels such as crude oil and natural gas. According to the organization of petroleum exporting countries (OPEC), the chemical industry accounted for 14% of the total oil demand in 2022.[25] Meanwhile, the international energy agency (IEA) claimed in their most recent report that: ''petrochemicals are rapidly becoming the largest driver of global oil consumption. They are set to account for more than a third of the growth in oil demand to 2030, and nearly half to 2050.''[26] This is in contrast with other sectors, including transportation and residential use, as their projected growth in oil demand will stagnate or even decline in the future. This discrepancy is linked to the chemical industry's unique dependency on fossil fuels. More than half of the fossil fuel demand in the chemical industry is used as feedstock for value-added components rather than merely as an energy resource, setting it apart from all other sectors. This strong dependency on a finite, geographically unequally distributed, non-renewable feedstock poses a significant challenge for the chemical industry.[27] Another drawback associated with the consumption of fossil fuels is their greenhouse gas (GHG) emission, which can be illustrated by the ethylene production process. As an energy- and carbon-intensive process, steam cracking generates a carbon footprint that varies from 1.0 to 1.7 tons of CO_2 released per ton of ethylene produced, depending on the hydrocarbon feedstock. In total, this emission accounts for approximately 20% of the annual petrochemical CO_2 emission and 5% of the annual total industrial CO_2 emission.[26,28,29]

Furthermore, apart from these drawbacks related to fossil fuels, today's aliphatic amine industry faces significant safety and health concerns. Its highly strained epoxide ring makes EO thermally unstable, highly flammable and very reactive to other substances, causing a permanent explosion risk and complicating its use and transport. Moreover, EO is classified as carcinogenic, mutagenic and reprotoxic according to the REACH regulations.[30,31] Similarly, REACH classifies EDC as a hazardous compound due to its high flammability, toxicity and carcinogenicity.[32] Additionally, the EDC process leads to stoichiometric amounts of HCl which, in order to prevent corrosion, are neutralized using caustic soda (NaOH) or lime, resulting in significant amounts of waste salts. According to REACH regulations, both substances are listed as substances of very high concern (SVHCs) which should be progressively replaced by less dangerous substances or technologies.[31,32]

1.4. Scope of the Review

All mentioned shortcomings (in)directly arise from the use of fossil-derived resources, highlighting the need for safer and more sustainable resources and production routes. A promising solution can be found in the use of biomass as a renewable feedstock for the chemocatalytic production of aliphatic amines. The increasing academic and industrial interest in bio-based aliphatic amines can be exemplified by the number of high-quality reviews dedicated to this topic that have been published in recent years.[33–37] To date, however, all these reviews primarily focus on the state-of-the-art amination methods, thereby reporting only one, yet essential, aspect of the future bio-based aliphatic amine industry. This Review aims to cover the bio-based aliphatic amine industry from a holistic perspective by relating their production methods to biomass valorization and addressing potential sustainable applications of these amines. In this way, this Review consists of three sections: (i) from biomass as a feedstock to renewable substrates, (ii) from renewable substrates to bio-based aliphatic amines, and (iii) from bio-based aliphatic amines to sustainable applications. The first section, from biomass feedstock to renewable substrates, summarizes the key chemocatalytic valorization reactions of cellulose and hemicellulose. In these reactions, the feedstock is converted into a range of oxygenate substrates characterized by the presence of hydroxyl and carbonyl functional groups. The second section, from renewable substrates to bio-based aliphatic amines, reports the most prominent catalytic amination methods that convert these oxygenate substrates into aliphatic amines. Here, particular emphasis is placed on the range of oxygenate substrates used and the product selectivity. Notably, the use of biomass enables the formation of both drop-in and novel aliphatic amine products. The final section, from bio-based aliphatic amines to sustainable applications, highlights three sustainable domains and related applications, namely CO_2-reactive applications, polymerization and quaternary ammonium compounds (QACs), where different types of aliphatic amines, drop-in or novel, are indispensable components or improve the *status quo* of the current state-of-the-art technologies.

The other, complementary approach toward sustainable bio-based aliphatic amines, *i.e.*, handling the sustainability concerns related to the synthesis of ammonia and other nitrogen sources, is out of the scope of this Review. Nevertheless, the amount of research devoted to green ammonia production proves its utmost importance.[38–41]

2. From biomass as a feedstock to renewable substrates

2.1. Biomass: setting the scene

Biomass is an umbrella term that encompasses all organic (macro)-molecules produced by living organisms, covering a wide range of different chemical structures. Contrary to fossil resources, it is defined as a renewable carbon source since it is replenished within a reasonable period. In general, biomass is considered a promising alternative resource for the production of fuels and chemicals if it is abundantly available, has little initial value, and is susceptible to chemical transformations.[42–45] A type of biomass that fulfills all these requirements is lignocellulose. As the major structural building block of plant cell walls, lignocellulose is universally recognized as the largest source of organic carbon on Earth and the largest fraction of biomass. Furthermore, it is readily available from various currently underused, low-value, non-edible waste streams such as wood residues from the construction or paper industry and agricultural waste (*e.g.*, corn stover, rice and wheat straw, sugarcane bagasse), bypassing land-use competition with food crops. Lignocellulose is a composite material primarily consisting of cellulose, hemicellulose and lignin. Cellulose is a linear homopolysaccharide containing up to 10 000 glucose units linked *via* β-1,4-glycosidic bonds, whereas hemicellulose is a branched heteropolysaccharide containing both pentose (*e.g.*, xylose, arabinose) and hexose (*e.g.*, galactose, glucose, mannose) monomers with a degree of polymerization from 50 up to 300 units. Lignin, on the other hand, is an irregularly crosslinked aromatic polymer formed by radical polymerization of three monolignol monomers, namely *p*-coumaryl alcohol, coniferyl alcohol and sinapyl alcohol.[46–48] In the context of bio-based aliphatic amines, the carbohydrate fraction of lignocellulose (*i.e.*, cellulose and hemicellulose) emerges as a promising feedstock. Carbohydrates are safe in use and consist of a functionalized and tunable aliphatic carbon backbone. In addition to lignocellulose, natural oils and lipids, encompassing fatty acid constituents, can serve as a potentially interesting feedstock in the production of long-chain aliphatic amines.[34,35]

Although out of the Review's scope, it is worth mentioning that the polysaccharide chitin is another important biomass resource. Chitin is present in the cell wall of certain fungi and in the exoskeletons of arthropods (*i.e.*, crustaceans and insects) and cephalopods (*i.e.*, octopuses and squids). It is generated in significant amounts as a waste product in the food industry (*e.g.* seafood industry, insect farms). Remarkably, being a linear amino polymer composed of *N*-acetol-D-glucosamine monomers, chitin is one of the few forms of biomass, next to proteins, containing biogenic nitrogen. Chitin valorization, also referred to as ''shell biorefinery'', presents a unique opportunity for the formation of fully bio-based amines. Current research efforts are mainly focused on chitin recovery and its conversion into value-added components.[49–53]

2.2. Lignocellulose valorization: general principles

In the biorefinery, lignocellulose valorization comprises three consecutive steps, namely fractionation, depolymerization and upgrading, comprehensively reviewed by Schutyser *et al.*[54]

Fractionation, the first step in the lignocellulose biorefinery consists of lignocellulose pretreatment into its three main constituents. A variety of physical, chemical, thermochemical and biological pretreatment methods exist, targeting the different lignocellulose fractions.[55–57] So does, for example, Kraft pulping, a well-established process in the paper and pulp industry, result in high-quality cellulose and hemicellulose fractions,[58] whereas various delignification methods, such as lignin-first techniques (*e.g.*, reductive catalytic fractionation (RCF)),[59,60] focus on lignin recovery.[61–63]

In the next two steps, the isolated cellulose and/or hemicellulose fractions are first depolymerized into their respective monomers which subsequently can be further upgraded into value-added compounds. Depolymerization and upgrading are often, but not necessarily, combined in one process. Three distinctive strategies are generally applied: (i) thermochemical (*e.g.*, gasification,[64,65] pyrolysis,[64,66] thermal cracking[67]), (ii) biotechnological (*e.g.*, enzymatic hydrolysis, fermentation)[68,69] and (iii) chemocatalytic transformation. The latter will be discussed in more detail (Fig. 2).

2.2.1. (Hemi)cellulose valorization by depolymerization and chemocatalytic upgrading. (Hemi)cellulose depolymerization is an acid-catalyzed hydrolysis reaction cleaving the glycosidic linkages.[70,71] In the literature, various catalytic systems have been explored, which will be discussed when addressing the formation of glucose and xylose (Section 2.3.1.). The resulting monosaccharide building blocks can undergo a final valorization step, *i.e.*, chemocatalytic upgrading. In this upgrading step, a diverse set of platform oxygenates is obtained by applying and combining four elementary key reactions: isomerization, retro-aldol condensation, dehydration and (de)hydrogenation. A brief summary of the catalytic requirements of each of these key reactions will be given.

2.2.1.1. Isomerization. Carbohydrate isomerization, comprehensively reviewed by Delidovich *et al.*[72,73] and Li *et al.*,[74] is the

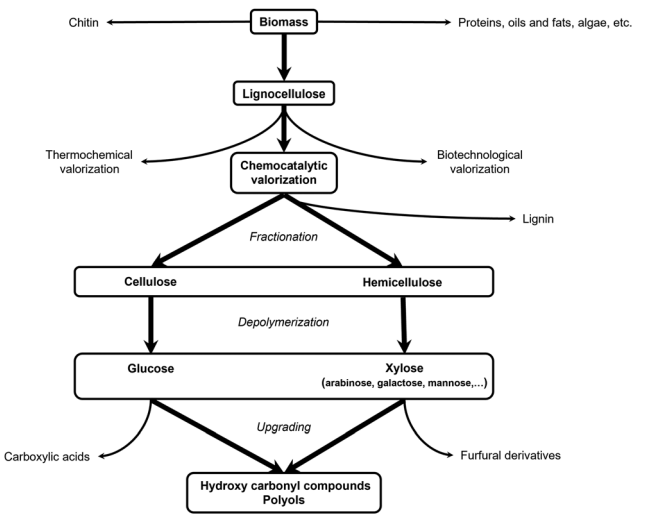

Fig. 2 Schematic overview of the biomass valorization pathway covered in this Review.

interconversion reaction between an aldose and ketose isomer. In general, carbohydrate isomerization reactions are carried out in an aqueous solution and are restricted by both their thermodynamic equilibrium and thermal stability.[75] Isomerization can be catalyzed by both homogeneous and heterogeneous basic or acidic catalysts.

Base-catalyzed isomerization, or Lobry de Bruyn-Alberda van Ekkenstein isomerization, follows an enediol mechanism by proton abstraction at the C2 position of the aldose. Initially, soluble alkali catalysts, such as NaOH and KOH, were employed but they suffer from a low isomerization rate together with the formation of various acidic by-products through alkaline degradation.[76] However, the isomerization efficiency of these soluble base catalysts can be significantly improved by adding a complexing agent such as borate ($Na_2B_4O_7$). This complexing agent preferentially forms a more stable complex with ketoses than with aldoses, resulting in an equilibrium shift in favor of the ketose isomer.[72] Interestingly, organic amines (*e.g.*, triethylamine, ethylenediamine, piperidine, morpholine, *etc.*) can be used as effective isomerization catalysts as they display desirable isomerization yields combined with reduced saccharide degradation.[77] Furthermore, various suitable heterogeneous basic isomerization catalysts have been reported such as Mg–Al hydrotalcites, metal oxides (*e.g.*, ZrO_2, MgO) and cation-exchanged zeolites (*e.g.*, type A zeolite).[72,74,78]

The acid-catalyzed isomerization, on the other hand, follows a 1,2-hydride transfer mechanism in which an intramolecular hydride shift takes place between the C2 and C1 positions of the aldose. Lewis acids, especially in heterogeneous forms such as Sn-BEA zeolites, are preferred over Brønsted acids as they minimize the formation of dehydrated by-products. Sn-BEA zeolites, in contrast to homogeneous Lewis acids, maintain their catalytic activity as their catalytic sites are protected from hydration and deactivation by the hydrophobic zeolite matrix.[75,79–81]

Both bases and Lewis acids also catalyze the epimerization reaction.[72,74] While most catalytic systems favor the isomerization reaction, some are more selective toward epimerization. Most notable are the molybdenum catalysts developed by Bílik.[82] This reaction, also referred to as the Bílik reaction, follows a 1,2-intramolecular carbon shift. Bílik initially studied molybdic acid but the catalyst scope has expanded over time to other highly active Mo(VI)-catalysts such as Mo-based heteropolyacids (*e.g.* $H_3PMo_{12}O_{40}$, $Ag_3PMo_{12}O_{40}$, *etc.*).[83]

2.2.1.2. Retro-aldol condensation. In the retro-aldol condensation of carbohydrates, the C–C bond of monosaccharide substrates is cleaved at the β-position relative to their carbonyl group to form shorter oxygenates.[84] The non-catalytic retro-aldol condensation of carbohydrates in the presence of (supercritical) water, referred to as hydrothermal cracking, proceeds at elevated temperatures (400–600 °C).[67,85] The use of a catalyst can significantly reduce this temperature requirement to around 200 °C.[86]

As reviewed by Zheng *et al.*,[84] both basic and transition metal catalytic systems can be used in the retro-aldol reaction of carbohydrates. In general, all metal oxides and hydroxides containing alkali (*e.g.*, NaOH, KOH) and alkaline earth elements (*e.g.*, $Ca(OH)_2$) are active retro-aldol catalysts *via* their basic sites. However, their selectivity toward retro-aldol is limited due to competing reactions such as the abovementioned isomerization.[84] Similarly, in addition to their isomerization activity, tin-based catalysts such as Sn-BEA also demonstrate retro-aldol activity.[87,88] Other transition metal catalysts, in specific tungsten and related metals (*i.e.*, Mo and Cr), are regarded as the most efficient and selective retro-aldol catalysts.[84,89]

Recently, Liu *et al.* proposed an alternative mechanism for the tungsten-catalyzed retro-aldol reaction, deviating from the conventional base-catalyzed mechanism where only the β-hydroxyl group is required.[90,91] They studied the WO_3-catalyzed retro-aldol reaction of various carbohydrate substrates and found that both an α- and β-hydroxyl group are essential for the selective C–C bond cleavage. Once absorbed on the catalytic surface, the substrate forms a tridentate complex by coordinating its carbonyl group and α- and β-hydroxyl groups with two adjacent tungsten atoms, identifying the W–O–W structure as the catalytic active site. According to Liu and co-workers, all literature-reported active tungsten catalysts, including tungstic acid (H_2WO_4), hydrogen tungsten bronze (H_xWO_3), *meta*- and paratungstate salts, heteropolyacids (*e.g.*, $H_3PW_{12}O_{40}$), and even tungsten metal and tungsten carbide (W_2C), derive their catalytic activity *via* intrinsic or *in situ* generated W–O–W sites despite their diverse compositions and structures.[91]

2.2.1.3. Dehydration. Dehydration, another key cleavage reaction, involves the breaking of C–O carbohydrate bonds *via* acid-catalyzed H_2O elimination. A wide variety of acidic catalysts has been used for these dehydration reactions: mineral (*e.g.*, HCl, H_2SO_4) and organic acids (*e.g.*, oxalic acid), soluble Lewis acids (*e.g.*, $CrCl_3$, $ZnCl_2$), acid resins (*e.g.*, Amberlyst-15), zeolites (*e.g.*, MFI, BEA), metal oxides (*e.g.*, Al_2O_3, ZrO_2, TiO_2), *etc.* Besides catalyst type, the effect of other reaction conditions such as reaction temperature (100–200 °C) and solvent (H_2O, DMSO, ionic liquids, *etc.*) have been studied extensively.[92–97]

2.2.1.4. (De)hydrogenation. Carbohydrates, containing a carbonyl functional group, are reduced to polyols or sugar alcohols by catalytic hydrogenation. In general, hydrogenation occurs as the final step in a carbohydrate upgrading process as polyol products are more stable and less susceptible to side reactions than their hydroxy carbonyl equivalents.[42] In the presence of molecular hydrogen, carbohydrates can be hydrogenated by both homogeneous and heterogeneous metal catalysts. The latter, however, are preferred on an industrial scale due to their ease of recovery and reusability in combination with high product yields and selectivity.[98] The catalytic efficiency of heterogeneous hydrogenation catalysts depends on both the active metal species and the catalytic support. Metals such as Ru, Pt and Ni typically demonstrate the highest hydrogenation activity of carbonyl functional groups. Contrary, Pd, another

well-known hydrogenation metal, displays limited activity in reducing carbonyl bonds.[99] The use of support materials beneficially leads to improved structural stability, surface area, and spatial distribution and can additionally induce metal–surface interactions that affect the catalyst's performance. Frequently used support materials include, but are not limited to, activated carbon, alumina, silica and titania.[100]

In dehydrogenation, the reverse reaction, a polyol or sugar alcohol is oxidized by catalytical removal of hydrogen yielding a carbonyl-containing product (*e.g.* sorbitol to glucose or fructose, and xylitol to xylose). While hydrogenation is an exothermic reaction, dehydrogenation is an endothermic reaction and requires a higher reaction temperature. Dehydrogenation is usually the first step in the catalytic upgrading of sugar alcohols as more reactive hydroxy carbonyl substrates are obtained.[101] The same heterogeneous metal catalysts used for hydrogenation can be applied in dehydrogenation reactions. Similar to hydrogenation, the dehydrogenation capacity of a heterogeneous metal catalyst depends on both the metal active species and support material.[101–103]

2.3. (Hemi)cellulose-derived oxygenates

In (hemi)cellulose valorization, hydrolysis and the four upgrading reactions can be combined to unravel a plethora of oxygenate molecules. The product scope ranges from large monosaccharides containing five or six oxygen atoms (**O5** and **O6** oxygenates) to small diols (**O2** oxygenates). In this regard, selectivity control, *i.e.*, favoring desired reactions and inhibiting undesired reactions, is of critical importance. Zheng *et al.* describe this selectivity challenge as ''dancing on eggs'', in which the dancer's weight needs to be distributed subtly on each egg to achieve a desirable result.[84] As a heavily studied topic in the literature, this overall conversion of (hemi)cellulose is referred to as hydrogenolysis.[104,105] In general, the complexity of these hydrogenolysis reactions increases when targeting smaller oxygenates, as more consecutive reaction steps are required. Hence, hydrogenolysis of (hemi)cellulose targeting their corresponding monomers (**O6-5** oxygenates) is first evaluated, after which the complexity gradually increased by assessing **O4** and **O3** oxygenates (containing four and three oxygen atoms) ultimately followed by the discussing **O2** oxygenates.

2.3.1. O6-5 oxygenates. **O6** and **O5** oxygenates are the monomeric building blocks of the polysaccharides cellulose and hemicellulose. As a homopolysaccharide, cellulose solely consists of glucose monomers (**O6** oxygenate) while hemicellulose, a heteropolysaccharide, comprises both **O5** and **O6** oxygenate monomers.[44] These monosaccharides are obtained *via* hydrolysis (Section 2.3.1.1.) and can, in their turn, be converted into their corresponding sugar alcohols by consecutive hydrogenation (*i.e.*, hydrolytic hydrogenation, Section 2.3.1.2.).

2.3.1.1. Monosaccharides (glucose and xylose). Depolymerization of cellulose into glucose monomers is challenging due to its rigid, crystalline structure. This characteristic originates from the excessive network of both inter- and intramolecular hydrogen bonds as well as the stable β-1,4-glycosidic bonds.[48] Chemocatalytic depolymerization of cellulose is an acid-catalyzed hydrolysis reaction in which traditionally aqueous soluble mineral acids, such as H_2SO_4, are used as they enable good accessibility to insoluble, solid cellulose chains. This process can either be performed using diluted or concentrated mineral acids.[70,71] In the former, hydrolysis is typically conducted with 0.5–1% H_2SO_4 at elevated temperature (>200 °C) and pressure (>2 MPa). Under these conditions, glucose is significantly degraded, limiting its yield to 60%. In the latter process, glucose yields above 80% can be obtained by operating with a concentrated H_2SO_4 solution (60–90%) due to decrystallization of the cellulose feed.[106,107] However, mineral acids are highly corrosive to the equipment making their industrial use not viable. Alternatively, organic acids (*e.g.*, carboxylic acids) or heteropolyacids (*e.g.*, $H_3PW_{12}O_{40}$, $H_4SiW_{12}O_{40}$) can be used. Nevertheless, all these acid catalysts suffer from difficult recyclability and product separation.[70,71] As a result, solid acids have gained increasing research interest over the past years. The explored heterogeneous catalysts range from metal oxides (both single and complex metal oxides) to H^+-form zeolites, acidic resins, sulfonated carbon catalysts, *etc.*[108–110] To prevent mass transfer limitations between the solid catalyst and solid cellulose feed catalyst design primarily focuses on creating a catalyst with strong binding sites for adsorption, strong acid sites for hydrolysis, and a high specific area to enhance the catalytic activity. Moreover, various feedstock pretreatment methods exist to increase its accessibility.[108] Optimized heterogeneous catalytic systems with glucose yields exceeding 90% have been reported in the literature.[111]

Hemicellulose, in contrast to cellulose, contains shorter and branched chains, which inhibit crystallization and enhance its solubility, thereby facilitating hemicellulose depolymerization.[44,112] This difference in ease of hydrolysis is illustrated by the work of Kobayashi *et al.*[113] In their work, a comparison between the acid-catalyzed hydrolysis of cellulose and hemicellulose (xylan type) was made using a heterogeneous carbon-based catalyst. Performing the hydrolysis reaction in an aqueous solution containing traces of HCl for 17 minutes at 215 °C resulted in glucose and xylose yields of 78% and 94%, respectively.[113]

2.3.1.2. Sugar alcohols (sorbitol and xylitol). Early research addressed the conversion of (hemi)cellulose into sugar alcohols, such as sorbitol and xylitol, using a binary catalytic system.[114] This system consists of (i) a soluble mineral acid to facilitate hydrolysis and (ii) a transition metal catalyst, typically Ru, to subsequently perform the hydrogenation of the monosaccharide into the sugar alcohol.[115,116] In 2006, Fukuoka and co-workers were the first to report a different approach, using an integrated multifunctional catalyst, bypassing the drawbacks of mineral acids.[117] In their work, cellulose was converted to sorbitol (25% yield) and mannitol (6% yield) using a Pt/γ-Al_2O_3 catalyst in the presence of 5 MPa H_2 pressure, at 190 °C for 24 h. The solid catalyst, consisting of a transition metal and an acidic support, both catalyzed the hydrolysis of cellulose and hydrogenation of glucose.[117] This finding paved the way for much follow-up research exploring various

transition metals (*e.g.*, Ni, Ru, Pt, Rh) and carbon-based supports (*e.g.*, activated carbon, zeolites, carbon nanotubes). Various of these studies have reported sugar alcohol selectivities exceeding 70%.[118–121] Importantly, selective multifunctional catalytic systems balance the activity of their acid sites and the activity of their hydrogenation sites. A catalyst with dominant acid sites results in fast hydrolysis followed by glucose degradation due to the high reaction temperature. Contrary, a catalyst with dominant hydrogenation sites additionally favors other metal-catalyzed reactions (*e.g.*, retro-aldol condensation, dehydration) resulting in smaller oxygenate by-products.[122,123]

2.3.2. O4-3 oxygenates. To date, little to no research has been dedicated to the selective formation of either **O4** or **O3** oxygenates *via* chemocatalytic (hemi)cellulose valorization. Instead, academic efforts have predominantly focused on the formation of various **O2** oxygenates, addressing **O4** and **O3** oxygenates as important reaction intermediates.

*2.3.2.1. **O4** oxygenates.* In theory, the **O4** oxygenate erythrose can be obtained *via* retro-aldol condensation of glucose. Erythrose, in its turn, can subsequently undergo keto–enol isomerization to form erythrulose or hydrogenation to yield erythritol.[124] Since currently no chemocatalytic processes exist, biotechnological routes dominate industrial production of these **O4** oxygenates.[125,126] Notably, the research team at Haldor Topsøe has proposed a chemocatalytic bottom-up pathway to produce these **O4** oxygenates.[127] In their study, they achieved the formation of these **O4** oxygenates through the aldol condensation of two glycolaldehyde (GA) molecules using shape-selective zeolites. For example, using a Sn-MFI catalyst at 80 °C in water for 30 minutes, they reported a total yield and selectivity for **O4** oxygenates of 74% and 97%, respectively.[127]

*2.3.2.2. **O3** oxygenates.* Within the scope of (hemi)cellulose valorization, three main **O3** oxygenates can be formed: 1,3-dihydroxyacetone (DHA), glyceraldehyde, and glycerol. In theory, the isomers DHA and glyceraldehyde can be produced *via* retro-aldol condensation of fructose, the ketose isomer of glucose. Subsequent hydrogenation of these **O3** isomers results in the formation of glycerol. In practice, glycerol is abundantly available being a major by-product in the biodiesel process. Approximately 100 g of glycerol is generated for every kg of biodiesel produced *via* transesterification of triglycerides.[128,129] Consequently, glycerol is the industrial feedstock to produce DHA and glyceraldehyde *via* fermentative or catalytic oxidation.[130,131]

2.3.3. O2 oxygenates. Hydrogenolysis of (hemi)cellulose-derived substrates into **O2** oxygenates has been a widely studied topic in biomass valorization. In the literature, three selectivity routes are addressed targeting different **O2** diols and their corresponding hydroxy carbonyl precursors: (i) ethylene glycol (EG) and glycolaldehyde (GA), (ii) 1,2-propylene glycol (1,2PG) and acetol, and (iii) 1,3-propylene glycol (1,3PG) and 3-hydroxypropanal. These three selectivity routes have been explored using various feedstocks, including (hemi)cellulose, its monosaccharides glucose and xylose, the sugar alcohols sorbitol and xylitol, and glycerol. Due to their chemical structure, hydrogenolysis of the **O5** substrates xylose and xylitol through retro-aldol condensation typically results in an equal and unselective formation of the products from the first two selectivity routes (*i.e.*, EG and 1,2PG).[132,133] In contrast, the **O6** substrates glucose and sorbitol can selectively favor all three routes, positioning them as ideal substrates to study the overall selectivity challenge in chemocatalytic hydrogenolysis.[105] Additionally, glycerol has been used to investigate the selectivity challenge between the latter two routes targeting 1,2PG and 1,3PG.[134]

2.3.3.1. Ethylene glycol (EG) and glycolaldehyde (GA). The chemocatalytic conversion of glucose to EG passes through three consecutive steps and two different key upgrading reactions: (i) retro-aldol condensation of glucose in erythrose and GA, (ii) consecutive retro-aldol condensation of erythrose in two additional GA molecules, and (iii) hydrogenation of GA into EG. Dehydration, isomerization, and preliminary hydrogenation of glucose and erythrose should all be suppressed or be less competitive than retro-aldol condensation to selectively form EG. A successful strategy consists in designing a catalytic system that contains both retro-aldol and hydrogenation activity. On the one hand, the catalyst can be a binary system comprising both a metal-based hydrogenation catalyst and a tungsten-based retro-aldol catalyst. For example, in Avantium's patented RAY process, a 72% EG yield could be obtained from an aqueous glucose solution by using a binary 5 wt% Ru/C–H_2WO_4 catalytic system (W-to-Ru molar ratio of 16 : 1) in a batch process at 180 °C and 5 MPa H_2.[135] Zhao *et al.* studied the conversion of an aqueous glucose solution with a binary 4 wt% Ru/C–ammonium metatungstate (AMT) catalytic system. They achieved a 76% EG yield by performing the reaction in a fed-batch set-up at 220 °C and 5 MPa H_2.[136] On the other hand, both hydrogenation and retro-aldol activity can be incorporated into one bimetallic catalyst. For instance, Ooms *et al.* developed a heterogeneous nickel–tungsten carbide catalyst (2 wt% Ni–30 wt% W_2C/AC) for the conversion of an aqueous glucose solution in a fed-batch process. Operating the reaction at 260 °C and 6 MPa H_2 yielded 66% EG.[137] It is noticeable that all reactions targeting EG are conducted at temperatures around or above 200 °C. Under applied reaction conditions, preliminary hydrogenation of glucose into sorbitol is the dominant side reaction. Although system-dependent, it is generally acknowledged that the activation energy of the retro-aldol condensation is significantly higher than that of the hydrogenation. For example, in the abovementioned Ru/C–AMT catalytic system, the activation energy for the retro-aldol condensation and hydrogenation of glucose are around 160 kJ mol^{-1} and 65 kJ mol^{-1}, respectively.[136] Therefore, conducting the reaction at an elevated temperature should beneficially affect the retro-aldol condensation at the expense of the preliminary hydrogenation.[137]

The chemocatalytic conversion of sorbitol to EG follows the same pathway as the hydrogenolysis of glucose, with the distinction that this substrate requires an initial

dehydrogenation step. The dehydrogenation–hydrogenation activity of the catalytic system is a crucial property of this hydrogenolysis reaction as substrate conversion generally is the rate-determining step. Liang *et al.* studied the dehydrogenation of sorbitol and observed the importance of the synergetic effect of ample acid–base pair sites. Comparing the catalytic activity of Ni/Al_2O_3 and Ni/ZSM-5, the first catalyst had both strong acidity and basicity and resulted in a higher dehydrogenation activity than the latter catalyst, which contained sufficient acidic but less basic sites.[103] Annuar *et al.* recently reviewed numerous heterogeneous catalysts used in sorbitol hydrogenolysis.[101]

In hydrolytic hydrogenolysis, acid-catalyzed hydrolysis of (hemi)cellulose is coupled with monosaccharide hydrogenolysis. Most hydrogenolysis catalytic systems are also effective hydrolytic hydrogenolysis catalysts since these catalysts already contain acidic properties to perform the retro-aldol condensation, isomerization and/or dehydration steps.[138,139] For example, the nickel–tungsten catalysts active in the hydrogenolysis of glucose to EG are also active catalytic systems in the conversion of cellulose to EG.[84]

2.3.3.2. 1,2-Propylene glycol (1,2PG) and acetol. The chemocatalytic conversion of glucose to 1,2PG involves a series of five sequential steps encompassing all four key reactions: (i) glucose isomerization to fructose, (ii) retro-aldol condensation of fructose leading to the isomers glyceraldehyde and DHA, (iii) dehydration of glyceraldehyde to pyruvaldehyde, (iv) hydrogenation of pyruvaldehyde to acetol, and finally (v) hydrogenation of acetol to yield 1,2PG. The primary challenge in achieving a desired 1,2PG selectivity *via* this hydrogenolysis process lies in the initial step, namely the isomerization reaction. To selectively obtain 1,2PG, it is important to favor glucose isomerization while minimizing preliminary glucose hydrogenation to sorbitol and retro-aldol condensation to erythrose and GA. Another selectivity challenge lies in the dehydration of glyceraldehyde as two other side reactions can occur, namely the retro-aldol condensation to GA and formaldehyde, and hydrogenation to glycerol. Consequently, a 1,2PG selective catalytic system should contain sufficient isomerization capacity alongside retro-aldol, dehydration and hydrogenation capacity. Analogous to selective EG formation, the two most studied strategies in selective 1,2PG formation are a binary catalytic system and a modified hydrogenation catalyst. For both strategies, numerous catalytic systems have been studied and were recently reviewed.[140,141] Here, both strategies are illustrated with a couple of suitable examples. Hirano *et al.* studied a binary Ru/C–ZnO catalytic system.[142] When only Ru/C was present, the direct hydrogenation of glucose into sorbitol was the dominant reaction pathway while the addition of ZnO steered the selectivity toward 1,2PG. They proposed that ZnO, acting as an amphoteric metal oxide, positively affected the isomerization, retro-aldol condensation and dehydration steps. The 1,2PG yield increased from 9% to 38% by adding ZnO to the 5 wt% Ru/C catalyst after 20 h reaction time at 180 °C and a stoichiometric hydrogen pressure (0.4 MPa H_2) to limit preliminary hydrogenation. Other tested metal oxides, including Fe_3O_4, La_2O_3 and CeO_2, were less effective but still selective toward 1,2PG.[142] Another selective 1,2PG binary system was proposed by Xiao *et al.*[143] They explored a binary system with on the one hand a Cu–Cr catalyst containing both hydrogenation and dehydration properties and on the other hand the base $Ca(OH)_2$ as an isomerization and retro-aldol condensation catalyst. With this catalytic system, they achieved a 1,2PG yield of 53% by conducting the reaction at 6 MPa H_2, first for 2 hours at 140 °C followed by 5 hours at 220 °C. In the second strategy, *i.e.*, developing a modified hydrogenation catalyst, the choice of support is crucial as it should introduce acid–base properties in the system. Liu *et al.* studied the Cu/Al_2O_3 catalytic system for the selective formation of 1,2PG.[144] Similar to ZnO used by Hirano *et al.*,[142] the amphoteric properties of the Al_2O_3 support significantly contributed to the isomerization, retro-aldol condensation and dehydration steps. At 180 °C and 4 MPa H_2, a 43% 1,2PG yield was obtained. Additionally, the incorporation of WO_x in the catalytic system ($Cu–WO_x(0.8)/Al_2O_3$) further increased the 1,2PG yield to 55% by beneficially influencing the retro-aldol condensation and glyceraldehyde dehydration.[144] In a successive study, the same researchers investigated the synergetic effect between Cu and Al_2O_3 in more detail. In addition to the intrinsic amphoteric character of the support, they found that Al_2O_3 could also induce the formation of oxidized $Cu^{\delta+}$ species which in their turn could act as Lewis acid sites promoting the isomerization, retro-aldol condensation and dehydration steps.[145] In line with these findings, Kirali *et al.* developed a Ce-promoted Cu/Al_2O_3 catalyst with optimized acid–base properties for the selective conversion of glucose into 1,2PG. After 6 h reaction time at 200 °C and 4 MPa H_2, the reaction catalyzed by 8 wt% Cu/Al_2O_3 yielded 31% 1,2PG. The 1,2PG yield was improved to 61% by performing the reaction with the $Ce–Cu/Al_2O_3$ catalyst.[146] While most studies focus on the production of 1,2PG, Deng *et al.* reported a catalytic system ($Ni–SnO_x/Al_2O_3$) with limited hydrogenation activity predominantly leading to acetol formation. The reaction yielded 3% 1,2PG and 53% acetol after 0.5 h at 200 °C and 6 MPa H_2.[147]

Glycerol hydrogenolysis mainly results in three diols, namely 1,2PG and 1,3PG and to a lesser extent in EG. 1,2PG and 1,3PG are produced *via* two consecutive steps: (i) acid-catalyzed dehydration of glycerol followed by (ii) hydrogenation of the hydroxy carbonyl intermediates. The dehydration of glycerol's two primary hydroxyl groups results in acetol which leads to 1,2PG after hydrogenation. The dehydration of the secondary hydroxyl group yields 3-hydroxypropanal and 1,3PG after hydrogenation.[134,148] From a kinetic point of view, the dehydration of the two primary hydroxyl groups and the subsequent formation of 1,2PG is favored. Contrary, from a thermodynamic point of view, the formation of 1,3PG *via* its more stable secondary carbocation is favored.[149] In practice, however, most investigated catalytic systems mainly yield the kinetic product 1,2PG. Moreover, 1,2PG can also be formed *via* a second pathway: (i) glycerol dehydrogenation into glyceraldehyde, (ii) glyceraldehyde dehydration into pyruvaldehyde,

(iii) subsequent hydrogenation of pyruvaldehyde into 1,2PG. EG can be formed as a minor by-product *via* this pathway if retro-aldol condensation of glyceraldehyde is competitive with its dehydration. Similar to other mentioned hydrogenolysis reactions, the catalytic system for glycerol hydrogenolysis consists of a transition hydrogenation metal (Cu, Ni, Ru, Pt, *etc.*), potentially accompanied by a promoter, and a support material. Consequently, product selectivity is influenced by the dehydrogenation–hydrogenation activity and, especially, by the acid–base properties of the overall catalytic system.[104] An overview of tested catalytic systems can be found in the reviews by Wang *et al.*[134] and Basu *et al.*[148]

3. From renewable substrates to bio-based aliphatic amines

3.1. Reductive amination: principles and mechanism

The catalytic transformation of (hemi)cellulose-derived oxygenates into aliphatic amines essentially involves the transformation of a C=O or C–OH bond into a C–N bond *via* a reductive amination reaction. Over the years, multiple reductive amination approaches have been studied, ranging from biocatalytic techniques using transaminase[150,151] and amine dehydrogenase enzymes[152,153] to electrocatalytic[154,155] and chemocatalytic techniques. The latter technique will be reviewed in detail, in correspondence with the abovementioned chemocatalytic valorization of (hemi)cellulose.

From a mechanistic perspective (Scheme 2), the reductive amination of a carbonyl-containing substrate (*i.e.*, aldehyde or ketone) is a multi-step reaction that starts with the nucleophilic addition of an amine reactant onto the carbonyl group of the substrate resulting in a hemi-aminal intermediate. Subsequent dehydration of this intermediate yields an imine or enamine if the reactant is NH_3/primary amine or a secondary amine, respectively. This imine/enamine is ultimately reduced to yield an amine product.[2,156,157] In the chemocatalytic reductive amination process, various reducing agents can be used.[158] The most widespread reducing agents include metal hydrides (*e.g.*, borohydrides such as $NaBH_4$ and $NaBH_3CN$),[159] formic acid/formate,[160–162] CO,[163,164] and molecular H_2 in combination with a homogeneous or heterogeneous transition metal hydrogenation catalyst.[165,166] The latter heterogeneous reducing system is predominantly used in research and industry because it uses non-toxic, relatively inexpensive and potentially green H_2 gas, only leads to H_2O as a by-product, and the metal catalyst can be recycled.[158,167] The amination of a hydroxyl-containing substrate (*i.e.*, alcohol) starts with its activation into a more reactive aldehyde/ketone *via* oxidation. Afterward, the process proceeds *via* the same elementary steps as the reductive amination reaction. In the literature, this process is referred to as hydrogen borrowing amination since overall no net H_2 is consumed.[168] The hydrogen atoms necessary for imine/enamine reduction are initially obtained *via* alcohol activation. In practice, however, most hydrogen borrowing amination reactions are conducted under (limited) hydrogen pressure to suppress catalyst deactivation and detrimental amine disproportionation (*vide infra*).[169] In hydrogen borrowing amination, substrate activation by oxidation is generally recognized as the rate-determining step. Consequently, these reactions typically require higher reaction temperatures than reductive amination (150–250 °C) and the presence of a transition metal catalyst that contains both dehydrogenation and hydrogenation activity.[170–172]

Both the reductive amination and hydrogen borrowing amination reactions encompass a wide scope of potential side reactions, influenced by the activity of the catalyst and the reactivity of the various components involved.[156,157] First, the choice of catalyst is crucial as it significantly contributes to the overall efficiency and selectivity of the process. In reductive amination, uncontrolled, fast hydrogenation of the unreacted aldehyde/ketone substrate into the corresponding alcohol inevitably depletes the substrate (Scheme 2, side reaction A).[166] In hydrogen borrowing amination, substrate activation, as the rate-determining step, emphasizing the need for a catalytic system with excellent dehydrogenation properties.[172] Second, all components throughout the reaction pathway (*i.e.*, substrate, reactant, intermediates and product) can undergo various side reactions, thereby decreasing the selectivity of the desired product. In general, aldehydes are considered to be more reactive than ketones due to electronic and steric effects. Consequently, aldehyde-containing substrates are not only more susceptible to the amination reaction but also more reactive to side reactions such as aldol condensation, caramelization and other degradation reactions, leading to depletion of the substrate (Scheme 2, side reaction B).[178,179] Moreover, both the amine reactant and product can undergo amine disproportionation, as it is catalyzed by a metal catalyst at elevated temperatures (*i.e.*, typical for hydrogen borrowing amination), resulting in the interconversion of primary, secondary and tertiary amines (Scheme 2, side reaction C).[169] In addition, the amine product can suffer from overalkylation, since the alkylated amine product, in general, exhibits greater reactivity compared to the amine reactant due to its increased nucleophilicity.[180] Similar to amine disproportionation, overalkylation results in a mixture of alkylated amine products (Scheme 2, side reaction E). Furthermore, all amine intermediates, particularly the imine/enamine intermediates, are labile compounds that are prone to Maillard-type degradation reactions, which adversely impact product selectivity (Scheme 2, side reaction D).[178,179]

3.2. Oxygenate-derived amines

Over the past decades, various lignocellulose-derived compounds have been explored as potential substrates in the catalytic reductive amination yielding a plethora of amines.[181] Amination of lignin and its monomers results in phenolic and cycloalkyl amine products such as aniline, cyclohexylamine and their derivatives.[182–186] (Hemi)cellulose-derived carboxylic acids, for example levulinic acid or lactic acid, can be converted into heterocyclic pyrrolidines and pyrrolidones,[187,188] amino

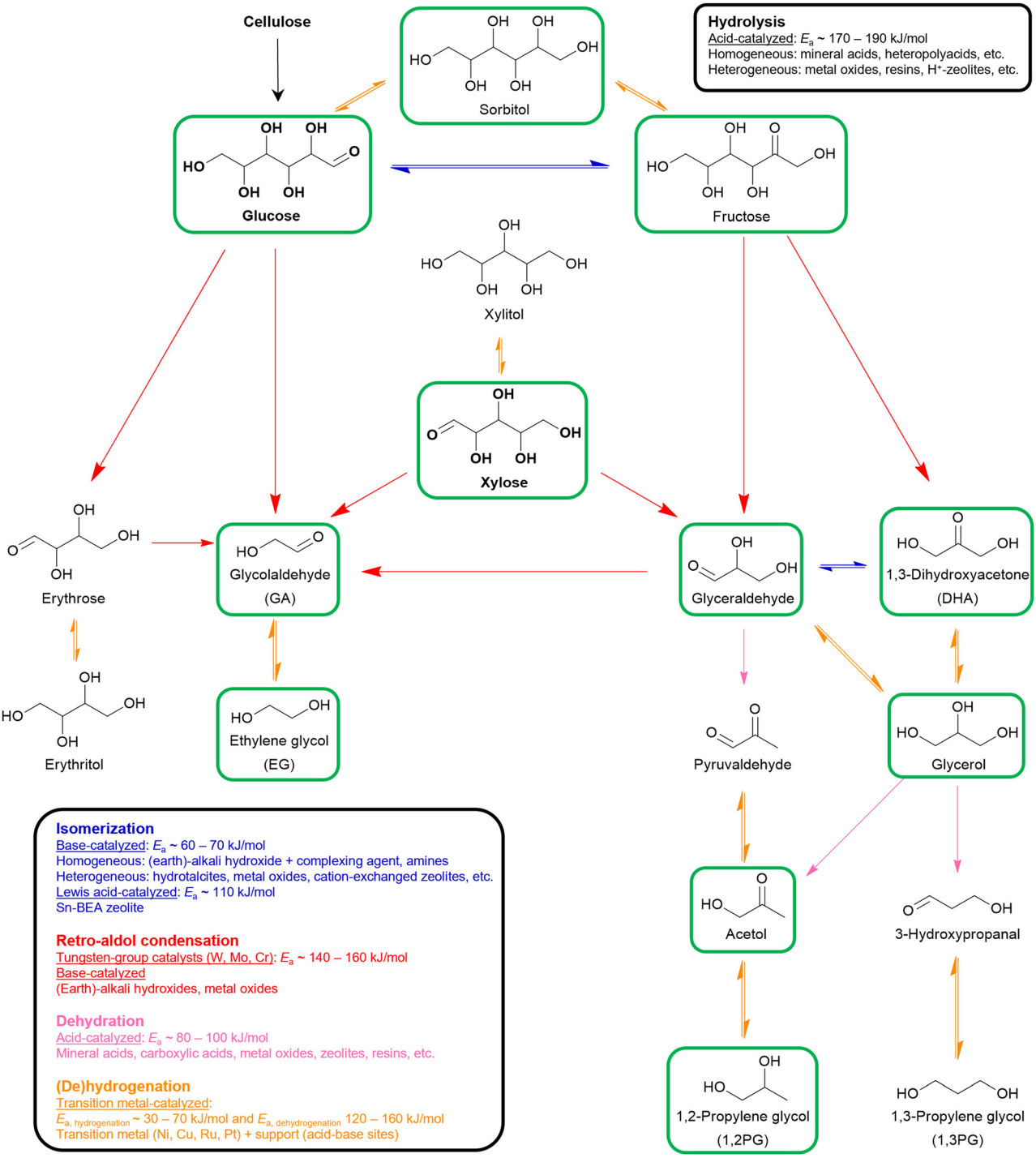

Scheme 1 Overview of the chemocatalytic valorization of (hemi)cellulose-derived monomers into hydroxy carbonyl and polyol oxygenates through hydrolysis and four upgrading key reactions. Oxygenates framed in green have already been assessed as viable substrates in the production of bio-based aliphatic amines. Reported activation energies (E_a) should be interpreted as an indication of the order of magnitude as they strongly depend on the studied catalytic system. References for hydrolysis,[70,71,108,173] isomerization,[72–74,174–176] retro-aldol condensation,[84,86,88,89,136] dehydration,[134,148,149,177] and (de)hydrogenation.[98,99,101,103]

acids[189] or even alkyl amines,[190] whereas (hemi)cellulose-derived furfurals predominantly yield furfuryl amines.[191–193]

In the scope of the Review, aliphatic amines are obtained from aliphatic (hemi)cellulose-derived oxygenates. Moreover, all three types of aliphatic amines, namely alkanolamines, alkyl polyamines and heterocyclic amines, are formed *via* the same reaction pathway due to the multi-oxygen nature of these oxygenate substrates. Hence, steering the selectivity toward

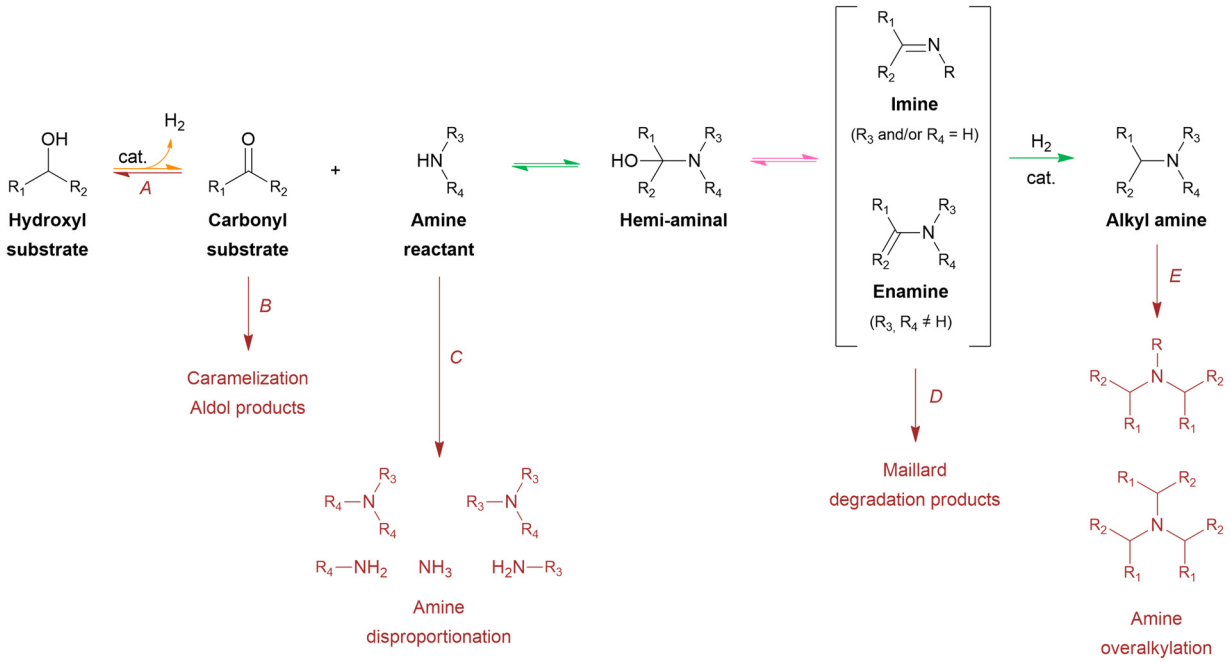

Scheme 2 General mechanism of the reductive amination of an oxygenate into an alkyl amine. Each elementary reaction is represented by a color; amination (green), dehydration (pink) and (de)hydrogenation (orange). Reactions in dark red represent the most important side reactions.

one desired product while reducing the formation of other products and undesired side reactions is the key challenge in governing the catalytic reductive amination of carbohydrate substrates. Strikingly, product selectivity is affected by the same four elementary key reactions that influence the chemocatalytic valorization of (hemi)cellulose, in addition to the nucleophilic amination step. While, two key reactions are inherently present in the reductive amination mechanism (*i.e.*, (de)hydrogenation and dehydration, Scheme 2), all four key reactions can occur as pre-amination reactions preceding reductive amination and further complicating product selectivity. In general, the complexity of the overall amination reaction, associated with the occurrence of these pre-amination reactions, increases with an increasing number of oxygen atoms in the oxygenate substrate (Scheme 3). In this regard, the reductive amination of **O2** substrates is first evaluated, after which the complexity gradually increases by assessing **O3** substrates followed by **O5** and **O6** substrates.

3.2.1. O2 substrates. **O2** substrates, as the simplest oxygenates, contain two oxygen atoms in their molecular structure. They encompass both dihydric alcohols, *i.e.*, diols, and hydroxy carbonyl components, which include hydroxy aldehydes and hydroxy ketones. As the oxygen-containing functional groups in nearly all (hemi)cellulose-derived oxygenates are separated by two carbon atoms, α-diols and α-hydroxy carbonyl components are the prevailing **O2** substrates. Additionally, both symmetric and asymmetric **O2** oxygenates can be obtained *via* chemocatalytic valorization. The use of these various **O2** substrates makes it possible to study the selectivity control challenge inherently associated with reductive amination while keeping the reaction network free from additional complexity.

The general pathway for the catalytic reductive amination of **O2** substrates is given in Scheme 4. Prior to the reductive amination reaction steps, two additional pre-amination reactions can or need to take place. First, when using a diol (Scheme 4, **S1**), an initial activation step is required. This activation involves the dehydrogenation of the diol, resulting in the formation of an α-hydroxy carbonyl component (**S2** or **S3**). Second, when using an asymmetric α-hydroxy carbonyl (*i.e.*, if $R_1 \neq R_2$), an isomerization reaction can occur. If one of the substituents is a proton (*i.e.*, if R_1 or R_2 = H), the isomerization involves the interconversion between an α-hydroxy ketone and an α-hydroxy aldehyde, resembling the aldose – ketose isomerization in carbohydrate upgrading. After these pre-amination reactions, the reductive amination of the α-hydroxy carbonyl substrates initially proceeds *via* the general reductive amination mechanism. First, the nucleophilic addition of an amine reactant onto the **O2** substrate results in a hemi-aminal intermediate (**I1**). Secondly, dehydration of **I1** leads to an imine (**I2**) or enamine (**I3**) intermediate. In their turn, **I2** and **I3** can interconvert *via* an imine-enamine tautomerization.[194,195] Due to the unique structure of α-hydroxy carbonyl components, the formed enamine (**I3**) can further undergo a keto–enol tautomerization reaction, yielding an α-amino carbonyl intermediate (**I4**). The overall isomerization of **I2** to **I4**, passing through two successive tautomerization reactions, is commonly referred to as the acid-catalyzed Amadori or Heyns rearrangement, depending on whether the substrate is an α-hydroxy aldehyde or α-hydroxy ketone, respectively.[196,197] In the presence of molecular hydrogen and a heterogeneous metal catalyst, **I2**, **I3** and **I4** can all be hydrogenated into a (substituted) alkanolamine product (**P1**). Alternatively, **I4** can undergo a second

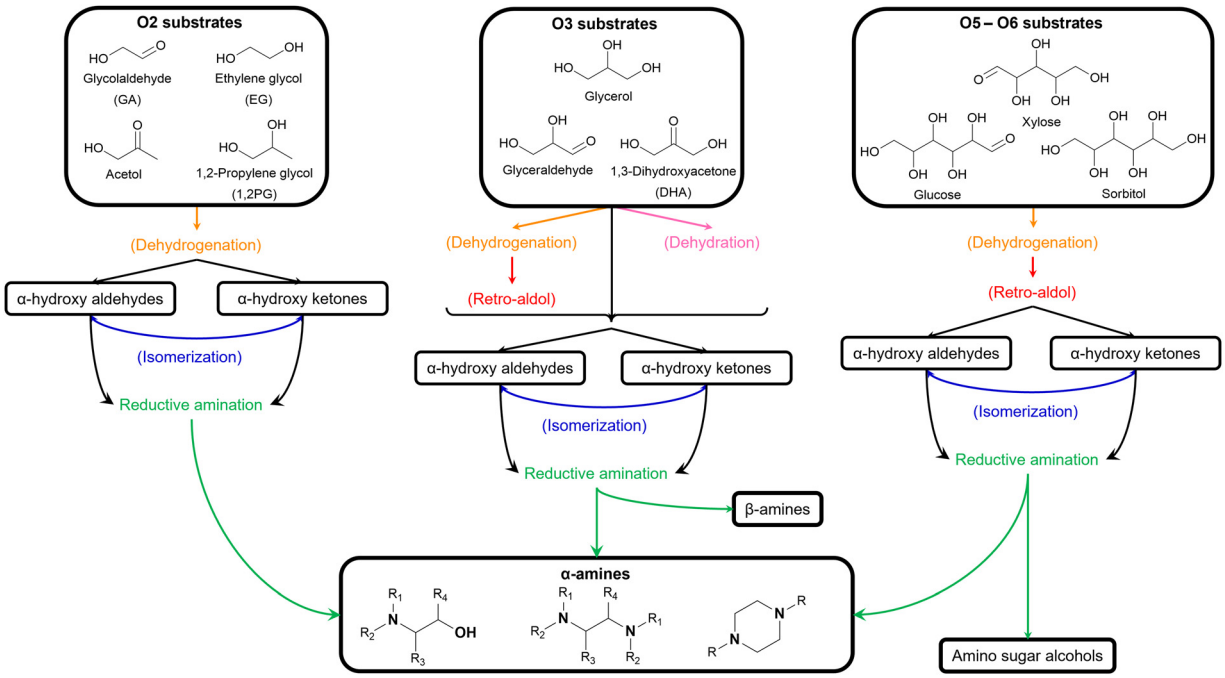

Scheme 3 Overview of the possible reductive amination pathways of different (hemi)cellulose-derived oxygenate substrates.

nucleophilic addition reaction on its carbonyl functional group, resulting in a second hemi-aminal intermediate (**I5**). Dehydration of **I5** results in an imine (**I6**) or enamine (**I7**) intermediate, which both yield the (substituted) alkyl polyamine product (**P2**) after hydrogenation. Under dehydrogenation conditions, the alkanolamine product (**P1**) could potentially be reactivated into **I4**, eventually resulting in the alkyl polyamine product (**P2**). Aliphatic heterocyclic piperazines (**P3**) can be formed from both amine products.[21] In Scheme 4 the amination reaction is depicted using the **S2** hydroxy carbonyl substrate. In the case of asymmetry, the amination of the isomer **S3** would result in the same polyamine (**P2**) and an isomeric ethanolamine (**P1**) compared to the **S2**-related amine products.

Four different **O2** substrates have been predominantly studied in literature and will be here reviewed systematically: (i) the symmetric α-hydroxy aldehyde glycolaldehyde (GA), (ii) the symmetric α-diol ethylene glycol (EG), (iii) the asymmetric α-hydroxy ketone acetol, and (iv) the asymmetric α-diol 1,2-propylene glycol (1,2PG).

3.2.1.1. Glycolaldehyde (GA). As the smallest reducing sugar, GA (Scheme 4, **S2**: $R_1 = R_2 = H$) is the most suitable model component to study the selectivity control challenge in catalytic reductive amination.[30]

Multiple researchers have used GA to qualitatively study the reductive amination reaction in order to develop handles that steer the product selectivity toward the formation of either ethanolamines or ethylene polyamines. In their work, Faveere *et al.* developed a set of guidelines for highly selective ethanolamine formation from GA.[198,199] They achieved a quantitative *N*,*N*-dimethylethanolamine (DMEA, Table 1 entry 3) yield (97%) in the one-step reductive amination of GA with DMA after 1 h at 100 °C. Three main aspects contribute to this high yield. First, they performed a fast and selective hydrogenation reaction of **I3** (Scheme 4) by conducting the reaction under high H_2 pressure (7 MPa H_2) in the presence of an effective C=C hydrogenation catalyst (*e.g.*, 5 wt% Pd/C). Second, they conducted the reaction in MeOH, a protic solvent that assists the different proton-transfer reactions throughout the amination pathway. Performing the same reaction in H_2O or THF decreased the DMEA yield to 67% and 57%, respectively. Although a protic solvent, performing the reaction in the presence of H_2O negatively affects the dehydration step. Third, they applied a low amine-to-substrate (ATS) molar ratio to stoichiometrically prevent the formation of the polyamine product. Similar to the fossil-based processes, the ATS molar ratio is an efficient tool to influence product selectivity. For example, in the reductive amination of GA with MMA in MeOH for 1 h at 100 °C and 7 MPa H_2 with a 5 wt% Pd/C hydrogenation catalyst, increasing the ATS molar ratio drastically shifted the product selectivity. At a molar ratio of 0.5 : 1, the yield of the overalkylated diethanolamine *N*-methyldiethanolamine (MDEA, Table 1 entry 5) amounted to 91%, while its yield strongly decreased to 18% at a stoichiometric molar ratio of 1 : 1 in favor of the ethanolamine *N*-monomethylethanolamine (MMEA, Table 1 entry 2), yielding 64%. A maximum MMEA yield of 91% was achieved at a molar ratio of 3 : 1.[198,199] These three control handles were further validated by expanding the amine reactant scope.[200] In agreement with the insights of Faveere *et al.*,[199] the reductive amination of GA with the reactant *N*-monoethylamine yielded 94% of the ethanolamine *N*-monoethylethanolamine (MEEA, Table 1 entry 4) under optimized conditions (MeOH as solvent,

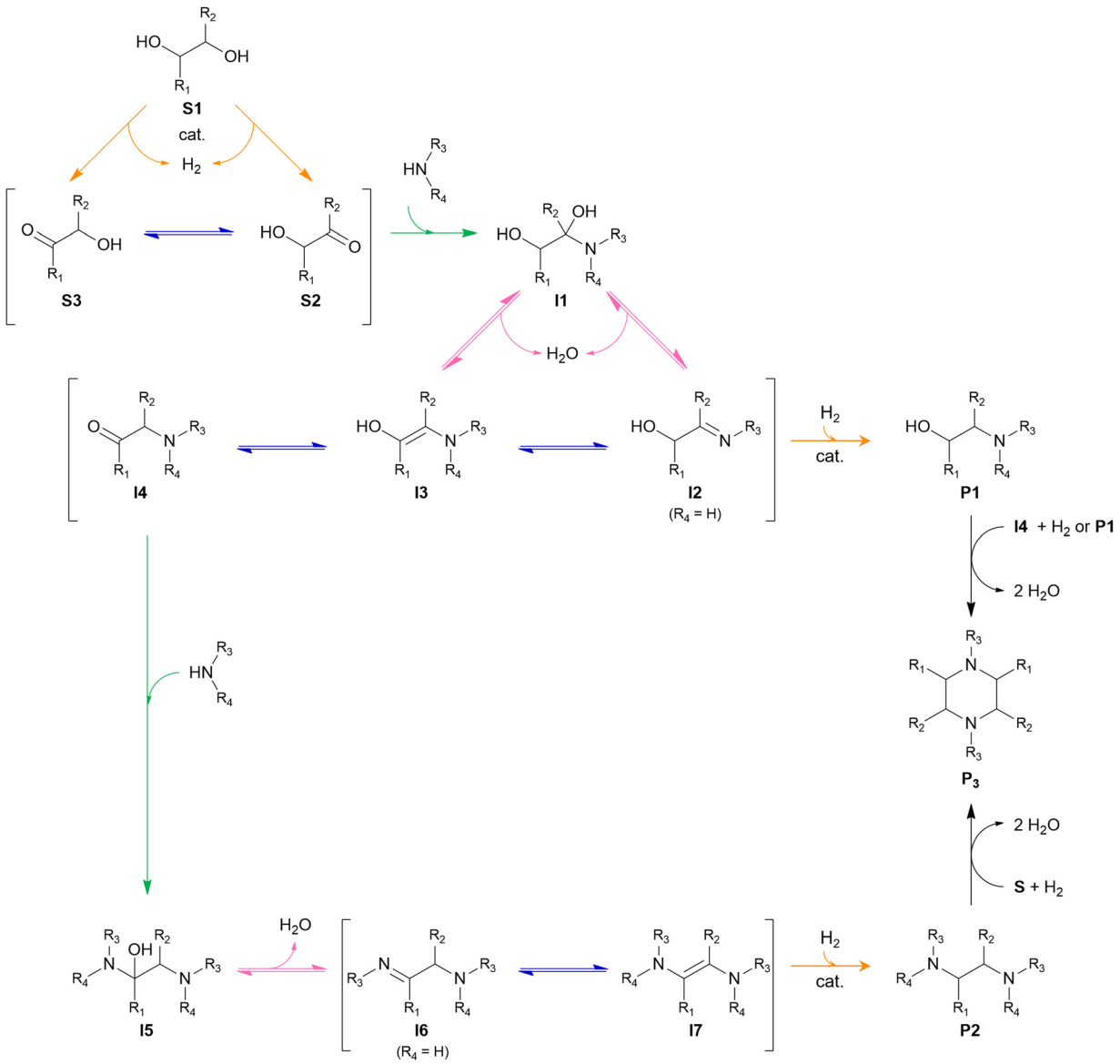

Scheme 4 General reaction mechanism of the reductive amination of O2 substrates. Each elementary key reaction is represented by a color: amination (green), isomerization (blue), dehydration (pink), and (de)hydrogenation (orange).

1 h, 120 °C, 8 MPa H_2, 5 wt% Pd/C hydrogenation catalyst, ATS molar ratio of 2 : 1).[200] The ethanolamine guidelines are also applied in a recent patent application by Solvay.[201] A 94% DMEA yield was achieved by performing the reductive amination of GA with DMA for 3 h at 25 °C under selective hydrogenation conditions (4 MPa H_2 with 5 wt% Pd/C), in EtOH as the protic solvent, and a low ATS molar ratio of 2.4 : 1.[201] Recently, Van Praet *et al.* strengthened the viability of the ethanolamine guidelines in a scale-up study.[202] Whereas Faveere *et al.* typically performed their reactions at a 5 wt% GA concentration, Van Praet *et al.*[199] conducted the reductive amination of GA using a significantly more concentrated GA solution (40 wt%) to align with industrial productivity standards.[202] Although all control handles were validated, performing the reductive amination using this highly concentrated GA solution negatively impacted the DMAE selectivity compared to the conventional low GA concentration reactions. These results were ascribed to H_2 transfer limitations induced by the increased GA concentration. To overcome these transfer limitations, Van Praet *et al.* proposed to enhance the gas-phase mass transfer of the system. This could be achieved by increasing the stirring rate or implementing baffles adjacent to the stirrer to facilitate mixing while minimizing excessive stirring. For example, performing the reductive amination of a 40 wt% GA MeOH solution for 1 h at 100 °C and 2 MPa H_2, with a 10 wt% Pd/C hydrogenation catalyst, an ATS molar ratio of 2.5 : 1, and a stirring rate of 800 rpm resulted in unselective DMEA and TMEDA formation with yields of 44% and 45%, respectively. However, conducting the reaction under the same conditions in the presence of baffles shifted product selectivity

Table 1 Overview of reported bio-based aliphatic amines

#	Name	Structure	Oxygenate substrate	Reaction conditions [cat., ATS molar ratio, T, solvent]	X–S [%]	Ref.	Applications
				Alkanolamines			
				Ethanolamines			
			GA	Ru/ZrO_2, 10 : 1, 75 °C, H_2O	100–93	203	
				Co/MnO, 35 : 1, 100 °C, THF	100–83	204	
			EG	(1) Ni–Cu–Mo/ZrO_2, 15 : 1, 150 °C, —	43–29	205	
1	MEA	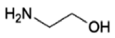		(2) Ru–Co/Al_2O_3, 15 : 1, 170 °C, —			CCUS
				Re–Ru–Co/ZrO_2, 20 : 1, 170 °C, —	35–32	206 and 207	
				Co—Cu/Al_2O_3, 5 : 1, 190 °C, H_2O	42–23	208 and 209	
			Cellulose	(1) H_2WO_4, —, 290 °C, H_2O	100–12	203	
				(2) Ru/ZrO_2, 3.5 : 1, 75 °C, H_2O			
2	MMEA	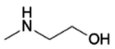	GA	Pd/C, 3 : 1, 100 °C, MeOH	100–91	199	CCUS
				Pd/C, 1 : 1, 100 °C, MeOH	100–97	199	
				Pd/C, 2.4 : 1, 25 °C, EtOH	100–94	201	
			GA	Pd/C, 2.5 : 1, 100 °C, MeOH	100–88	202	
				Cu/Al_2O_3, 12 : 1, 165 °C, —	100 - 74	210	
				Ni/SiO_2, 2.8 : 1, 130 °C, THF	100–76	211	
3	DMEA	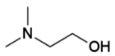	EG	Cu/Al_2O_3, 1 : 1, 230 °C, —	91–68	212	Epoxy
			Glyceraldehyde	Ni oxide, 8 : 1, 130 °C, MeOH	100–1	213 and 214	
			Xylose		100–2		
			Fructose		100–2		
			Glucose		100–4		
4	MEEA	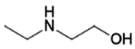	GA	Pd/C, 2 : 1, 120 °C, MeOH	100–94	200	CCUS
5	MDEA	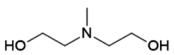	GA	Pd/C, 0.5 : 1, 100 °C, MeOH	100–91	199	CCUS
6	TriMAEEA	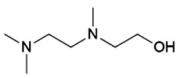	GA	Pd/C, 1 : 1, 100 °C, MeOH	100–95	215	PUR
				Propanolamines			
			Acetol	Cu/Cr_2O_3, 50 : 1, 210 °C, —	100–2	216	
			1,2PG	Rh–In/C, 10 : 1, 180 °C, H_2O	38–42	217	
				Co/Nb_2O_5, 9 : 1, 160 °C, H_2O	37–36	218	
7	1A2P			(1) Cu–PdO–Bi_2O_3–In_2O_3/Al_2O_3, —, 180 °C, —	100–99	219	
				(2) Ni–V_2O_5–Y_2O_3/Al_2O_3, 3 : 1, 200 °C, —			
			Acetol	(1) —, 2 : 1, 100 °C, EG	100–90	220	
				(2) Ru/C, 2 : 1, 50 °C, EG			
8	1DMA2P		Glyceraldehyde	Ni oxide, 8 : 1, 130 °C, MeOH	100–14	213 and 214	CCUS
			Xylose		100–13		
			Fructose		100–11		
			Glucose		100–5		
9	1TriMEDA2P	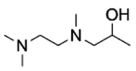	Acetol	(1) —, 2 : 1, 100 °C, EG (2) Ru/C, 2 : 1, 50 °C, EG	100–89	220	
				Ru/ZrO_2, 10 : 1, 65 °C, H_2O	100–26	203	
				Ni–Cu/Cr_2O_3, 4 : 1, 150 °C, H_2O	100–51	221	
			Acetol	Ru–Ni/C, 11 : 1, 65 °C, H_2O	100–52	222	
				(1) —, 3 : 1, RT, H_2O	100–94	223	
				(2) Ni oxide, 3 : 1, 85 °C, H_2O			
10	2A1P			Cu/Cr_2O_3, 50 : 1, 210 °C, —	100–47	216	
			1,2 PG	Rh–In/C, 10 : 1, 180 °C, H_2O	38–26	217	
				Co/La_3O_4, 9 : 1, 160 °C, H_2O	69–89	218	
			Fructose	Ru–W_2C/C, 80 : 1, 180 °C, H_2O	100–1	222	
			Cellulose	(1) W_2C, —, 235 °C, H_2O	100–2	222	
				(2) Ru–W_2C, 20 : 1, 65 °C, H_2O			
11	2iPA1P	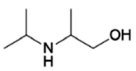	Acetol	Ni–Cu/Cr_2O_3, 4 : 1, 100 °C, EtOH	100–64	221	
12	2TriMEDA1P	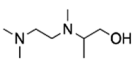	Acetol	Pd/C, 1 : 1, 50 °C, MeOH	77–75	220	
				(1) —, 2.8 : 1, 20 °C, H_2O–MeOH			
13	2A1,3PG	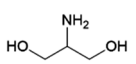	DHA	(2) RANEY® Ni, 2.8 : 1, 70 °C, H_2O–MeOH	100–99	224	
				RANEY® Ni, 10 : 1, 65 °C, H_2O–MeOH	100–91	225	

Table 1 (*continued*)

#	Name	Structure	Oxygenate substrate	Reaction conditions [cat., ATS molar ratio, T, solvent]	X–S [%]	Ref.	Applications
				Ru/ZrO_2, 10 : 1, 55 °C, H_2O	100–82	203	
14	3A1,2PG	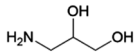	Glyceraldehyde	(1) —, 2.8 : 1, 20 °C, H_2O (2) Pd/C, 2.8 : 1, 50 °C, H_2O	100–95	224	
15	1,2DA3P	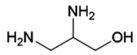	Glycerol	RANEY® Ni, 32 : 1, 200 °C, H_2O	91–21	226	
			Sugar alcohols				
16	Glucamine	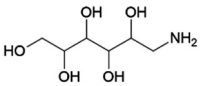	Glucose	RANEY® Ni, 5 : 1, 100 °C, MeOH	100–26	227	
17	DEGA	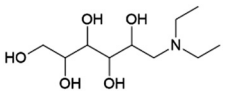	Glucose	Ru/C, 3 : 1, 45 °C, MeOH	100–95	228	
			Alkyl polyamines				
			Ethylene polyamines				
			GA	Ru/ZrO_2, 10 : 1, 75 °C, H_2O	100–2	203	
				Co/MnO, 35 : 1, 100 °C, THF	100–6	204	
			EG	(1) Ni–Cu–Mo/ZrO_2, 15 : 1, 150 °C, —	43–50	205	
18	EDA	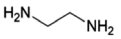		(2) Ru–Co/Al_2O_3, 15 : 1, 170 °C, —			CCUS Epoxy
				Re–Ru–Co/ZrO_2, 20 : 1, 170 °C, —	35–52	206 and 207	
				Co–Cu/Al_2O_3, 5 : 1, 190 °C, H_2O	42–46	208 and 209	
			Glycerol	RANEY® Ni, 32 : 1, 200 °C, H_2O	91–8	226	
			Glucose	RANEY® Ni, 32 : 1, 200 °C, H_2O	100–15	229	
			Sorbitol		100–8		
			GA	(1) —, 12 : 1, 25 °C, EG (2) Pd/C, 12 : 1, 130 °C, EG	100–91	199	
				Ni/SiO_2, lactic acid, 2.8 : 1, 130 °C, THF	100–63	211	
19	TMEDA	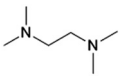	EG	Cu/Al_2O_3, 1 : 1, 230 °C, —	91–21	212	multiQAC
			Glyceraldehyde	Ni oxide, 8 : 1, 130 °C, MeOH	100–4	213 and 214	
			Xylose		100–34		
			Fructose		100–24		
			Glucose		100–66		
20	BHEDMEDA	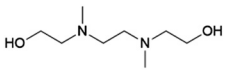	Glucose	(1) —, 70 : 1, 130 °C, MMEA (2) Ni oxide, 70 : 1, 130 °C, MMEA	100–92	213 and 214	
21	HMTriETA	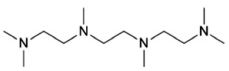	GA	(1) —, oxalic acid, 4 : 1, 30 °C, EG (2) Pd/C, oxalic acid, 4 : 1, 100 °C, EG	100–82	215	ATRP multiQAC
			Propylene polyamines				
			Acetol	Ru/ZrO_2, 10 : 1, 65 °C, H_2O	100–10	203	
				Ru/C, 11 : 1, 65 °C, H_2O	100–5	222	
22	1,2PDA		1,2PG	Co/Fe_3O_4, 9 : 1, 160 °C, H_2O	25–15	218	
			Glycerol	RANEY® Ni, 32 : 1, 200 °C, H_2O	91–22	226	
			Glucose	RANEY® Ni, 32 : 1, 200 °C, H_2O	100–13	229	
			Sorbitol		100–12		
			Acetol	(1) —, 2 : 1, 100 °C, MeOH (2) Pd/C, 4 : 1, 100 °C, MeOH	100–87	220	
23	1,2TMPDA		Glyceraldehyde	Ni oxide, 8 : 1, 130 °C, MeOH	100–6	213 and 214	
			Xylose		100–7		
			Fructose		100–6		
			Glucose		100–7		
24	1,2HMPBEDA	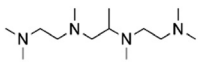	Acetol	(1) —, 2 : 1, 100 °C, MeOH (2) Pd/C, 4 : 1, 100 °C, MeOH	100–90	220	
25	PTriA	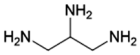	Glycerol	Ni–Cu–Co/ZrO_2, 32 : 1, 200 °C, H_2O	77–17	226	
			Aliphatic heterocyclic amines				
26	PZ		EG	Ni–Cu–Mo/ZrO_2, 15 : 1, 150 °C, —	43–7	205	CCUS
				Ru–Co/Al_2O_3, 15 : 1, 170 °C, —			
				Re–Ru–Co/ZrO_2, 20 : 1, 170 °C, —	35–10	206 and 207	
				Co–Cu/Al_2O_3, 5 : 1, 190 °C, H_2O	42–18	208 and 209	
27	DMPZ		1,2PG	Rh–In/C, 10 : 1, 180 °C, H_2O	38–26	217	

Table 1 (*continued*)

#	Name	Structure	Oxygenate substrate	Reaction conditions [cat., ATS molar ratio, T, solvent]	X–S [%]	Ref.	Applications
			Amino ketones				
			Acetol	—, 2 : 1, 100 °C, EG	100–93	220	
			Glycerol	$Cs_{2.5}H_{0.5}PMo_{12}O_{40}$, 1.5 : 1, 250 °C, —	47–70	230	
28	1-DMA-2-propanone			$H_3PW_{12}O_{40}$, 2.5 : 1, 300 °C, —	100 - 33	231	
			Glyceraldehyde	Ni oxide, 8 : 1, 130 °C, MeOH	100–8	213 and 214	
			Xylose		100–4		
			Fructose		100–6		
			Glucose		100–1		
29	1-TriMEDA-2-propanone	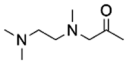	Acetol	—, 2 : 1, 100 °C, EG	100–93	220	
30	1-DMA-3-propanone	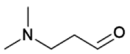	Glycerol	$H_6P_2W_{18}O_{62}$, 2.5 : 1, 300 °C, —	100–81	231	

if favor of the ethanolamine, with DMEA and TMEDA yields amounting to 88% and 2%, respectively.[202]

Other researchers have primarily focused on catalyst development to obtain high ethanolamine yields under conditions which diverge from the benchmark approach. BASF patented a gas-phase reductive amination reaction to overcome the limitations of working with aqueous solutions.[210] In this gas-phase reaction, an aqueous GA solution was evaporated and reacted with gaseous DMA in the presence of a 56 wt% Cu/Al_2O_3 catalyst. Under investigated conditions (165 °C, ATS molar ratio of 12 : 1, H_2-to-GA molar ratio of 56 : 1 and a catalyst loading of 0.17 kg L h^{-1}), the DMEA, TMEDA and EG yields amounted to 74%, 4% and 1%, respectively.[210] In their work, Liang *et al.* conducted the reductive amination of GA with aqueous NH_3, for 12 h at 75 °C, 3 MPa H_2, and an ATS molar ratio of 10 : 1. They achieved a 93% MEA yield by using a bifunctional 5 wt% Ru/ZrO_2 hydrogenation catalyst. The remarkable activity of the Ru/ZrO_2 catalyst stood out as Ru on other supports (*e.g.*, activated carbon, Al_2O_3, SiO_2) or other transition metals (*e.g.*, Pd, Pt, Ir) on ZrO_2 did not result in a comparably high yield. They reasoned that RuO_2 species act as Lewis acid sites, facilitating imine formation by activating the carbonyl group of GA, whereas the metallic Ru^0 species function as active hydrogenation sites to subsequently yield MEA.[203,232] In another patent by BASF, researchers developed a Co/MnO catalyst for the reductive amination of GA with NH_3 in THF. An 82% MEA yield was obtained by conducting the reaction for 8 h, at 100 °C, 8 MPa H_2, and an excessive ATS molar ratio of 35 : 1.[204] Both the work by Liang and the latter patent by BASF conducted the reductive amination with an excess of NH_3 reactant to limit overalkylation of the amine product.[203,204,232] Contrary, overalkylation does not occur when performing the reaction with secondary amines, which allows for the use of stoichiometric amounts of amine reactant.

Vermeeren *et al.* recently formulated a set of guidelines for the selective formation of ethylene polyamines from GA by investigating the reductive amination with various diamines such as *N*,*N*,*N*′-trimethylethylenediamine (TriMEDA).[215] In their work, the selectivity was shifted from the ethanolamine, obtainable in quantitative yields when employing the ethanolamine guidelines (*vide supra*), toward the ethylene polyamine product by three rational-design handles based on a profound understanding of the reaction network.[233] These handles were developed by demystifying the reaction network *via* intermediate analysis. The first hemi-aminal (Scheme 4, **I1**) and the unsaturated polyamine (Scheme 4, **I7**) were identified as the predominant intermediates in the studied reaction system. Each selectivity control strategy successfully contributed to the fast and selective reaction of **I1** to **I7**. The first handle consisted of kinetically and thermodynamically enhancing the dehydration reaction by smart solvent choice. Out of a comprehensive polar solvent screening, EG stood out as the solvent with the highest dehydration capacity. In the second handle, **I7** formation was favored over hydrogenation of **I3** and **I4** by physically separating in time the amination reactions and hydrogenation, employing a one-pot-two-step method. The third handle involved the use of trace amounts of a carboxylic acid catalyst, already present as natural impurities in crude GA, to increase both the rate of dehydration and keto–enol tautomerization. Integrating these three handle in one general selectivity control strategy yielded ethylene polyamine products exceeding a yield of 80%. For example, carrying out the reductive amination of GA with the diamine TriMEDA in a one-pot-two-step approach in EG, with an ATS molar ratio of 4 : 1, 10 mol% oxalic acid, and a 5 wt% Pd/C hydrogenation catalyst, yielded 82% of the ethylene polyamine *N*,*N*,*N*′,*N*′,*N*″,*N*″,*N*‴,*N*‴-hexamethyltriethylenetetramine (HMTriETA, Table 1 entry 21). The first, intermediate, step was performed for 1 h at 30 °C under an inert atmosphere, whereas the second, hydrogenation, step was performed for 1 h at 100 °C and 3 MPa H_2.[215] The work by Faveere *et al.*[199] and a patent by BASF[211] both support the different control handles of this guideline for selective ethylene polyamine formation. Faveere *et al.* obtained a 91% yield of the polyamine *N*,*N*,*N*′,*N*′-tetramethylethylenediamine (TMEDA, Table 1 entry 19) by performing the reductive amination of GA with DMA in a one-pot-two-step reaction in EG. Contrary to Vermeeren *et al.*, they performed the reaction with an ATS molar ratio of 12 : 1, for

5 h under an inert atmosphere during the intermediate step, and at an elevated temperature of 130 °C during the hydrogenation step.[199] In the BASF patent, carboxylic acids were used to shift the selectivity from the ethanolamine DMEA to the ethylene polyamine TMEDA. The reductive amination of GA with DMA was performed in THF, for 1 h, at 130 °C, 17.5 MPa, with a 64 wt% Ni/SiO_2 catalyst, and an ATS molar ratio of 2.8 : 1. Conducting the reaction in absence of lactic acid yielded 26% TMEDA and 76% DMEA, while the presence of 20 mol% lactic acid shifted the yields to 63% TMEDA and 23% DMEA.[211]

3.2.1.2. Ethylene glycol (EG). As the simplest symmetric diol, EG (Scheme 4, **S1**: $R_1 = R_2 = H$) is the ideal model component to study the hydrogen borrowing amination, *i.e.*, dehydrogenation followed by reductive amination. Notably, most of the research up to now has essentially been focused on the dehydrogenation reaction, which is regarded as the rate-determining step, and centered around the search for an optimal catalytic dehydrogenation–hydrogenation system.[234]

Already since the 1960s, multiple articles and patents have been published on the gas- and liquid-phase amination of EG.[235,236] For example in 1964, Moss *et al.* patented a Ni–Cu/Cr_2O_3 dehydrogenation–hydrogenation catalyst for the hydrogen borrowing amination of EG with aqueous NH_3 in a fixed bed reactor.[235] More recently, van Cauwenberge and co-workers patented a continuous two-step fixed bed process.[205] The first fixed bed contained a Ni–Cu–Mo/ZrO_2 dehydrogenation catalyst while the second bed was equipped with a Ru–Co/Al_2O_3 hydrogenation catalyst. The amination of EG with NH_3 was performed at 150 °C (first reactor) and 170 °C (second reactor), with a total H_2 pressure of 20 MPa, and an ATS molar ratio of 15 : 1. At an EG conversion of 43%, the product selectivity of EDA, MEA and PZ amounted to 50%, 29% and 7%, respectively.[205] In two related patents, Heidemann and Becker developed several dehydrogenation–hydrogenation catalysts containing at least one or a combination of the following metals: Co, Ru, Ni, Cu or Sn dispersed on a ZrO_2 or Al_2O_3 support.[206,207] The hydrogen borrowing amination of EG with NH_3 was tested in a fixed bed reactor at 150 °C, 17 MPa H_2, and an ATS molar ratio of 10 : 1. At an EG conversion of 35%, the selectivities toward EDA, MEA and PZ on average amounted to 50%, 30% and 10%, respectively.[206,207] Recently, An and co-workers quantitatively and qualitatively investigated the performance of various Co-based dehydrogenation–hydrogenation catalysts for the hydrogen borrowing amination of EG with aqueous NH_3.[208] They were able to ascribe the catalytic activity of these Co-based catalysts to the amount of acid and base sites of the different metal oxide catalyst supports as determined by NH_3- and CO_2-TPD. The catalytic activity (*i.e.*, EG conversion) significantly increased when the metal oxide support possessed sufficient acid–base amphoteric sites (*e.g.*, Al_2O_3, ZrO_2, MgO) in comparison with metal oxide supports with a reduced number of base sites (*e.g.*, SiO_2, TiO_2, Nb_2O_5). DFT calculations indicated that the base sites promote O–H bond cleavage in the substrate while the acid sites promote C–H bond cleavage, underlining the importance of this synergetic effect between acid–base sites. Co/Al_2O_3, as the most active catalyst, resulted in an EG conversion of 57% alongside an unselective formation of EDA (29% selectivity), MEA (25%) and PZ (23%). This optimized reaction was carried out with aqueous NH_3, for 12 h, at 175 °C, 3 MPa H_2, and an ATS molar ratio of 12 : 1.[208] In a supplementary study, An *et al.* evaluated different Co-based bimetallic dehydrogenation–hydrogenation catalytic systems.[209] Compared to Co/Al_2O_3, the presence of a second metal (*e.g.*, Cu, Ni, Ru or Pt) improved the activity and selectivity of the ethylene polyamine product. It was hypothesized that Co and the second metal could separately facilitate the dehydrogenation of EG and the subsequent reductive amination. In addition to the choice of the second metal, other preparation conditions, such as metal loading and calcination and reduction temperature, strongly affected the catalytic performance. The Co–Cu/Al_2O_3 catalytic system demonstrated the highest activity and selectivity as it led to an EG conversion of 42% and an EDA, MEA and PZ selectivity of 46%, 23% and 18%, respectively. The optimized reaction was conducted with aqueous NH_3, for 12 h, at 190 °C, 4 MPa H_2, and an ATS molar ratio of 5 : 1.[209]

To the best of our knowledge, only one research article qualitatively addresses the product selectivity challenge in the hydrogen borrowing amination of EG.[212] Runeberg *et al.* systematically screened four reaction conditions (*i.e.*, temperature, ATS molar ratio, H_2 pressure and addition of H_2O) and assessed their effect on the selectivity by monitoring both the ethanolamine and ethylene polyamine product as well as the unsaturated polyamine intermediate (Scheme 4, **I7**). Moreover, they related these conditions and corresponding results to the proposed reaction mechanism. Of all screened conditions, only the temperature had a significant, positive effect on EG conversion. The ATS molar ratio, H_2 pressure and presence of water all had no significant effect on EG conversion, suggesting that neither the amine nor H_2 nor H_2O are involved in the rate-determining step. This is in agreement with the general assumption that the dehydrogenation of EG is the rate-determining step. In contrast, these three reaction conditions did have a significant effect on product selectivity. Increasing the ATS molar ratio negatively affected the ethanolamine yield in favor of both the polyamine and **I7**. In the absence of H_2 pressure, the reaction favored **I7** formation. Increasing the H_2 pressure positively affected the yields of both the ethanolamine and polyamine at the expense of **I7**. Finally, the addition of H_2O to the reaction system steered the product selectivity in favor of the ethanolamine product.[212] All these findings unambiguously support the selectivity control handles that were applied in the guidelines for GA amination (*vide supra*).

3.2.1.3. Acetol. Acetol (Scheme 4, **S2**: $R_1 = H$, $R_2 = CH_3$) can be regarded as a potential model substrate for asymmetric α-hydroxy ketone substrates. As an asymmetric oxygenate, acetol possesses the ability to undergo an aldose–ketose isomerization reaction forming the α-hydroxy aldehyde 2-hydroxypropanal (lactaldehyde).[237,238] Interestingly, the amination of acetol or lactaldehyde would lead to the same α-propylene polyamine but

result in two different isomeric α-propanolamine products. To date, the reductive amination of acetol has gained limited research interest and has mainly been focused on the formation of the acetol-derived α-propanolamines.

In their patent, Cavitt and co-workers studied the formation of the α-propanolamine 2-amino-1-propanol (2A1P, Table 1 entry 10) by the reductive amination with aqueous NH_3 and a Ni–Cu/Cr_2O_3 hydrogenation catalyst.[221] They obtained a product yield of 51% by carrying out the reaction for 1 h, at 150 °C, 3.4 MPa H_2, and an ATS molar ratio of 4 : 1. Furthermore, they performed the reductive amination of acetol and isopropylamine both in H_2O and EtOH as the solvent. The reaction in EtOH significantly outperformed the reaction in H_2O as the corresponding α-propanolamine (*i.e.*, 2-isopropylamino-1-propanol, Table 1 entry 11) yield in EtOH and H_2O amounted to 64% and 33%, respectively. Both reactions were performed for 1 h, at 100 °C, 20.6 MPa H_2, and an ATS molar ratio of 4 : 1. Throughout the patent, no α-propylene polyamine or other amine products were reported.[221] Liang *et al.* reported a low 2A1P yield in the reductive amination of acetol with aqueous NH_3, although their $RuZrO_2$ catalyst was very selective toward the formation of MEA in the reductive amination of GA. Under optimized conditions (6 h, 65 °C, 3 MPa H_2, ATS molar ratio of 10 : 1), they achieved a 2A1P and 1,2-propylenediamine (1,2PDA, Table 1 entry 22) yield of 26% and 10%, respectively.[203] Recently, Boulos *et al.* studied the use of bimetallic Ru–Ni/C catalysts in the reductive amination of acetol with aqueous NH_3.[222] Compared to Ru/C (5 wt%), using a Ru–Ni/C (4.5 wt% Ru and Ni) enhanced the 2A1P yield from 37% to 52% at full acetol conversion under optimized reaction conditions (3 h, 65 °C, 6 MPa H_2, ATS molar ratio of 11 : 1). Next to 2A1P, this optimized reaction resulted in a 1,2PG yield of 28%.[222] In their granted patent, P&G reported a highly selective two-step reductive amination process for the production of 2A1P.[223] In the first step, aqueous NH_3 was dropwise added to a reactor containing acetol while stirring at room temperature for 90 minutes until an ATS molar ratio of 3 : 1 was obtained. In the second step, the reactor was loaded with a Ni oxide on kieselguhr hydrogenation catalyst, pressurized with H_2 to 15 MPa and heated to 85 °C. In this way, a 94% 2A1P yield was obtained after the reaction.[223] Trégner *et al.* studied the reductive amination of acetol to 2A1P in a gas-phase continuous fixed bed reactor with a Cu/Cr_2O_3 catalyst.[216] In the optimized reaction (WHSV = 0.078 h^{-1}, 210 °C, molar ratio of acetol : H_2 : NH_3 of 1 : 50 : 50) a 2A1P yield of 47% was obtained at full acetol conversion. In addition, they identified numerous by-products *via* GC-MS and proposed their corresponding reaction mechanism. Under these conditions, the major by-products were heterocyclic PZ-related and aromatic amines. Interestingly, they also reported trace amounts (~2% yield) of 1-amino-2-propanol (1A2P, Table 1 entry 7), the α-propanolamine product that originates from lactaldehyde, the isomer of acetol.[216] In line with their work on GA,[215] Vermeeren *et al.* recently used the same bottom-up methodology to qualitatively study the selectivity control challenge in the catalytic reductive amination of acetol with TriMEDA as the aminating agent.[220] This methodology, consisting of intermediate identification and control handle evaluation, ultimately resulted in three distinct control strategies targeting the two isomeric alkanolamines: *N*,*N*,*N*′-trimethyl-2-ethylenediamino-1-propanol (2TriMEDA1P, Table 1 entry 12) and *N*,*N*,*N*′-trimethyl-1-ethylenediamino-2-propanol (1TriMEDA2P, Table 1 entry 9), analogues to 2A1P and 1A2P, respectively, and the propylene polyamine product *N*,*N*,*N*′,*N*″,*N*‴,*N*‴′-hexamethyl-1,2-propylenebis(ethylenediamine) (1,2HMPBEDA, Table 1 entry 24). The first control strategy, targeting 2TriMEDA1P, encompassed catalyst selection, solvent choice and reaction temperature as the most influential control handles. After fine-tuning, this strategy obtained a product selectivity up to 75%. Notably, the two other strategies, targeting 1TriMEDA2P and 1,2HMPBEDA, harnessed the formation of a highly stable α-amino ketone intermediate, *N*,*N*,*N*′-trimethyl-1-diamino-2-propanone (1-TriMEDA-2-propanone, Table 1 entry 29) in a one-pot-two-step reaction configuration. In both strategies, the reaction temperature proved to be the crucial control handle in the first process step to achieve intermediate selectivities exceeding 90%. Subsequently in the second process step, product selectivity could be consciously steered toward 1TriMEDA2P or 1,2HMPBEDA by judicious hydrogenation catalyst selection. In this way, these two strategies resulted in excellent 1TriMEDA2P and 1,2HMPBEDA selectivity, amounting to 95% and 90%, respectively. These two one-pot-two-step strategies were successfully validated by expanding the reactant and substrate scope. As a proof of concept, the one-pot-two-step polyamine strategy could be modified to accommodate the formation of high-value asymmetric polyamines consisting of different vicinal amino groups. This proof of concept elucidated the importance of both the relative reactivity of the two amine reactants and the stability of the formed α-ketone intermediate.[220]

3.2.1.4. 1,2-Propylene glycol (1,2PG). The asymmetric α-diol 1,2PG (Scheme 4, **S1**: R_1 = CH_3, R_2 = H) has received limited research interest, despite its potential significance. In theory, the dehydrogenation of 1,2PG can yield acetol (α-hydroxy ketone) or lactaldehyde (α-hydroxy aldehyde). In practice, most research has still targeted the formation of the acetol-derived α-propanolamine. However, it can be noticed that in general the selectivity toward the lactaldehyde-derived α-propanolamine increases by using 1,2PG instead of acetol. Analogous to EG amination research, all 1,2PG hydrogen borrowing amination studies essentially focus on the development of a suitable dehydrogenation–hydrogenation catalytic system.

Takanashi *et al.* studied the hydrogen borrowing amination of 1,2PG with aqueous NH_3 in the presence of a 5 wt% Rh–In/C catalyst.[217] With this catalytic system under applied conditions (24 h, 180 °C, 5 MPa H_2, ATS molar ratio of 10 : 1), the two isomeric α-propanolamines, namely 2A1P (42% selectivity) and 1A2P (47%), were obtained as major products and dimethylpiperazine (DMPZ, Table 1 entry 27) (10%) as the by-product at a 1,2PG conversion of only 11%. The Rh/C catalyst, in the absence of In, was unable to convert 1,2PG while the combination of the individually supported metals, Rh/C and In/C, resulted in a reduced 1,2PG conversion of 6% with similar product distribution. They reasoned that the presence of In enhanced the resistance to catalyst deactivation during the

dehydrogenation step. By extending the reaction time from 24 h to 160 h with the Rh–In/C catalyst, the 1,2PG conversion increased to 38%. In addition, extending the reaction time had a significant effect on product selectivity. While the selectivity of 1A2P remained unchanged (42%), the selectivity of 2A1P decreased to 26% in favor of DMPZ (26%).[217] Niemeier *et al.* investigated Ru/C as an effective catalytic system in hydrogen borrowing amination of various alcohols. Although the catalyst was active for some alcohol substrates, only a 1,2PG conversion of 10% was obtained by performing the reaction with aqueous NH_3 for 6 h, at 170 °C, 1 MPa H_2, and an ATS molar ratio of 10 : 1. No distinctive product analysis was performed.[239] Yue *et al.* evaluated the activity and selectivity of various Co-based dehydrogenation–hydrogenation catalysts in the hydrogen borrowing amination of 1,2PG with aqueous NH_3.[218] Next to the formation of the acetol-derived α-propanolamine 2A1P, they also monitored the formation of the lactaldehyde-derived α-propanolamine 1A2P and the diamine 1,2PDA. During the initial catalyst screening (6 h, 160 °C, N_2 atmosphere, ATS molar ratio of 9 : 1), three catalysts displayed promising activity. Co/Al_2O_3, Co/La_3O_4 and Co/Nb_2O_5 achieved 1,2PG conversions of 50%, 40% and 38%, respectively. Although Co/Al_2O_3 exhibited the highest activity, its selectivity toward 2A1P (54%) was moderate, while 1A2P (21%) and 1,2PDA (13%) were also formed at lower selectivities. In contrast, Co/Nb_2O_5 demonstrated comparable selectivities toward both α-propanolamine isomers 2A1P (40%) and 1A2P (36%), with a minor formation of 1,2PDA (14%). Notably, Co/La_3O_4 exhibited a high selectivity toward 2A1P (75%), with significantly lower selectivities toward 1A2P (18%) and 1,2PDA (3%). After finetuning the Co/La molar ratio, the 2A1P selectivity reached an optimum at 89%, together with a 1A2P selectivity of 9%, at a 1,2PG conversion of 69%. No further efforts were made to elucidate the role of the support in these selectivity differences. Without additional experimental insights, it is impossible to pinpoint if this support-induced selectivity was established during the initial dehydrogenation or later in the isomerization step.[218] A highly selective and quantitative two-step 1,2PG hydrogen borrowing amination process was patented by Shujie and co-workers.[219] In contrast to other research, this process targeted the formation of the lactaldehyde-derived α-propanolamine 1A2P. In the first step, a $Cu–Pd–Bi_2O_3–In_2O_3/Al_2O_3$ catalyst was used to selectively dehydrogenate 1,2PG into lactaldehyde. In the second step, the formed lactaldehyde subsequently underwent reductive amination into the corresponding 1A2P product in the presence of a $Ni–V_2O_5–Y_2O_3/Al_2O_3$ hydrogenation catalyst. Under optimized first-step reaction conditions (SV = 2 L h^{-1} L_{cat}^{-1}, 180 °C), 1,2PG was fully converted into lactaldehyde. Under optimized second-step reaction conditions (SV = 6 L h^{-1} L_{cat}^{-1}, 200 °C, H_2 : lactaldehyde molar ratio of 2 : 1, ATS molar ratio of 3 : 1), lactaldehyde, in its turn, was fully converted into 1A2P. Furthermore, the role of each metal oxide present in both catalysts was clarified through a series of comparative experiments. In the dehydrogenation catalyst, Cu was identified as the primary active site responsible for the dehydrogenation capacity, whereas Pd enhanced the catalyst activity. Additionally, the presence of Bi_2O_3 and In_2O_3 positively affected the selectivity toward lactaldehyde. In the hydrogenation catalyst, Ni contained the hydrogenation capacity while the presence of the metal oxides V_2O_5 and Y_2O_3 beneficially increased the selectivity toward 1A2P.[219]

3.2.2. O3 substrates. The complexity of the overall reaction builds up when working with **O3** substrates. Unlike **O2** substrates, which can undergo two pre-amination reactions (*i.e.*, (de)hydrogenation and isomerization), **O3** substrates have the potential to undergo all four elementary reactions (*i.e.*, (de)hydrogenation, isomerization, retro-aldol condensation and dehydration) prior to amination (Scheme 5). Afterward, the amination follows the general reductive amination mechanism as depicted in Scheme 4. Three **O3** substrates have been studied in the literature: (i) the α-hydroxy aldehyde glyceraldehyde, (ii) the α-hydroxy ketone 1,3-dihydroxyacetone (DHA), and (iii) the α-triol glycerol. Most research has been focused on the amination of glycerol due to its abundance and stability.

3.2.2.1. Glyceraldehyde. In theory, four different amination routes are possible from the α-hydroxy aldehyde glyceraldehyde (Scheme 5). The first route involves the direct reductive amination of glyceraldehyde's available carbonyl group, leading to a product containing one up to three amino groups (Scheme 5, route A). In the second route, glyceraldehyde isomerizes to DHA which can subsequently undergo reductive amination (Scheme 5, route B). In the third and fourth routes, amination is preceded by a cleavage reaction; dehydration (Scheme 5, route C) and retro-aldol condensation (Scheme 5, route D), respectively. Dehydration of glyceraldehyde yields pyruvaldehyde and acetol, whereas retro-aldol condensation leads to GA, which are all suitable amination substrates (*vide supra*). To date, research efforts concerning the reductive amination of glyceraldehyde have been limited.

Two authors have targeted the first route (Scheme 5, route A), namely the direct reductive amination of glyceraldehyde. In addition to GA and acetol, Liang *et al.* also explored glyceraldehyde as a substrate to assess the effectiveness of their Ru/ZrO_2 reductive amination catalyst. In an optimized one-step reaction with aqueous NH_3 (6 h, 55 °C, 2 MPa H_2, ATS molar ratio of 10 : 1), they reported a yield of 82% for the diolamine 3-amino-1,2-propylene glycol (3A1,2PG, Table 1 entry 14).[203] A patent by Merck outlined a two-step reductive amination process for the selective formation of 3A1,2PG.[224] In the first step, aqueous NH_3 is gradually added to an aqueous glyceraldehyde solution at a reduced temperature (20 °C) under continuous stirring for 1 h until an ATS molar ratio of 2.8 : 1 is obtained. In the second step, hydrogenation conditions are introduced (6.5 MPa H_2, 10 wt% Pd/C hydrogenation catalyst) and the reaction is further conducted at 50 °C for an additional 40 minutes, resulting in a notable 95% yield of 3A1,2PG.[224]

In the context of their glucose amination research (*vide infra*), Pelckmans *et al.* extended the substrate scope in one experiment to glyceraldehyde.[213] Noteworthy, this experiment solely focused on the amine products obtained *via* both cleavage routes (Scheme 5, routes C–D). They performed the

reductive amination of glyceraldehyde with DMA and a commercial Ni oxide catalyst (Ni-6458P, Engelhard) in MeOH, for 1 h, at an elevated temperature (130 °C), 8.5 MPa H_2, and an ATS molar ratio of 8 : 1. Under these conditions, product yields indicated that dehydration (Scheme 5, route C) was more prominent than cleavage *via* retro-aldol condensation (Scheme 5, route D). The dehydration-derived amination products, including the diamine *N*,*N*,*N*′,*N*′-tetramethyl-1,2-propylenediamine (1,2TMPDA, Table 1 entry 23), the α-propanolamine *N*,*N*-dimethyl-1-amino-2-propanol (1DMA2P, Table 1 entry 8), and the amino ketone intermediate (Scheme 4, **I4**) *N*,*N*-dimethyl-1-amino-2-propanone (1DMA-2-propanone, Table 1 entry 28), were formed in yields of 6%, 14%, and 8%, respectively. The formation of 1DMA2P and 1DMA-2-propanone illustrate the selectivity preference of the amine reactant to perform the nucleophilic addition at the aldehyde carbon of pyruvaldehyde rather than at its ketone carbon. The retro-aldol-derived products, namely the diamine TMEDA and the ethanolamine DMEA, were formed in trace amounts, with yields of 5% and 1%, respectively.[213]

3.2.2.2. 1,3-Dihydroxyacetone (DHA). The **O3** α-hydroxy ketone DHA can potentially undergo two amination routes. DHA can undergo direct reductive amination at its carbonyl group (Scheme 5, route A), or it can first isomerize to glyceraldehyde before proceeding with its corresponding amination routes (Scheme 5, route B). The first route has been targeted in the scarce literature available.

Complementary to the two-step process for glyceraldehyde reductive amination, the patent by Merck likewise reported a two-step process for DHA reductive amination under similar conditions.[224] In the first step, aqueous NH_3 was gradually added to a MeOH solution containing DHA at 20 °C until an ATS molar ratio of 2.8 : 1 was obtained. Hydrogenation conditions (10 MPa H_2, RANEY® Ni hydrogenation catalyst) were introduced in the second step and the reaction was performed at 70 °C for an additional 40 minutes. The diethanolamine 2-amino-1,3-propylene glycol/serinol (2A1,3PG, Table 1 entry 13) was formed in a quantitative yield of 99%.[224] In another patent, Hegde and co-workers performed the same reaction using a one-step process.[225] During a period of 3 h, a DHA–MeOH mixture was gradually added to the reaction mixture containing aqueous NH_3 and RANEY® Ni, operating at 65 °C and 1.7 MPa H_2, until an ATS molar ratio of 10 : 1 was achieved. The reaction was then prolonged for an additional 3 h. This one-step approach resulted in an excellent 2A1,3PG yield of 91% with the overalkylated bis adduct as a minor by-product (7%).[225]

3.2.2.3. Glycerol. As an α-triol substrate, glycerol requires an activation step before amination can occur. In this regard, two distinctive activation routes can be applied. In the first route, glycerol is dehydrogenated to form its corresponding aldehyde (*i.e.*, glyceraldehyde) or ketone (*i.e.*, DHA) substrate, similar to **O2** diol activation. In the second route, glycerol is activated *via* dehydration, leading to the formation of acetol (Scheme 5, route E) or 3-hydroxypropanal (Scheme 5, route F). Both routes have been explored as viable amination strategies in the literature.

In the first activation strategy, glycerol is dehydrogenated into glyceraldehyde/DHA in the presence of a dehydrogenation catalyst. To promote the initial dehydrogenation step, this strategy is typically carried out at elevated temperatures which additionally also favor cleavage reactions such as retro-aldol condensation and dehydration. Therefore, although glyceraldehyde and DHA are susceptible to undergo reductive amination

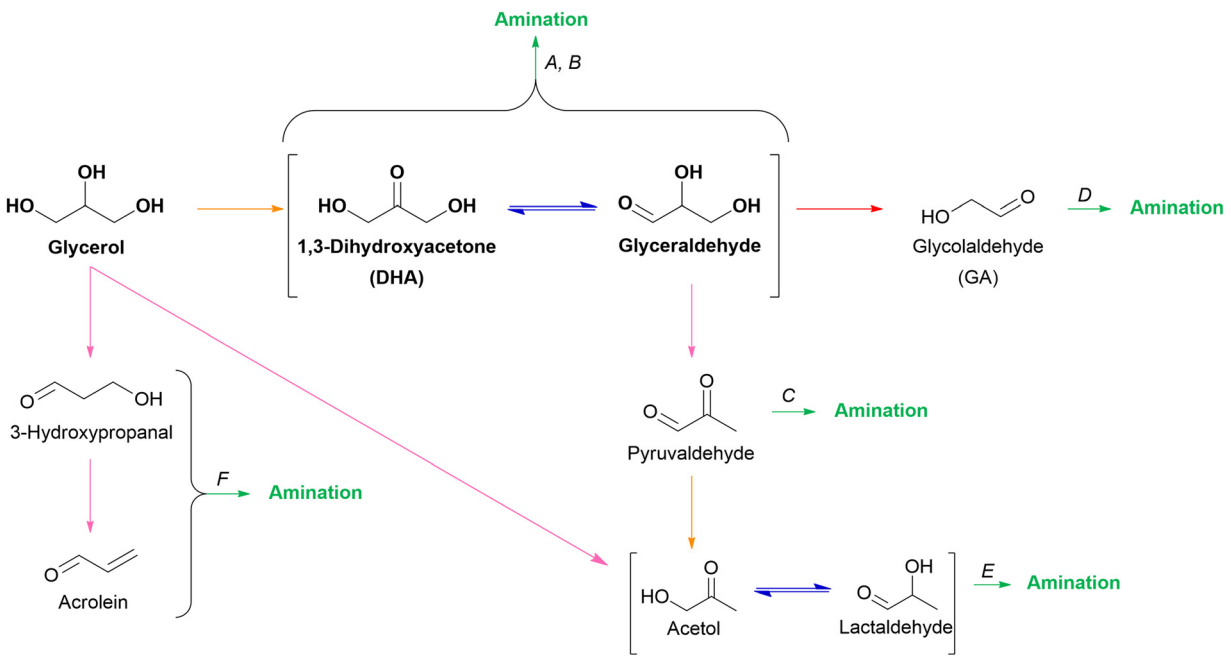

Scheme 5 Overview of different pre-amination pathways in **O3** oxygenate reductive amination. Each elementary step is represented by a color: amination (green), isomerization (blue), retro-aldol condensation (red), dehydration (pink) and (de)hydrogenation (orange).

(*vide supra*), most of the formed amine products *via* this strategy are obtained by the amination of smaller oxygenates such as GA and pyruvaldehyde/acetol. In a patent by BASF, Ernst *et al.* performed the hydrogen borrowing amination of glycerol with aqueous NH_3 in the presence of a number of dehydrogenation–hydrogenation catalysts (*e.g.*, RANEY® Ni, RANEY® Co, Cu–Ni–Co/ZrO_2).[226] At standardized conditions (200 °C, 2 MPa H_2 while heating and 20 MPa H_2 when attaining the desired reaction temperature, and an ATS molar ratio of 32 : 1) resulting in full glycerol conversion, the amination reactions led to a plethora of amine products. On the one hand, they monitored **O3**-derived amines such as the propanoldiamine 1,2-diamino-3-propanol (1,2DA3P, Table 1 entry 15) and the triamine 1,2,3-propylenetriamine (PTriA, Table 1 entry 25). On the other hand, they also observed **O2**-derived amines such as EDA, 1,2PDA and three PZ derivatives. In general, all tested catalytic systems favored the formation of PZ and its derivatives at the expense of the other amine products. For example, the reaction in the presence of a commercial RANEY® Ni catalyst resulted in three major products after 36 h: 1,2DA3P at a 21% yield, 1,2PDA at 22%, and the PZ derivatives at 26%. By extending the reaction time to 48 h, the yield of the PZ derivatives increased to 59% at the expense of 1,2DA3P and 1,2PDA.[226] In a similar concept, Du *et al.* studied the reductive amination of glycerol with aqueous NH_3 in the presence of 5 wt% Ru/C as the dehydrogenation–hydrogenation catalyst.[240] However, the main objective of this research was not to form **O3**- and **O2**-derived amines, but rather simple alkylamines such as MMA, *N*-monoethylamine and *N*-monopropylamine. In their proposed reaction mechanism, these alkylamines result from excessive hydrogenation and dehydration of initially formed **O3** and **O2** substrates and amines. As a consequence, these harsh reaction conditions additionally led to undesirable glycerol hydrogenolysis products such as 1,2PG, EG and MeOH. Under optimized conditions (48 h, 200 °C, 10 MPa H_2, and an ATS molar ratio of 6 : 1), the selectivity toward these alkylamines, PZ derivates and hydrogenolysis products were 51%, 8% and 19%, respectively, at full glycerol conversion.[240]

In the second activation strategy, glycerol is dehydrated into either acetol or 3-hydroxypropanal, which can subsequently undergo amination. In a study conducted by Safariamin *et al.*, the dehydrative amination of glycerol was carried out using DMA as the reactant in a fixed bed reactor equipped with a silica-supported heteropolyacid catalyst ($Cs_{2.5}H_{0.5}PMo_{12}O_{40}$).[230] This research primarily targeted the amino ketone components (Scheme 4, **I4**) derived from acetol and 3-hydroxypropanal, as the catalyst lacked any inherent hydrogenation capacity. The experimental results, however, demonstrated only the occurrence of 1DMA-2-propanone, the α-amino ketone derived from the acetol-isomer lactaldehyde. These findings suggest that the catalyst, under applied conditions, facilitated both the selective dehydration of the primary hydroxyl groups of glycerol and the isomerization of acetol to lactaldehyde. Under optimized conditions (reactant flow of 10 L h^{-1}, 250 °C, and an ATS molar ratio of 1.5 : 1) a 1DMA-2-propanone selectivity of 70% was achieved at a glycerol conversion of 47%.[230] Ding *et al.* further optimized this strategy and elaborated on the mechanism as they explored the same reaction with two different Zr-MCM-41-supported heteropolyacid catalysts (*i.e.*, $H_3PW_{12}O_{40}$ and $H_6P_2W_{18}O_{62}$).[231] Next to 1DMA-2-propanone, the reaction also produced *N*,*N*-dimethyl-1-amino-3-propanone (1DMA-3-propanone, Table 1 entry 30), the β-amino ketone derived from 3-hydroxypropanal. Based on the presence of trace amounts of acrolein, the researchers proposed an alternative mechanism for the formation of 1DMA-3-propanone. According to this pathway, glycerol undergoes two consecutive dehydration reactions resulting in acrolein. Subsequently, acrolein preferentially undergoes hydroamination at its unsaturated carbon site rather than amine addition at its carbonyl group, yielding 1DMA-3-propanone. Under optimized reaction conditions (GHSV = 3 h^{-1}, 300 °C, ATS molar ratio of 2.5 : 1, full glycerol conversion), both heteropolyacid catalysts favored the formation of 1DMA-3-propanone over 1DMA-2-propanone. In the dehydrative amination catalyzed by the heteropolyacid $H_3PW_{12}O_{40}$, the selectivities of 1DMA-3-propanone and 1DMA-2-propanone were 62% and 33%, respectively. The use of the heteropolyacid $H_6P_2W_{18}O_{62}$ additionally enhanced the product distribution in favor of 1DMA-3-propanone. In this reaction, the selectivities of 1DMA-3-propanone and 1DMA-2-propanone reached 81% and 11%, respectively. Ding *et al.* related this difference in selectivity to the relative amount of Brønsted acid sites in both catalysts. Glycerol, so they postulated, would preferentially be dehydrated into 3-hydroxypropanal on Brønsted acid sites, whereas glycerol dehydration would favorably produce acetol on Lewis acid sites. In accordance with this hypothesis, the heteropolyacid with relatively more Brønsted acid sites resulted in a higher selectivity toward 1DMA-3-propanone.[231] Dai *et al.* reported a glycerol amination process that seems to balance between the two activation strategies.[241] In this process, glycerol is reacted with morpholine into the α-amino ketone component 1-morpholine-2-propanone (Scheme 4, **I4**) using a Cu–Ni/AlO_x catalyst in the presence of K_2CO_3. Although the authors provided no mechanistic insights, the formation of the amino ketone product indicates that glycerol has undergone dehydrative C–C cleavage during the reaction, directly or after dehydrogenation into glyceraldehyde. The presence of both the heterogeneous Cu–Ni/AlO_x catalyst and the inorganic base K_2CO_3 were required to obtain excellent activity and selectivity. At a morpholine conversion of 91%, a quantitative selectivity of 99% was achieved by conducting the reaction in 1,4-dioxane for 12 h, at 150 °C, under an Ar atmosphere, and a sub-stoichiometric ATS ratio of 0.2 : 1. Performing the same reaction in absence of K_2CO_3 reduced both the conversion and selectivity to 80% and 41%, respectively.[241]

3.2.3. O5-6 substrates. **O5** and **O6** substrates, the monomeric building blocks of polysaccharides, can also serve as amination substrates. Similar to **O3** substrates, these monomers can undergo direct amination resulting in amino sugar alcohols or yield shorter amine products resulting from C–C bond cleavage. Within the scope of (hemi)cellulose valorization, xylose and glucose are the prevailing **O5** and **O6**

monomers, respectively. However, scientific interest has predominantly centered around glucose.

The direct reductive amination of glucose, resulting in glucamine-based products, has been studied throughout time.[242,243] In 1940, Wayne and Adkins reported the straightforward formation of glucamine (Table 1 entry 16) from glucose with a NH_3–MeOH solution in the presence of a RANEY® Ni hydrogenation catalyst.[227] An isolated glucamine yield of 26% was obtained when conducting the reaction for 1 h, at 100 °C, 15 MPa H_2, and an ATS molar ratio of 5 : 1. They attributed this poor yield to the purification step as they commented that the difficulty in obtaining glucamine was not in the amination reaction but solely in the isolation of the product.[227] Recently, Seddig *et al.* obtained a *N*,*N*-diethylglucamine (DEGA, Table 1 entry 17) yield of 95% in the reductive amination of glucose with *N*,*N*-diethylamine.[228] This excellent yield was obtained by performing the reaction in MeOH for 18 h, at 45 °C, 9 MPa H_2, an ATS molar ratio of 3 : 1, and a 5 wt% Ru/C hydrogenation catalyst. Carrying out the reaction in H_2O instead of MeOH drastically slowed down the reaction and additionally led to a significantly diminished DEGA yield of 35%.[228]

The other approach, referred to as reductive aminolysis in the literature, involves the formation of shorter aliphatic amine products. BASF has patented an aminolysis process that applies to both sorbitol and glucose.[229] By employing a dehydrogenation–hydrogenation catalyst (*e.g.*, RANEY® Ni, Cu–Ni–Co/ZrO_2) and aqueous NH_3, the substrates were converted into the diamines EDA and 1,2PDA, as well as various heterocyclic PZ-related amines. Under tested conditions (32 h, 200 °C, 20 MPa, and an ATS molar ratio of 32 : 1) and full glucose conversion, the amination of glucose catalyzed by RANEY® Ni resulted in equivalent yields of EDA and 1,2PDA, 15% and 13%, respectively, alongside a cumulative yield of 23% for the PZ-derivatives. The same reaction conducted with sorbitol yielded a similar product distribution, with yields of EDA, 1,2PDA and PZ-derivatives amounting to 8%, 12% and 20%, respectively.[229] In their work, Boulos *et al.* expanded the substrate scope from acetol to fructose.[222] They explored the reductive aminolysis of fructose with aqueous NH_3 using a bimetallic Ru–W_2C/C (7.5 wt% Ru and 36 wt% W_2C). Under tested reaction conditions (3 h, 180 °C, 7.5 MPa H_2, an ATS molar ratio of 80 : 1) full fructose conversion yielded a wide range of amine and oxygenate products in trace amounts: MEA (5%), EDA (1%), 2A1P (1%), 1,2PDA (1%), EG (1%), and 1,2PG (1%).[222] The fundamental mechanistic insights of this aminolysis reaction were clarified by Pelckmans and co-workers (Scheme 6).[213,214,244,245] They reasoned that the retro-aldol C–C scissions in the substrate are induced by the amine reactant itself, mimicking the

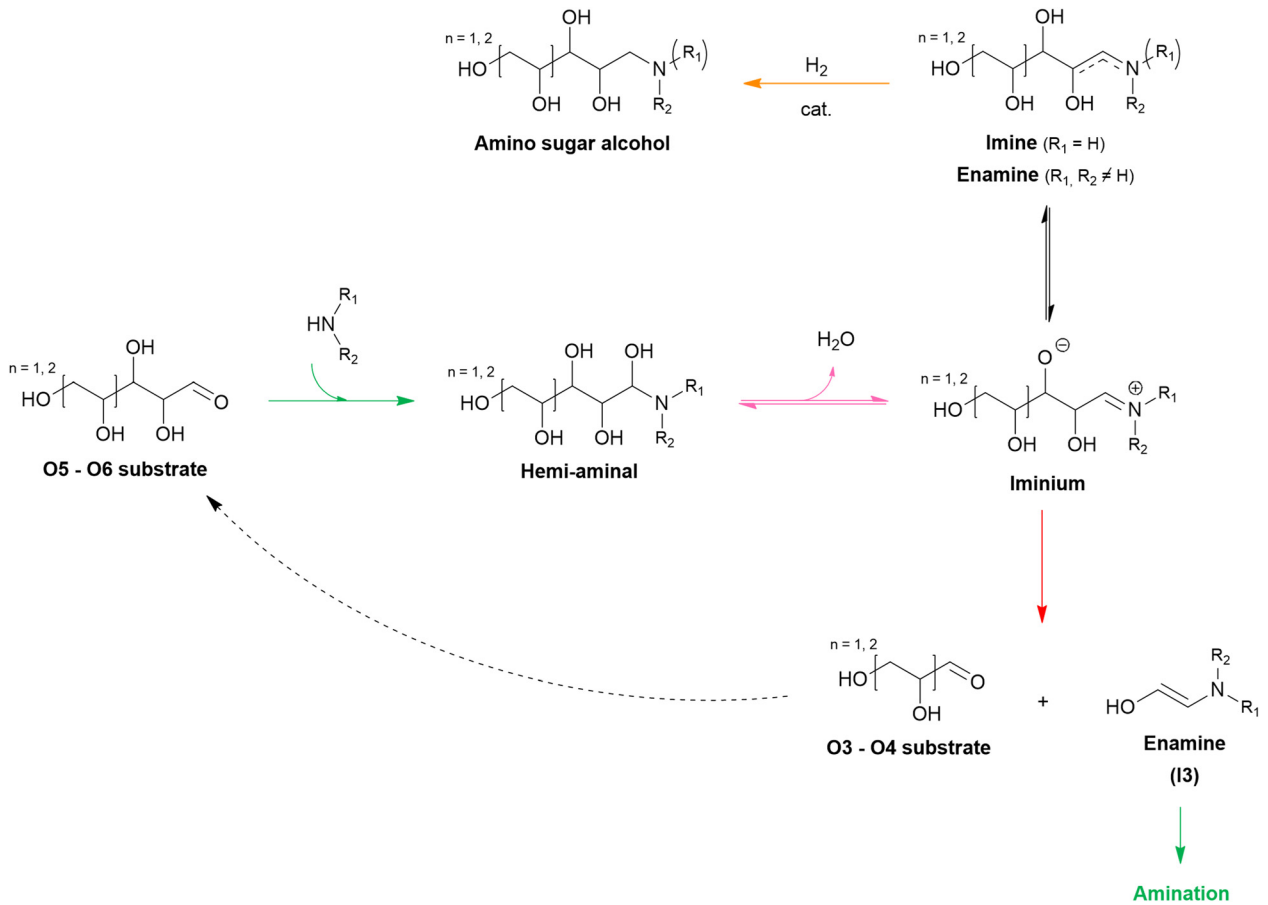

Scheme 6 General reaction mechanism of the reductive amination of **O5** and **O6** substrates. Each elementary key reaction is represented by a color: amination (green), retro-aldol condensation (red), dehydration (pink) and (de)hydrogenation (orange).

mechanism of (retro-)aldolase enzymes. To start, the amine reactant performs a nucleophilic attack on the carbonyl of the substrate, forming a zwitterionic iminium intermediate through dehydration. Subsequently, two distinct reaction pathways can occur. On the one hand, this iminium intermediate can undergo intramolecular proton transfer, yielding an amino sugar alcohol product upon hydrogenation of the imine/enamine intermediate. On the other hand, this iminium intermediate can undergo amine-facilitated retro-aldol condensation, forming a C2-enamine intermediate and a smaller α-hydroxy carbonyl. The latter component can re-enter the reaction as a substrate, whereas the C2-enamine proceeds *via* the established **O2** amination reaction pathway (Scheme 4), resulting in an ethanolamine or ethylene polyamine product. The proposed pathway was verified *via* theoretical DFT calculations and supported by experimental data. For example, carbohydrate hydrogenolysis was experimentally excluded as a cause of C–C scission as sorbitol was not converted under applied reaction conditions.[213,244] Advantageously, the amine-facilitated retro-aldol condensation can be carried out at temperatures significantly lower than the typical retro-aldol temperatures of around 200 °C. As a result, this approach mitigates numerous temperature-induced side reactions. Notably, besides the formation of these retro-aldol-derived C2 amines, so-called C3 amines, such as the diamine 1,2TMPDA and the α-propanolamine 1DMA2P, were also observed. Based on their structure, these C3 amines essentially originate from the amination of pyruvaldehyde or acetol species that can be formed *in situ via* the retro-aldol condensation of fructose or xylose (as depicted in Scheme 1). Although the reaction mechanism remains unclear, the authors still provided some preliminary findings. In theory, glucose–fructose isomerization prior to amination could be a major pathway. However, the reductive aminolysis of glucose and fructose led to the same product distribution of C2 and C3 amines, indicating that fructose is not the main precursor of the C3 amines. Approximately 75% of formed aliphatic amines were C2 amines when using both substrates under reductive aminolysis conditions (1 h, 130 °C, 7.5 MPa H_2, Ru/C hydrogenation catalyst, aqueous DMA, ATS molar ratio of 12 : 1). Alternatively, the reductive aminolysis of xylose did result in a 50–50 distribution of C_2 and C_3 amines, which strongly relates with its retro-aldol product distribution. Noteworthy, diamines were preferentially formed over alkanolamines in both C2 and C3 amines for each substrate. This phenomenon is most likely attributed to the retro-aldol requirements, such as an elevated reaction temperature and a high ATS molar ratio.[214] Furthermore, the choice of solvent significantly affected the product yields and selectivity. Using MeOH instead of H_2O as the solvent enhanced the total yield of all amine products and steered the selectivity more in favor of C2 amines relative to C3 amines. All these insights were combined in an optimization experiment (1 h, 130 °C, 8.5 MPa H_2, commercial Ni oxide hydrogenation catalyst, 2 M DMA MeOH solution, ATS molar ratio of 8 : 1), yielding 66% of the C2 diamine TMEDA and minor amounts of the C_3 diamine 1,2TMPDA (7%), the C_2 ethanolamine DMEA (4%) and the C3 α-propanolamine 1DMA2P (5%). Additionally, the solvent-free reductive amination of glucose with MMEA, serving both as amine reactant and solvent, (2 h, 130 °C, 8.5 MPa H2, commercial Ni oxide hydrogenation catalyst) yielded a remarkable 84% product yield of the C2 polyamine *N*,*N*′-bis(2-hydroxyethyl)-*N*,*N*′-dimethylethylenediamine (BHEDMEDA, Table 1 entry 20). This notably high yield was attributed to the formation of a stable, cyclic C2-enamine adduct, namely a heterocyclic 5-membered oxazolidinic compound, favoring the subsequent formation of BHEDMEDA through hydrogenation.[213]

3.2.4. Cellulose. Only two research groups have attempted the two-step conversion of cellulose into aliphatic amines. Both studies similarly focused on converting cellulose into an **O2** hydroxy carbonyl substrate using a tungsten-based catalyst followed by reductive amination. Liang *et al.* conducted cellulose valorization using H_2WO_4 in hot water (290 °C) for 60 s, targeting GA formation. After purification a GA yield of 21% was achieved. Reductive amination of the recovered GA with aqueous NH_3 using a Ru/ZrO_2 catalysts yielded 52% MEA (12 h, 75 °C, 3 MPa H_2, ATS molar ratio of 3.5 : 1).[203] The overall yield, from cellulose to MEA, amounted to 10%. Boulos *et al.* performed cellulose valorization with 30 wt% W_2C/C in hot water (235 °C) for 30 minutes and 4 MPa H_2, targeting acetol formation. An acetol yield of 12% was obtained after purification. Reductive amination of this recovered acetol with aqueous NH_3 using a Ru–W_2C/C (7.5 wt% Ru and 36 wt% W_2C) catalyst yielded 18% 2A1P, resulting in an overall yield, from cellulose to 2A1P, of 2%.[222]

4. From bio-based aliphatic amines to sustainable applications

Aliphatic amines are omnipresent in a plethora of applications due to their reactivity and structural diversity. This is illustrated by considering three diverse domains in which aliphatic amines play a pivotal role as a catalyst or an active component. These three domains cover all different types of aliphatic amines as they each require distinct functional features of the amine in question. The three domains include (i) CO_2-reactive applications, (ii) polymerization, and (iii) quaternary ammonium compounds.

4.1. CO_2-reactive applications

4.1.1. Carbon capture, utilization and/or storage (CCUS)

4.1.1.1. Introduction. The ever-rising importance of fossil fuels as an energy and chemical resource has led to a substantial increase in atmospheric CO_2 concentration from below 300 ppm to above 400 ppm since the industrial revolution. The increase in atmospheric CO_2 has been causing global greenhouse effects, which destabilize the climate and contribute to climate change and global warming.[246] In the context of long-term climate change mitigation, a shift towards non-fossil alternatives, such as biomass, solar and wind energy, presents a promising strategy to reduce CO_2 emissions. However, during this transition, the primary focus remains on curbing

anthropogenic CO_2 emissions in the existing fossil-based industries. In this regard, the concept of carbon capture, utilization and/or storage (CCUS) has gained extensive research interest.[247,248] A wide range of technologies has been studied to perform CO_2 capture, *i.e.*, the initial step in CCUS, to remove CO_2 from a gaseous stream such as flue gas. Among these, the post-combustion CO_2 capture process utilizing aqueous (alkanol)amine solvents as CO_2 absorbents has emerged as a prominent and well-established industrial-scale technology.[249,250]

This chemical absorption process involves the reversible, temperature-dependent reaction of CO_2 with an aqueous amine solution. In a typical set-up, a CO_2-rich gas stream is pumped through an absorption column where CO_2 reacts with an aqueous amine solution at temperatures around 30–60 °C and atmospheric pressure, generating a CO_2-lean gas stream and a CO_2-rich amine solution. Subsequently, the CO_2-rich amine solution is sent to a desorption column where CO_2 is released from the amine absorbent upon heating, typically by steam. This regeneration step is usually carried out around 120–140 °C and results in a concentrated CO_2 stream and a lean amine solution that can be recycled back to the absorption unit for a new absorption–desorption cycle.[250] The mechanism of CO_2 absorption is influenced by the type of amine. Primary and secondary amines following a zwitterion mechanism, forming a carbamate and a protonated amine upon reacting with CO_2. Stoichiometrically, one CO_2 molecule reacts with two amine molecules, yielding a maximum CO_2 loading of 0.5 mol CO_2/mol amine:

$$CO_2 + 2R_1R_2NH \rightleftharpoons R_1R_2NCOO^- + R_1R_2NH_2^+$$

On the other hand, tertiary amines, which lack a nucleophilic proton, function as base catalysts, resulting in the formation of bicarbonate through CO_2 hydration. Consequently, the theoretical maximum CO_2 loading of tertiary amines is 1 mol CO_2/mol amine:

$$CO_2 + H_2O + R_1R_2R_3N \rightleftharpoons HCO_3^- + R_1R_2R_3NH^+$$

From a kinetic point of view, primary and secondary amines generally demonstrate significantly higher CO_2 absorption rates (*i.e.*, one or two orders of magnitude higher) compared to tertiary amines. Thermodynamically, carbamates are more stable compounds than bicarbonate, leading to higher heat of reaction values for primary and secondary amines than tertiary amines. Therefore, tertiary amines are more readily regenerated than primary and secondary amines. Another important parameter to evaluate the performance of an amine absorbent is the cyclic capacity. It is defined as the difference between the CO_2 concentration in the rich and lean amine solution and thus combines the CO_2 loading and heat of reaction of the amine absorbent. The cyclic capacity is characteristic for a specific amine absorbent but also strongly depends on reaction conditions such as gas flow. Additionally, an ideal amine absorbent should also be resistant to degradation, non-volatile, non-toxic, non-corrosive, cheap, sustainable, and maintain low viscosity; properties which are not always taken into account.[249,251]

Aqueous solutions containing 20–30 wt% MEA and MDEA have been established as benchmark absorbents for primary/secondary and tertiary amines, respectively. These two reference solutions illustrate the tradeoff between fast absorption kinetics and ease of regeneration. The primary amine MEA readily absorbs CO_2, however, CO_2 desorption requires a substantial amount of energy. On the other hand, CO_2 absorption proceeds slower with the tertiary amine MDEA, but less energy is required to desorb CO_2.[250,252] In the literature, various strategies have been investigated to address this tradeoff, aiming to reduce the energy required for CO_2 desorption while maintaining favorable absorption kinetics. These strategies focus either on the reactor configuration,[253] the use of a catalyst[254,255] or the amine absorbent. In general, the latter strategy is approached by developing either new effective aqueous amine absorbents or so-called water-lean amine solutions. Both approaches will be discussed in more detail in following subsections.

4.1.1.2. Novel aqueous amine absorbents. The search for new aqueous amine absorbents should target the specific shortcoming of each type of amine without compromising its beneficial properties (Fig. 3). The high energy requirements in CO_2 desorption, the bottleneck for primary and secondary amine, can be addressed by two approaches. First, the energy requirements can be reduced by using amines with a lower heat of reaction than MEA. When reacting with CO_2, sterically hindered primary/secondary amines will form less stable carbamate species which correspond to a lower heat of reaction. The sterically hindered primary amine, 2-amino-2-methyl-1-propanol (AMP), has been studied by multiple researchers as a suitable alternative for MEA.[251,256] The heat of reaction of AMP ($\Delta H = -80$ kJ mol^{-1} CO_2) was experimentally verified to be lower than that of MEA ($\Delta H = -85$ kJ mol^{-1} CO_2).[257,258] Furthermore, stability studies indicated that AMP is more resistant to thermal and oxidative degradation than MEA.[259,260] In addition to AMP, other sterically hindered primary/secondary amines have been investigated as potential CO_2 absorbents based on their heat of reaction. In a study conducted by Chowdhury and co-workers, *N*-monoisopropylethanolamine (MiPEA) emerged as a favorable absorbent compared to MEA and other hindered amines due to its reduced heat of reaction (-64 kJ mol^{-1} CO_2) combined with a comparable absorption rate to that of MEA.[257] Other promising sterically hindered amines were observed in the research by El Hadri *et al.* The amines of interest, namely *N*-monomethylethanolamine (MMEA) and *N*-monoethylethanolamine (MEEA), exhibited similar kinetics as MEA in addition to a reduced heat of reaction of -74 kJ mol^{-1} CO_2 and -69 kJ mol^{-1} CO_2, respectively.[258] Second, the energy requirements of the desorption step can be reduced by enhancing the cyclic capacity of the amine absorbent as less solvent is required to react with a given amount of CO_2. In this regard, polyamines are a potentially interesting group of amines as, in theory, each nitrogen atom in the absorbent can react with CO_2. Singh *et al.* systematically assessed the effect of the number of functional groups in the absorbent on the CO_2 loading and the cyclic capacity. The tested polyamines

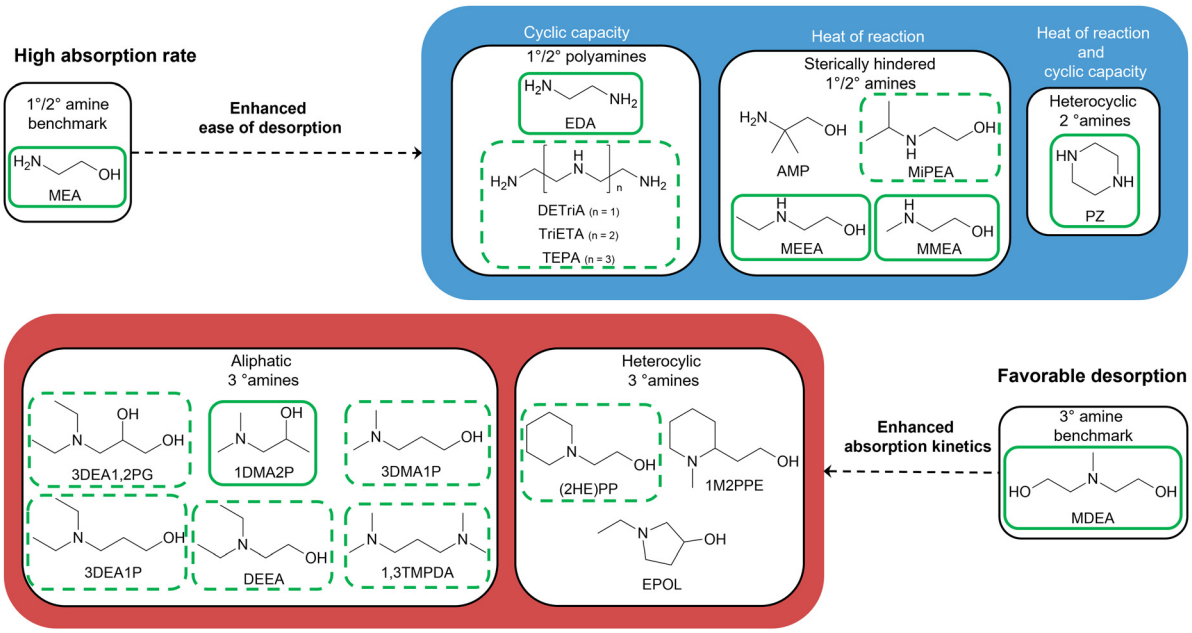

Fig. 3 Overview of novel aqueous amine absorbents reported in the literature. Amine absorbents that have been produced from (hemi)cellulose-derived oxygenates are framed in green, whereas amines that could potentially be produced from these oxygenates are framed in dashed green.

(*i.e.*, EDA, DETriA, TriETA and TEPA) all exhibited a higher CO_2 loading and cyclic capacity than MEA. Moreover, both the CO_2 loading and cyclic capacity gradually improved with an increasing number of nitrogen atoms present in the absorbent.[261,262] Interestingly, both energy reduction approaches can be combined by using heterocyclic polyamine absorbents such as piperazine (PZ). Aqueous PZ solutions display a superior overall performance in CO_2 capture compared to MEA since PZ demonstrates fast kinetics, a high cyclic capacity, and relatively low heat of reaction.[263]

Tertiary amines, on the other hand, generally suffer from slow absorption kinetics. Multiple researchers have conducted screening experiments in the search for tertiary amines with faster absorption rates compared to the benchmark MDEA. In their study, Chowdhury and co-workers identified four better-performing aliphatic alkanolamines than MDEA, namely *N*,*N*-diethylethanolamine (DEEA), *N*,*N*-diethyl-3-amino-1,2-propylene glycol (3DEA1,2PG), *N*,*N*-diethyl-3-amino-1-propanol (3DEA1P), and *N*,*N*-dimethyl-1-amino-2-propanol (1DMA2P).[264] In addition to 1DMA2P, El Hadri *et al.* also found that the β-propanolamine *N*,*N*-dimethyl-3-amino-1-propanol (3DMA1P) and the diamine *N*,*N*,*N*′,*N*′-tetramethyl-1,3-propylenediamine (1,3TMPDA) outperformed MDEA in terms of absorption rate.[258] Xiao *et al.* drew similar conclusions as Chowdhury *et al.* and El Hadri *et al.* as they reported 3DMA1P and DEEA as interesting tertiary amine absorbents.[265] Consistent with the primary and secondary amine absorbents, also various heterocyclic piperidine- and pyrrolidine-derived tertiary amines outperformed the MDEA in terms of absorption rate.[264,266,267] From a mechanistic point of view, one could intuitively reason that the absorption rate predominantly correlates with the basicity of the amine, *i.e.*, the corresponding pK_a value. In practice, however, this straightforward relationship is rather limited and not entirely compelling.[267,268] Recently, Rozanska *et al.* developed an empirical and predictive model to quantitatively assess the absorption rate of tertiary amines.[269] In their model, the key determinants for the reaction rate were the concentrations of CO_2 and OH^- and the Gibbs free energy of activation of the reaction between these two species. Hence, the pK_a value of the amine absorbent indirectly influences the absorption rate by affecting the concentration of the OH^- species *via* acid–base chemistry.[269] In a follow-up study, Orlov *et al.* successfully employed this model by screening 100 structurally diverse tertiary amines. This screening verified existing experimental reaction rates and additionally highlighted pyrrolidinol (*e.g.*, 1-ethyl-3-pyrrolidinol (EPOL)) as a promising yet unexplored class of tertiary amines.[270]

Despite all research interests, it is still challenging to obtain an amine that combines the fast absorption kinetics of primary/secondary amines and the ease of regeneration of tertiary amines. Consequently, amine blends, which contain two or more amines with complementary properties, have gained attention as a suitable solution. Currently, the blend of PZ and AMP is the best-known absorbent formulation. The blend of these two absorbents exceeds the individual amines in terms of absorption rate, ease of desorption and cyclic capacity.[249,271] In addition to the PZ/AMP formulation, PZ has been employed as a rate-enhancing additive for various aqueous tertiary amines including MDEA.[270,272] The effectiveness of these amine blends is demonstrated by the fact that almost all industrial amine-based absorption technologies utilize commercial amine blends such as KS-1 (MHI), Cansolv (Shell) and OASE (BASF).[250,252,273]

4.1.1.3. Water-lean absorbents. The second strategy to decrease energy consumption involves the elimination of water

from the solvent system. Amine absorbents typically contain water to maintain their solubility and minimize the viscosity of the CO_2-rich solution. However, the relatively high specific heat capacity and vaporization heat of water have a large parasitic effect on the overall cost and energy requirements of heating and recondensing the absorbent solution throughout the absorption–desorption cycles.[274,275] Different so-called water-lean approaches have been studied in the literature.[276] The most straightforward water-lean approach consists of replacing water with an organic solvent that has a lower specific heat capacity and higher CO_2 solubility such as MeOH, EtOH or EG. In practice, however, water is not completely eliminated from the capture system as most water-lean approaches still rely on steam to regenerate the CO_2-rich solvent. This approach primarily focuses on solvent design while utilizing the same group of amines used in traditional aqueous amine absorbents.[274]

In the context of this Review, a noteworthy water-lean approach involves the substitution of aqueous amine solutions with a tailor-made single amine absorbent system (Fig. 4). Since no additional solvent is present, the amine absorbent should be liquid both in the absence and presence of CO_2 while preventing a substantial increase in viscosity. Furthermore, the amine absorbent should at least contain one primary/secondary amino group to form carbamates upon CO_2 absorption as no bicarbonate can be formed in the absence of water.[276] Barzagli *et al.* investigated a number of *N*-alkylated ethanolamines as potential single-component absorbents. Among these, *N*-monobutylethanolamine (MBEA) stood out as the most promising absorbent due to its high absorption efficiency, high boiling point (*i.e.*, low volatility), thermal stability and moisture tolerance.[277] Recently, Heldebrant and co-workers have explored various single-component systems in a series of publications.[278–280] In their initial work, they presented six promising single-amine absorbents based on computational screening *via* molecular simulations.[278] Subsequently, they experimentally evaluated two of these amines, namely *N*-(2-ethoxyethyl)-3-morpholinopropyleneamine (2EEMPA)[279] and *N*-(2-ethoxyethyl)-*N*′,*N*′-diisopropylethylenediamine (2EEDiPEDA).[280] Comparing the two, 2EEDiPEDA exhibited a lower viscosity and stronger affinity for CO_2, relative to 2EEMPA.[279,280] Through a comprehensive techno-economic analysis, they estimated that employing the 2EEDiPEDA absorbent could potentially lead to a 20% reduction in the overall capture cost when compared to the commercially available Cansolv absorbent.[280]

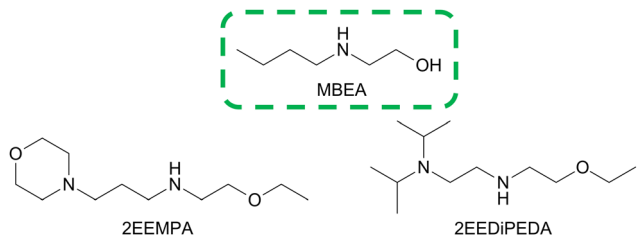

Fig. 4 Examples of novel water-lean absorbents reported in the literature of which some could potentially be produced from (hemi)cellulose-derived oxygenates (green dashed frame).

4.1.2. CO_2-switchable solvents

4.1.2.1. Introduction. Apart from CO_2 capture, the acid–base interaction between CO_2 and an amine can also be harnessed in so-called switchable materials such as switchable solvents. This group of designer solvents employs CO_2 as a smart chemical switch to alter specific solvent properties. These property changes are reversible as CO_2 can be removed from the solvent *via* steam stripping or sparging with non-acid gases such as N_2 or air, with or without heating.[281] Since 2005, Jessop and collaborators have been pioneers in the development of such CO_2-switchable solvents.[282,283] Two types of CO_2-switchable solvents that require aliphatic amines, namely switchable water (SW) and switchable hydrophilicity solvents (SHS), will be discussed in more detail (Fig. 5).

4.1.2.2. CO_2-switchable water (SW). Switchable water (SW) is a single-phase aqueous solution, both in the absence and presence of CO_2, that contains a water-miscible organic base (referred to as the ionogen), generally an aliphatic amine. Upon introduction of CO_2, the amine reacts with CO_2 to yield a bicarbonate salt which triggers a significant increase in the ionic strength of the aqueous solution (Fig. 5A). Additionally, also the conductivity, viscosity and osmotic pressure will increase.[284]

The altering ionic strength can be exploited to efficiently separate or purify water-soluble organic compounds from an aqueous environment. In the CO_2-lean solvent, the organic solute is highly soluble due to the ionogen acting as a hydrotrope. In the CO_2-rich solvent, however, the ionic strength increases and the organic solute is salted out because the ionogen–solute interaction changes from attractive to repulsive.[285] Mercer *et al.* have experimentally illustrated this salting-out effect by separating THF from an aqueous solution.[286,287] Interestingly, these studies have postulated a number of structural requirements for the amine ionogen as it strongly affects the performance of the SW. First, tertiary and bulky secondary amines are preferred as they exclusively form bicarbonate salts instead of carbamate salts. The formation of carbamate salts is detrimental as it complicates the reversibility of the reaction and leads to the formation of fewer ions, thus, decreasing the ionic strength. Furthermore, using a polyamine ionogen will lead to a higher ionic strength than a monoamine ionogen as each amino group can enhance the ionic strength upon protonation.[286] Second, incomplete protonation of the amino group(s) of an ionogen has an adverse effect on the performance of the SW. Consequently, the basicity of the amine

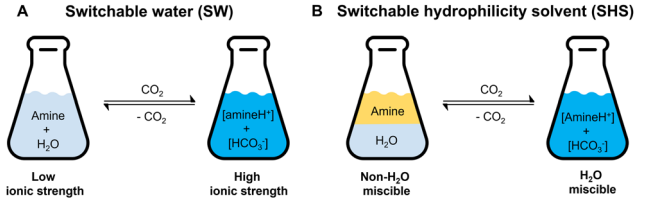

Fig. 5 General principle of (A) switchable water and (B) switchable hydrophilicity solvents.

(*i.e.*, pK_a) plays a vital role. If the basicity of the amine is too low, it will not be fully protonated in the presence of CO_2. Conversely, if the basicity is too high, the amine will already be partially protonated in the CO_2-lean aqueous solution. These lower and upper pK_a limits are dependent on the amine concentration, temperature and CO_2 pressure.[288] In this regard, polyamines with a two-carbon linkage between the different amino groups tend to perform poorly. The protonation of one amino group diminishes the basicity of the adjacent amino group(s), rendering it unprotonated in the carbonated solution. On the other hand, polyamines with a three- or four-carbon linkage display an improved performance because the longer linkage ensures that each amino group can undergo protonation.[287] In line with these insights, the best-performing ionogens in the studies of Mercer *et al.* were propylene polyamines, namely the diamine 1,3TMPDA and the tetramine *N*,*N*,*N*′,*N*″,*N*‴,*N*‴′-hexamethyltripropylenetetramine (HMTriPTA). Under reaction conditions (THF-to-H_2O wt ratio of 1 : 1, 0.8 molal amine loading, 30 min, 25 °C), a THF separation of 82% and 85% was achieved by employing 1,3TMPDA and HMTriPTA, respectively, while both amines retained for more than 99% in the aqueous phase.[286,287] By elaborating on this salting-out effect, SW can also be used as a reaction medium in a chemical process, facilitating the separation of the organic product after the reaction (Fig. 6A). For example, Püschel *et al.* performed an auto-tandem reductive hydroformylation reaction in a SW medium.[289] Noteworthy, they employed the ethanolamine DEEA both as a catalytic ligand and as an ionogen in the SW. After completion of the reaction, CO_2 was added to the reaction system in order to separate the alcoholic products from the aqueous phase containing DEEA and the catalyst. In this way, an alcohol yield of 99% and a turnover frequency of 764 h^{-1} were successfully achieved.[289]

4.1.2.3. CO_2-switchable hydrophilicity solvents (SHSs). A switchable hydrophilicity solvent (SHS) represents a basic, hydrophobic liquid that, when combined with water, results in a biphasic system. Upon introducing CO_2, however, the SHS becomes hydrophilic and readily miscible with water (Fig. 5B).[281,290] The hydrophobic form of SHSs typically comprises a tertiary or bulky secondary amine, while its hydrophilic counterpart corresponds to its respective bicarbonate salt.[291] The altering miscibility of SHSs can be exploited to efficiently dissolve or extract hydrophobic organic compounds without the need for a distillation step (Fig. 7A). Initially, these organic compounds are dissolved in the hydrophobic SHS. Afterward, the desired organic compound can be purified by removing the SHS with carbonated water. In this way, the hydrophobic phase solely contains the organic compound and is separated from the aqueous phase that comprises the amine as a bicarbonate salt.[283,284]

An effective SHS must fulfill two primary requirements. First, the SHS should be able to fully dissolve the targeted hydrophobic compound in the absence of CO_2. Second, the presence of CO_2 should trigger the SHS to move completely toward the aqueous phase. These two requirements can be quantified by two intrinsic parameters, namely the octanol–water partition coefficient (log K_{ow}) and the basicity (pK_a). In general, all tertiary and bulky secondary monoamines with log K_{ow} values between 1.2 and 2.5 and pK_a values between 9.5 and 11 are applicable as SHSs.[292] Amines with log K_{ow} values lower than 1.2 are miscible with water and do not result in a biphasic system, while amines with log K_{ow} values higher than 2.5 remain non-water-miscible regardless of the applied CO_2 pressure. On the other hand, amines with pK_a values below 9.5 are not easily protonated by the carbonated water, whereas those with pK_a values above 11 lack reversible behavior under mild conditions.[292] The most commonly studied monoamine as an SHS is *N*,*N*-dimethylcyclohexylamine (DMCHA). For example, DMCHA has been employed as an SHS to extract lipids from algae,[293,294] phospholipids from dairy[295] and the carotenoid astaxanthin from bacteria.[296] Furthermore, Samori *et al.* employed DMCHA as an SHS to successfully recycle polyethylene and aluminum from multilayer packaging materials.[297]

In addition to monoamines, polyamines have also been explored as suitable SHSs. However, polyamines exhibit some differences in properties compared to monoamines. For example, polyamine SHSs generally require larger log K_{ow} values than monoamines, as they partition more favorably into the aqueous

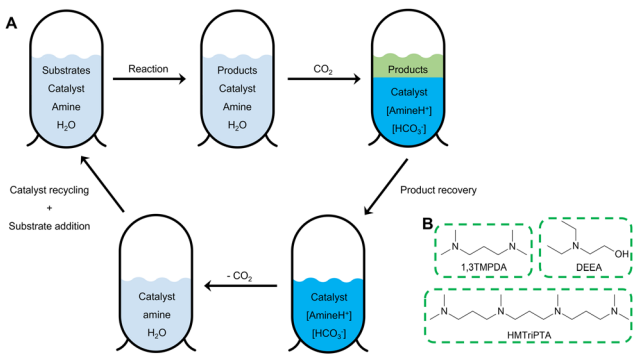

Fig. 6 (A) Illustration of a reaction performed in switchable water. (B) Examples of switchable water ionogens which could potentially be produced from (hemi)cellulose-derived oxygenates (green dashed frame).

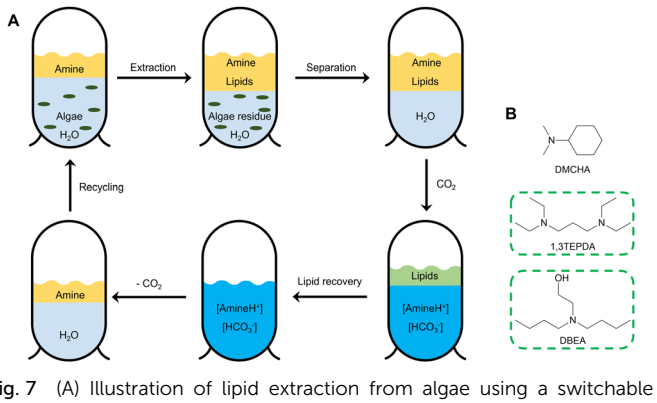

Fig. 7 (A) Illustration of lipid extraction from algae using a switchable hydrophilicity solvent. (B) Examples of aliphatic amines as switchable hydrophilicity solvents which could potentially be produced from (hemi)-cellulose-derived oxygenates (green dashed frame).

phase. Consequently, the use of polyamine SHSs can lead to an enhanced separation as the residual polyamine amount in the hydrophobic phase is reduced compared to monoamines. One drawback associated with polyamine SHSs is their relatively longer transition time when switching between the hydrophobic and hydrophilic states, in comparison to monoamine SHSs.[298] The diamine *N*,*N*,*N*′,*N*′-tetraethyl-1,3-propylenediamine (1,3TEPDA) is an example of a frequently studied SHS. 1,3TEPDA has been used in multiple extraction studies, for example in the extraction of lipids from algae[299] or extraction of heavy oil in oil-solid separation.[300] Besides their use in extraction processes, SHSs can also be used in chemical reactions. A case in point is the work of Viner *et al.*, who employed the ethanolamine *N*,*N*-dibutylethanolamine (DBEA) both as a solvent and recoverable base catalyst in the transesterification of soybean oil to long-chain fatty acid methyl esters (FAMEs). They achieved a very good FAME yield of 80–85% along with an excellent DBEA recovery rate of approximately 92%.[301]

4.2. Polymerization

Aliphatic amines are widespread as (reactive) catalysts in numerous polymerization reactions. This will be illustrated by discussing the role of aliphatic amines in three distinct polymers and their polymerization process, namely (i) epoxy polymers, (ii) polyurethane (PUR), and (iii) atom transfer radical polymerization (ATRP).

4.2.1. Epoxy polymers

4.2.1.1. Introduction. Epoxy polymers or epoxies are an important and versatile class of thermosetting polymers. They are known for their outstanding mechanical strength and toughness, excellent chemical, moisture and corrosion resistance, as well as remarkable thermal, adhesive and electrical properties. Consequently, epoxies find extensive applications in various fields, ranging from coatings and adhesives to electronic insulation, composites and construction.[302] Epoxy polymers are produced by the polymerization and crosslinking of mono- and oligomeric epoxy resins or epoxy prepolymers. These epoxy resins are aliphatic, cycloaliphatic, aromatic or nonhydrocarbon structures containing at least one epoxide functional group. To date, diglycidyl ether of bisphenol A (DGEBA) is the most commonly used epoxy resin monomer.[303–305] In recent years, however, the production of epoxy resins derived from various biomass sources such as lignin, carbohydrates, vegetable oils and plant extracts (*e.g.*, tannins and terpenes) has gained increasing research interest and poses numerous sustainable alternatives.[306–311]

The polymerization and crosslinking of these resins occur in the presence of so-called curing agents or hardeners as they irreversibly transform the epoxy resins into a solid, infusible and insoluble three-dimensional thermoset network. The curing agent plays a pivotal role in determining the type of chemical bonds formed and the degree of crosslinking. Furthermore, the curing process can be either catalytic or co-reactive. In a catalytic curing process, the curing agent functions as a catalyst, activating another curing agent or the homopolymerization of the epoxy resin. In a co-reactive curing process, on the other hand, the curing agent acts as a reactive co-monomer and is incorporated into the polymeric network *via* polyaddition. Consequently, the choice of curing agent has a direct impact on the properties of the final epoxy polymer product.[305] A wide scope of basic and acidic curing agents has been extensively studied and industrially applied.[302–305] Notably, aliphatic amines stand out as a prominent group within this diverse range of curing agents.

4.2.1.2. Aliphatic amine curing agents. Primary and secondary aliphatic amines are widely used as co-reactive curing agents. They have a low viscosity and are highly reactive, which enables them to initiate curing at ambient temperatures. Adversely, their high reactivity makes primary and secondary aliphatic amines sensitive to amine blush, which can compromise both the performance and aesthetic properties of the cured epoxy material.[312] Amine blush refers to the reaction between a primary or secondary amine hardener and moisture and CO_2 from the air. Similar to CO_2-related applications, this carbonation reaction will yield unreactive carbamate species, which appear as an oily, sticky film on the surface of the material.[313]

In the co-reactive polyaddition mechanism (Fig. 8A), the curing agent performs a nucleophilic addition onto the epoxide functionality of the epoxy resin, resulting in the formation of a hydroxyl group. This polyaddition process continues until all nucleophilic amine sites have either reacted or become unreactive (*e.g.*, due to steric hindrance). In order to perform effective crosslinking, the curing agent should be a polyamine containing at least two amino groups.[302–305] Recently, Mora *et al.* evaluated the reactivity of different types of primary and secondary polyamine curing agents.[314] The reactivity of the curing agent depends on both its nucleophilicity and steric hindrance. In general, primary polyamines are presumed to be more reactive than secondary polyamines due to steric hindrance. Additionally, primary aliphatic polyamines are

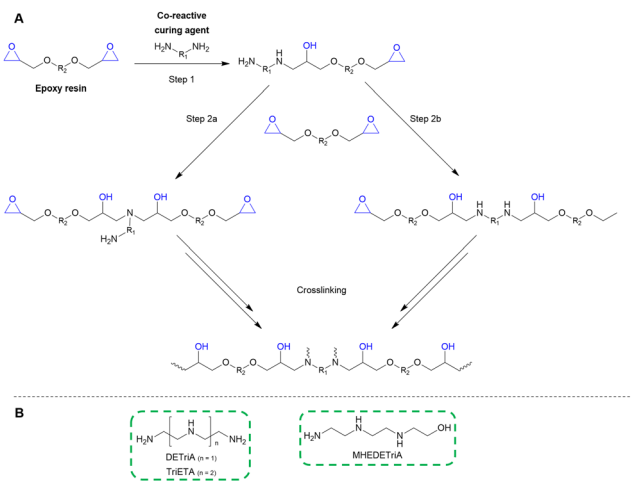

Fig. 8 (A) Mechanism of co-reactive polymerization of epoxy resins. (B) Examples of aliphatic amines as co-reactive curing agents which could potentially be produced from (hemi)cellulose-derived oxygenates (green dashed frame).

considered to be more reactive than their cycloaliphatic and aromatic counterparts. Among the primary aliphatic polyamines, DETriA and TriETA are regarded as the most reactive aliphatic amines due to the presence of two chain-end primary amino groups and one or two internal secondary amino groups, respectively.[314] In another study by the same research group, primary ethanolpolyamines emerged as a potentially valuable, yet insufficiently explored type of highly reactive aliphatic polyamines. The researchers related the enhanced reactivity of these primary ethanolpolyamines to their ability to form additional hydrogen bonds with the epoxy reactant through their hydroxyl group.[315] Secondary aliphatic amines are another type of underexplored curing agent. For example, little is known about the relative reactivity of *N*-methylated secondary aliphatic polyamines compared to primary aliphatic polyamines. Although more sterically hindered than primary aliphatic polyamines, *N*-methylation increases the nucleophilicity of these secondary aliphatic polyamines. In this regard, ethanolpolyamines, such as the DETriA adduct *N*-(2-monohydroxyethyl)-diethylenetriamine (MHEDETriA), are an interesting type of polyamines as they possess a primary amino group and a reactivity enhancing hydroxyl group.[302,314] Noteworthy, preliminary research also suggests that this type of curing agent demonstrates reduced skin-sensitizing effects compared to the more common primary aliphatic polyamines.[316]

Tertiary amines, unable to perform polyaddition, catalyze the anionic homopolymerization of the epoxy resins (Fig. 9A). Through their Lewis basicity, tertiary amines activate either the epoxy monomers itself or another curing co-catalyst.[314] In addition to commonly used aliphatic and aromatic monoamines (*e.g.*, TriEA and benzyldimethylamine), various alkanolamines, including DMEA, DEEA and *N*,*N*-dimethyl-2-amino-2-methyl-1-propanol (DMAMP), are employed as catalytic curing agents.[303–305,312]

4.2.2. Polyurethane (PUR)

4.2.2.1. Introduction. Polyurethane (PUR) is a highly versatile and commercially important group of specialty polymers. It encompasses all polymers formed by the polyaddition reaction that involves two types of monomers, namely polyfunctional isocyanates and polyols.[317] Regarding these monomers, industrial PUR production is dominated by aromatic polyisocyanates, particularly methylene diphenyl diisocyanate (MDI) and toluene diisocyanate (TDI). More than 90% of PURs are industrially produced from these aromatic polyisocyanates while a handful of (cyclo)aliphatic polyisocyanates, *e.g.*, hexamethylene diisocyanate (HDI) and isophorone diisocyanate (IPDI), are used in niche applications (*e.g.*, applications requiring stability to UV light). In contrast, a diverse set of polyols is used as a reaction partner for these isocyanates. The two most common types of polyols are polyether polyols and polyester polyols. Polyether and polyester polyols result from the polycondensation reaction of an initiator with a cyclic ether (*i.e.*, EO, PO) or a dicarboxylic acid (*e.g.*, adipic acid, terephthalic acid), respectively. These initiators typically include glycols (*e.g.*, EG, diethylene glycol, 1,2PG, 1,3PG), glycerol, 1,6-hexanediol, trimethylolpropane, bisphenol A, *etc.*[318] Some of these initiators

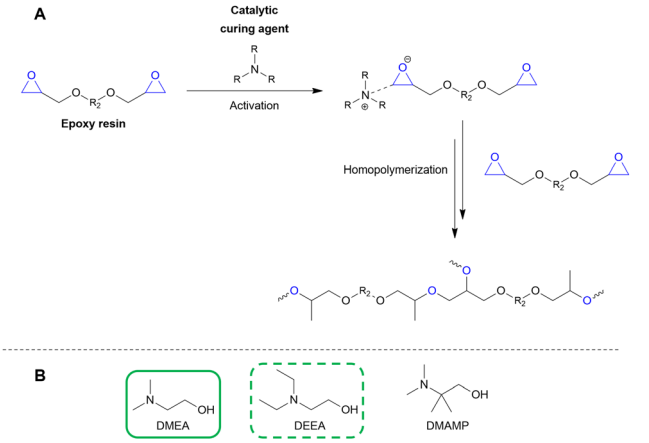

Fig. 9 (A) Mechanism of catalytic homopolymerization of epoxy resins. (B) Examples of aliphatic amines as catalytic curing agents which have been (green fame) or could potentially be (green dashed frame) produced from (hemi)cellulose-derived oxygenates.

can be derived from biomass. Moreover, partially or fully bio-based PUR polymers have experienced increased research activity in recent years. All different fractions of lignocellulose, as well as various vegetable oils, have been reported as suitable resources for the formation of bio-based drop-in polyols and isocyanates.[319–321] The seemingly endless choice of polyols, combined with a couple of isocyanates and various additives (*e.g.*, chain extenders, flame retardants, plasticizers) results in a diverse set of PUR materials. The structure of PUR spans from compact to foamed, from soft to rigid and comprises everything in between, whereas their applications extend from furniture and bedding to automotive components, construction materials, clothing, and thermal insulation.[317,322,323]

The polyaddition reaction of isocyanate and polyol leads to the linear urethane (or carbamate) link characteristic for PUR. In addition, isocyanate can undergo a plethora of alternative reactions with other active hydrogen compounds present in the reaction system (Fig. 10A). A second essential linear polyaddition reaction yields urea through the condensation of isocyanate with a primary or secondary amino group. The presence of these amines in the system can be deliberate or result from the reaction of isocyanate with water. When isocyanate reacts with water, carbamic acid is initially formed, which then spontaneously decomposes into an amine accompanied by the elimination of CO_2. The formed CO_2 expands and thereby promotes the formation of the porous structure in foams. In this regard, the formation of urea and CO_2 is known as the blowing reaction, while the formation of the rigid urethane bond is often referred to as the gelling reaction. The formed urethane and urea groups retain active hydrogen atoms in their structure and are therefore capable of engaging in crosslinking reactions with isocyanate, yielding allophanates and biurets, respectively. In addition to polyaddition reactions, isocyanate can also oligomerize, resulting in cyclic structures such as uretdione, isocyanurate and uretonimine.[317,318,322] Consequently, catalysis plays a crucial role in selectively controlling each of these reactions as they all distinctively contribute to the final

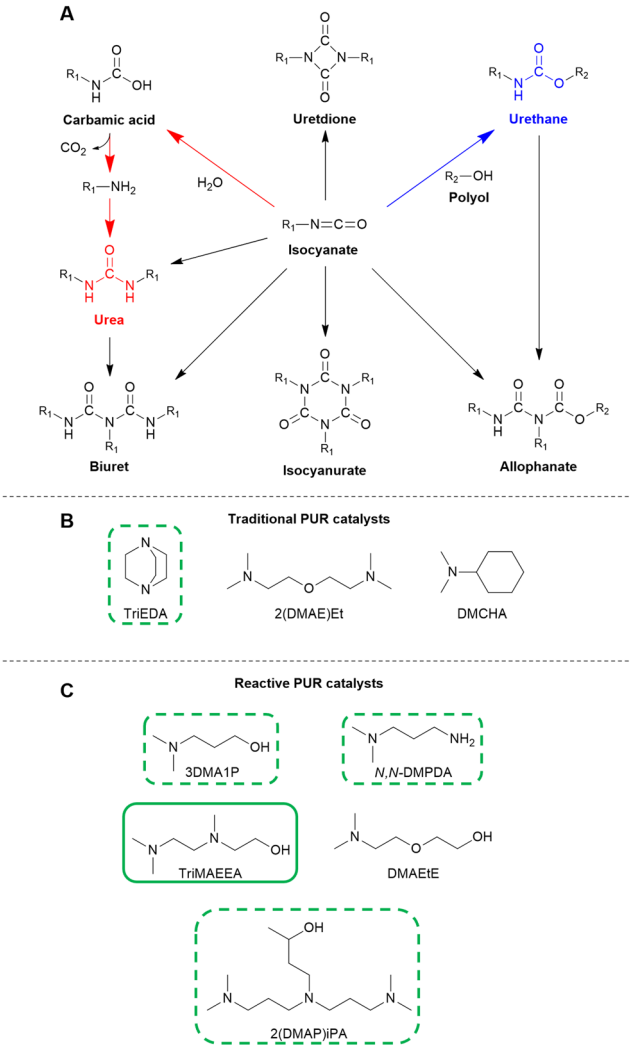

Fig. 10 (A) Overview of possible polymerization reactions in the synthesis of polyurethane. The two primary polymerization reactions, namely gelling (urethane formation) and blowing (urea formation) are highlighted in blue and red, respectively. Examples of (B) traditional PUR catalysts and (C) novel reactive PUR catalysts which have been (green frame) or could potentially be (green dashed frame) produced from (hemi)cellulose-derived oxygenates.

properties of the polymer. In general, two categories of catalysts are used: organometallic Lewis acid catalysts, with organotin compounds as most prominent class, and Lewis base tertiary amines.[324] The latter will be discussed in more detail in the scope of this Review.

4.2.2.2. Tertiary amine PUR catalysts. Tertiary amines catalyze both the isocyanate-polyol and isocyanate-water reactions (*i.e.*, the gelling and blowing reactions), as well as some side reactions such as the trimerization reaction forming isocyanurate. As Lewis bases, tertiary amines catalyze the polymerization reactions by activating the hydroxyl group of the polyol or water for nucleophilic addition (Farka's mechanism) and/or facilitating the proton transfer between hydroxyl and isocyanate by activating the isocyanate (Baker's mechanism).[325] Therefore, the catalytic activity of tertiary amines mainly depends on their basicity, steric hindrance and number of catalytic sites. Nonetheless, predicting the catalytic selectivity of tertiary amines *a priori* based on these properties remains challenging. Tertiary amines that preferentially interact with water molecules catalyze the isocyanate-water reaction and are called blowing catalysts, while those that favor the isocyanate-polyol reaction are referred to as gelling catalysts.[326–328]

In recent years, the use of traditional tertiary amines, such as triethylenediamine (TriEDA), DMCHA and bis-(2-dimethylaminoethyl)ether (Fig. 10B), has progressively declined in industrial applications. These amines possess relatively high volatility and are susceptible to oxidative degradation over time, which combined results in significant emissions of harmful volatile organic compounds (VOCs) and associated undesirable odors.[318,329] This limitation has prompted the development of nonvolatile catalysts such as reactive catalysts and autocatalytic polyols, which are both designed to chemically bind into the polymer matrix using isocyanate-reactive groups. Reactive catalysts are tertiary amines functionalized with a hydroxyl or primary/secondary amino group.[324,327] In contrast to traditional tertiary amine catalysts, larger quantities of reactive catalysts are required as they become less effective when incorporated into the polymer network. Furthermore, the choice of the reactive group strongly affects the catalytic activity. For example, reactive catalysts with a secondary hydroxyl group will exhibit a prolonged catalytic activity compared to those containing a primary hydroxyl group as they react more slowly with the polymer matrix. However, this advantage is offset by the risk of never being incorporated into the network. Conversely, a reactive catalyst with a primary or secondary amino group is highly likely to integrate into the polymer network, but it may rapidly lose its catalytic effectiveness. Some examples of commercially important reactive catalysts are given in Fig. 10C.[330–332] Autocatalytic polyols go a step further as they are polyols functionalized with catalytic sites. Similarly to traditional polyols, autocatalytic polyols are typically produced by reacting a cyclic ether or dicarboxylic acid with an initiator, in this case being a reactive tertiary amine catalyst.[317,333,334]

4.2.3. Atom transfer radical polymerization (ATRP)

4.2.3.1. Introduction. Reversible-deactivation radical polymerization (RDRP) is an umbrella term for well-controlled polymerization techniques that are based on establishing a dynamic equilibrium between a small number of actively propagating radicals and a large number of dormant species incapable of propagation and termination. In this way, the lifetime of the growing polymer chains is significantly extended from mere seconds to several hours or even days, allowing to precisely control of the composition, topology, functionality and complex architecture of the synthesized polymer.[335] IUPAC recently described this technology as a revolution in polymer synthetic chemistry and has included it in its top 10 emerging chemical innovations that can change the world.[336]

Atom transfer radical polymerization (ATRP), independently developed by Matyjaszewski[337] and Sawamoto[338] in 1995, is one

of the most robust and widely used methods of RDRP. In ATRP, a broad range of monomers (*e.g.*, styrenes, acrylonitrile, (meth)acrylates, (meth)acrylamides) can be polymerized into well-defined and uniform polymers applicable in various applications. Over the years, several companies have successfully commercialized ATRP-derived polymers.[339]

From a mechanistic perspective, ATRP is a catalytic reversible-deactivation method wherein the activation and deactivation of radicals occur through a concurrent atom and electron transfer reaction regulated by a catalyst (Fig. 11A). A successful ATRP reaction requires a minimal amount of termination reactions, uniform growth of all chains, and fast initiation coupled with rapid reversible deactivation. These three requirements all heavily rely on the choice of catalyst as it regulates the equilibrium dynamics between active and dormant species (*i.e.*, k_{act}, k_{deact} and K_{ATRP}). The catalyst is typically a homogeneous complex consisting of a transition metal and a ligand. While Cu is frequently employed as the transition metal, other transition metals (*e.g.*, Ti, Fe, Ru, Co, Pd) have also been explored. In combination with Cu, nitrogen-containing ligands, particularly aliphatic tertiary polyamines and pyridine derivatives, stand out as the most active ligands.[340,341] The aliphatic polyamine ligands connect to the interest of this review and will be addressed in more detail.

4.2.3.2. ATRP aliphatic polyamine ligands. Although already reported in 1997,[342] traditional linear tertiary polyamines, namely *N*,*N*,*N*′,*N*″,*N*‴-pentamethyldiethylenetriamine (PMDETriA) and HMTriETA, are still regarded as robust and active ATRP ligands, demonstrating an excellent control over molecular weight and molecular weight distribution. As a rule of thumb, the performance of these linear aliphatic polyamine ligands generally improves with increasing number of nitrogen atoms and decreasing length of carbon linker (*i.e.*, C2 ≫ C3 > C4). Later, the branched aliphatic polyamine tris(2-dimethylaminoethyl)amine (3(DMAE)A) was developed to further improve the catalytic performance. To date, the Cu-3(DMAE)A complex is one of the most active and selective ATRP catalysts reported in the literature (Fig. 11B).[343,344]

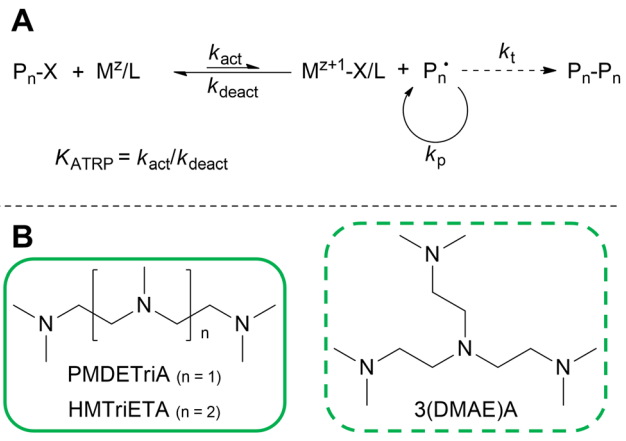

Fig. 11 (A) General principles of atom transfer radical polymerization. (B) Examples of ATRP catalytic ligands which have been (green frame) or could potentially be (green dashed frame) produced from (hemi)cellulose-derived oxygenates.

4.3. Quaternary ammonium compounds (QACs)

Quaternary ammonium compounds (QACs) constitute a fourth distinct type of functional amino group, in addition to primary, secondary and tertiary amines. Unlike the other three amino groups, QACs lack basicity and nucleophilicity due to the absence of a lone electron pair at the nitrogen atom. Instead, QACs are cationic as the nitrogen center contains four substituents (R_4N^+).[345] QACs are generally formed through the exhaustive alkylation of an amine with an electrophilic alkylation agent. In this way, an extensive scope of QACs can be obtained from various amines and alkylation agents, thereby broadening their utility in a wide range of applications.[346] For example, QACs can be used as phase-transfer catalysts in organic synthesis,[347] as framework templates in supramolecular chemistry such as zeolite synthesis,[348] as cationic amphiphilic surfactants in detergents and fabric softeners,[199,349] and as biocides in pesticide and antimicrobial formulations.[350] The latter application will be discussed in more detail to highlight the potential of QACs.

4.3.1. QACs as antibacterial agents. QACs used as antibacterial agents have an amphiphile structure consisting of a polar, charged head (*i.e.*, cationic nitrogen atom) and long non-polar carbon chain substituents. QACs target the bacterial cell membrane through electrostatic interactions between the cationic QAC head and the negatively charged cell membrane. Subsequently, the non-polar QAC side chains permeate into the intramembrane region of the cell, causing leakage of cytoplasmic material and ultimately cellular lysis. Their use is widespread as they demonstrate antibacterial activity against various microorganisms including multiple pathogenic ESKAPE bacteria (*e.g.*, *Staphylococcus aureus*, *Pseudomonas aeruginosa* and *Enterobacter* species). Consequently, antibacterial QACs have found their way in various formulations (*e.g.*, antiseptics, disinfectants, preservatives, sterilization agents) and are omnipresent in medical, industrial, agricultural, and household settings. The most common QACs have been extensively used for more than 70 years due to their effective antibacterial activity in combination with their relatively low toxicity, simplicity and ease of preparation. Examples of commonly used QACs include benzalkonium chloride (BAC), dimethyldodecylammonium chloride or bromide (DDAC or DDAB), cetyltrimethylammonium bromide (CTAB), and cetylpyridinium chloride (CPC) (Fig. 12).[346,350,351] However, their extensive use also has a major downside. Current commercial antibacterial QACs do not readily (bio)degrade and consequently accumulate in the environment. As a result, bacterial populations are exposed to diluted, sublethal QAC concentrations which catalyze the development of resistance. Over the past years, the rate at which bacteria have developed QAC resistance is concerning and is further amplified by the rise of multi-drug-resistant species.[352]

Consequently, the development of next-generation antibacterial QACs that are less susceptible to resistance development,

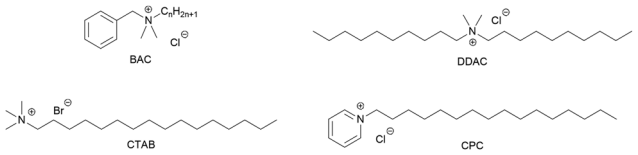

Fig. 12 Traditional monoQACs employed as antibacterial agents.

is of utmost importance. An ideal next-generation QAC should meet four criteria: (i) high antibacterial activity, particularly against resistant bacteria, (ii) minimal toxicity, *i.e.*, exhibiting high selectivity towards microbial cells over eukaryotic cells, (iii) resilience against the development of resistance, and (iv) biodegradability to avoid accumulation in the environment. In this regard, the research groups of Minbiole and Wuest have synthesized and assessed more than 200 QACs in the search for these next-generation QACs. Their research efforts have primarily focused on the development of multiQACs, characterized by the presence of more than one charged nitrogen atom.[353,354] Among all tested multiQACs, aliphatic multiQACs are regarded as the most promising next-generation QACs. These multiQACs are obtained by straightforward quaternization of aliphatic tertiary polyamines such as TMEDA, PMDETriA, HMTriETA, 3(DMAE)A and tris(2-dimethylaminopropyl)amine (3(DMAP)A), and fulfill multiple of the predetermined criteria. First, various tested multiQACs outperformed the traditional monoQACs in terms of antibacterial activity. Notably, activity did not increase with the number of cationic centers, as multiple bis-, tri- and tetraQACs resulted in comparably excellent activities. Furthermore, multiQACs containing symmetric alkyl side chains with a carbon length between 12 and 14 exhibited the highest activity as this length is required to successfully penetrate and disrupt bacterial cell membranes. However, the most active compounds also displayed the highest toxicity.[355,356] Second, experimental results indicated that aliphatic multiQACs, in contrast to monoQACs and aryl-containing QACs, were active against bacterial strains carrying QAC resistant genes,[357] which is likely at least partly attributable to their increased affinity to the bacterial cell surface.[358] Furthermore, no *de novo* resistance development was observed against aliphatic multiQACs after more than 500 generations. In contrast, resistance development was observed after a few hundred generations for mono- and bisQACs possessing aryl substituents.[359] These results indicate that to counteract aliphatic multiQACs, bacteria need to evolve a resistance mechanism that differs from the mechanism used against conventional QACs.[353] Third, these multiQACs can become ''soft'' antibacterials that are designed to biodegrade after a certain time or trigger by incorporating cleavable amide- or ester-containing side chains in their structure. All of these soft compounds were stable in water, but the ester-QACs rapidly decomposed in any sort of buffered solution while the amide-QACs only decomposed in acidic media. Interestingly, several of these soft multiQACs retained their excellent antibacterial activity.[360] Finally, these multiQACs are among the most potent QAC-based biofilm eradicators published to date. Both the polycationic character and the presence of the alkyl chains are vital for this activity.[359,361] Biofilms are complex three-dimensional communities of microorganisms and contribute to over 80% of all microbial infections. Furthermore, bacteria in biofilms are inherently more tolerant to antibacterial treatments, making it extremely difficult to treat and eradicate the pathogenic biofilm effectively.[362] The development of multiQACs with biofilm-eradicating properties is very promising but still requires more insights into the mechanism of action and a significant reduction in their toxicity. Overall, mutiQACs possess the potential to become the next-generation antibacterial QACs.[354] A summary of the most promising antibacterial multiQACs and their preparation methods are given in Table 2.

5. Critical discussion and conclusive remarks

Aliphatic amines encompass a versatile class of amines including alkyl polyamines, heterocyclic amines and alkanolamines. The characteristic amino group in aliphatic amines is connected *via* a linear or branched aliphatic carbon chain to either another amino group, in the case of alkyl polyamines and piperazine-related heterocyclic amines, or to a hydroxyl group, in the case of alkanolamines. Current aliphatic amine production heavily relies on fossil feedstock and is facing pressing sustainability, health and safety issues. These issues can be fundamentally resolved by shifting from fossil feedstock to biomass. Consequently, the academic and industrial interest in bio-based aliphatic amines has systematically increased over the past years. Similar to the current aliphatic amine industry, the production of these bio-based amines will be the middle part of a larger, ideally circular, industrial value chain. This value chain additionally includes, as the first part, the refinery of biomass to suitable substrates and, as the final part, the utilization of these amines across various applicative domains. Therefore, applying a holistic perspective already in the research stage enables to acknowledge the requirements and limitations of each part and to efficiently bridge knowledge gaps between the different parts (Fig. 13).

5.1. Chemocatalytic (hemi)cellulose valorization

Lignocellulose, the major structural constituent of plant cell walls, is universally recognized as an alternative feedstock for the production of chemicals due to its abundance, low cost and susceptibility to chemical modifications. In the context of the holistic bio-based aliphatic amine value chain, the carbohydrate fraction of lignocellulose, namely the aliphatic polymers cellulose and hemicellulose, emerges as a suitable feedstock. Carbohydrates circumvent many health and safety concerns associated with the current fossil-based amine process as they are non-toxic and safe to handle. Hence, the chemocatalytic transformation of lignocellulose-derived carbohydrate feedstock into suitable substrates is a heavily studied and well-known process that passes through two stages. In the first stage, the biopolymers are depolymerized into their

Table 2 Overview of the most promising antibacterial multiQACs

Component	Yield[a]	Antibacterial activity[b]			Toxicity[c]	Biofilm eradication[d]
	[%]	MIC [μM]			$Lysis_{20}$ [μM]	MBEC [μM]
		PA	SA	MRSA		MRSA
Common monoQAC						
BAC		63	8	32	63	>200
MultiQACs						
TMEDA		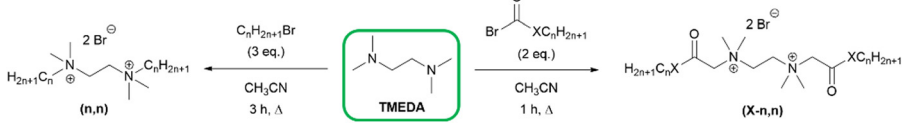				
12,12	94	4	1	0.5	8	75–100
E-12,12	77	32	2	4	16	N.R.
A-13,13	44	2	1	0.5	8	N.R.
PMDETriA		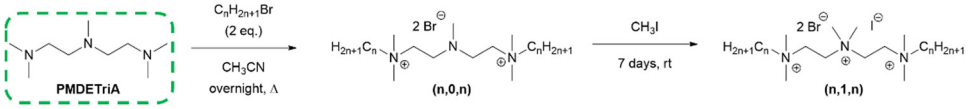				
12,0,12	95	4	1	0.5	8	75–100
12,1,12	90	1	1	1	16	50
HMTriETA		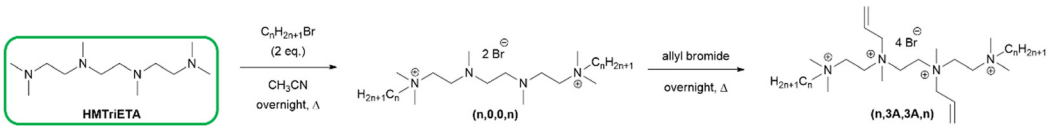				
12,0,0,12	93	4	1	1	4	100
12,3A,3A,12	91	2	1	1	8	150
3(DMAE)A		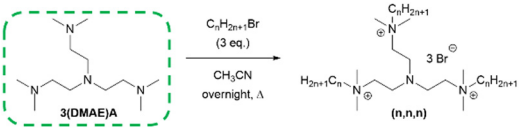				
12,12,12	82	8	1	2	8	>200
3(DMAP)A		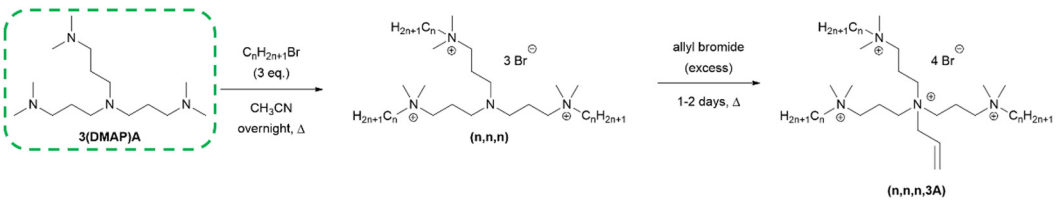				
12,12,12	99	4	0.5	0.5	4	200
12,12,12,3A	94	2	1	1	4	100

[a] QAC product yield after purification. [b] Minimum inhibitory concentrations (MIC) against *Pseudomonas aeruginosa* (PA), *Staphylococcus aureus* (SA) and methicillin-resistant *Staphylococcus aureus* (MRSA). [c] $Lysis_{20}$ values represent the compound concentration at which 20% or less of red blood cells are lysed. [d] Minimum biofilm elimination concentration (MBEC) against MRSA. N.R. = not reported. Results obtained from Minbiole *et al.*[355,356,359–361,363] Amine multiQACS that have been produced from (hemi)cellulose-derived oxygenates are framed in green, whereas amines that potentially could be produced from these oxygenates are framed in dashed green.

corresponding monomers (*e.g.*, glucose and xylose) *via* acid-catalyzed hydrolysis. In the second stage, these carbohydrate monomers are further upgraded into multiple smaller hydroxyl- and carbonyl-functionalized oxygenates. This chemocatalytic valorization involves a multi-step process comprising four elementary key reactions, namely isomerization, retro-aldol condensation, dehydration and (de)hydrogenation. Since these four elementary reactions occur consecutively, various oxygenates can be derived by chemocatalytic valorization from a single substrate. For example, glucose can simultaneously be converted into the sugar alcohol sorbitol, multiple polyols (*e.g.*, ethylene glycol (EG), 1,2-propylene glycol (1,2 PG), glycerol) and hydroxy carbonyl oxygenates (*e.g.*, glyceraldehyde, glycolaldehyde (GA), acetol).

5.1.1. State of the art. The advantage of selectively producing various oxygenates from a single feedstock can become a burden if the interplay between these key reactions is not properly regulated. Consequently, product selectivity control has been an extensively studied research topic in the chemocatalytic upgrading of carbohydrates and has led to a fundamental understanding of each individual reaction step as well as the overall mechanism.

In the state of the art, this product selectivity challenge is managed by consciously fine-tuning two aspects of the reaction

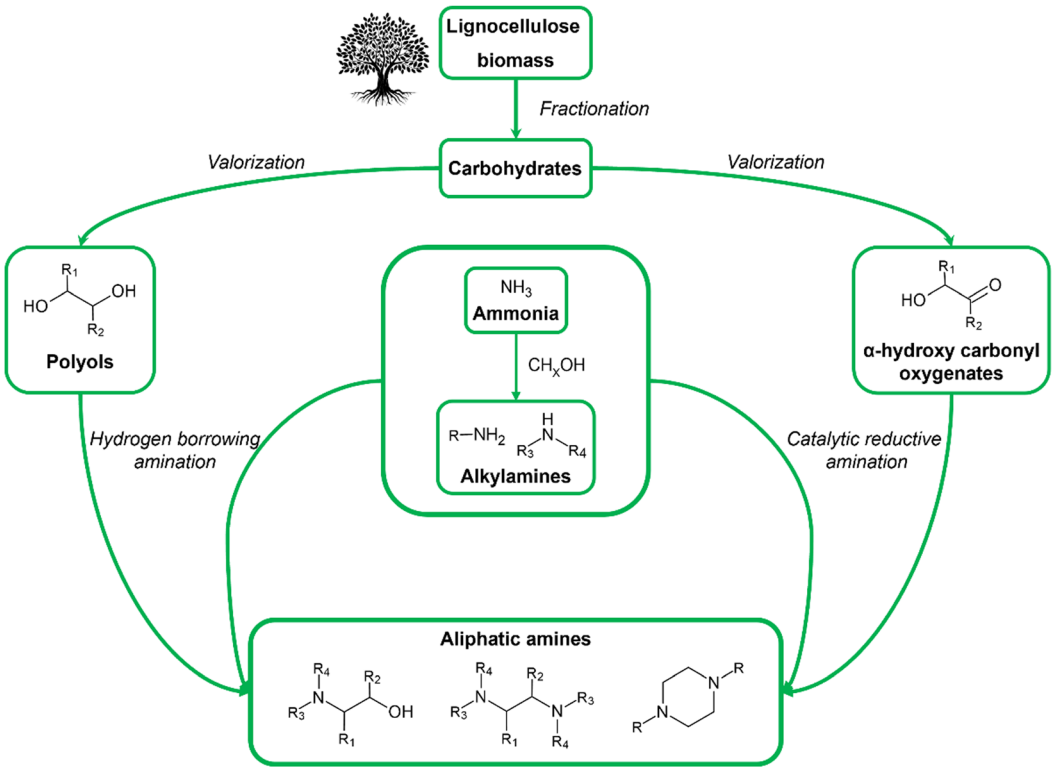

Fig. 13 Schematic overview of the holistic aliphatic amine industry. The carbon part of the aliphatic amines originates from oxygenates obtained *via* valorization of lignocellulose-derived carbohydrates. The nitrogen part originates from green ammonia and bio-alcohol-derived alkylamines.

system: (i) the reaction conditions and (ii) the catalytic system. On the one hand, reaction conditions such as temperature and H_2 pressure strongly affect product selectivity. For example, retro-aldol condensation and dehydrogenation, both endothermic reactions, benefit from an elevated reaction temperature, whereas hydrogenation is favored under an increased H_2 pressure. On the other hand, the intrinsic properties of the catalytic system determine which competitive key reactions are promoted. For instance, the presence of transition metals in the catalytic system is essential to facilitate (de)hydrogenation, which require noble (*e.g.*, Ru, Pt) or non-noble metals (*e.g.*, Cu, Ni), as well as retro-aldol condensation, which is catalyzed by tungsten-group metals. In addition, the presence of acid or base sites strongly influences the selectivity of the catalytic system. Acid sites favor dehydration, while basic sites facilitate both isomerization and retro-aldol condensation. Furthermore, acid–base pair sites improve the dehydrogenation activity of the catalytic system. In the state of the art, two successful approaches have been described in terms of catalytic system. It can either consist of one integrated multifunctional catalyst containing all required properties or a binary system in which two catalysts possess complementary properties.

These mechanism-derived handles can be grouped in a set of general strategies to selectively steer carbohydrate upgrading toward a variety of oxygenates.

5.1.2. Potential future research direction. Building on these insights, future research in chemocatalytic (hemi)cellulose valorization should aim to expand the product scope. While the state-of-the-art literature has mainly focused on the formation of stable **O2** diols (*i.e.*, EG and 1,2PG) two other subgroups deserve future research interest: (i) **O2** hydroxy carbonyl oxygenates (*i.e.*, GA and acetol) and (iii) higher **O3** and **O4** polyols (*i.e.*, glycerol and erythritol). Developing selective chemocatalytic pathways toward these subgroups would be both academically and industrially valuable, providing competitive alternatives to existing thermochemical and biological routes.

5.2. Bio-based aliphatic amines *via* catalytic reductive amination

Carbohydrate-derived oxygenates, ranging from bifunctional **O2** substrates such as GA and EG to **O6** substrates such as glucose, are chemocatalytically converted into aliphatic amines *via* catalytic reductive amination. Notably, reductive amination of oxygenates with at least two oxygen-containing functional groups is a multi-step process that yields all three types of aliphatic amines, encompassing alkanolamines, alkyl polyamines and aliphatic heterocyclic amines. In this way, a striking parallel emerges between carbohydrate upgrading and reductive amination. Both chemocatalytic processes encounter the same challenge of achieving a desirable product selectivity amidst multiple potential products originating from a single substrate. Furthermore, both multi-step processes are influenced by the same four elementary reactions, namely isomerization, retro-aldol condensation, dehydration and (de)hydrogenation. From a mechanistic point of view, reductive

amination inherently includes dehydration and (de)hydrogenation as elementary steps, while all four key reactions can take place as substrate-modifying, pre-amination reactions.

5.2.1. State of the art. In accordance with the state-of-the-art expertise in (hemi)cellulose valorization, bottom-up strategies have emerged as the most effective methodology to address the selectivity challenge present in catalytic reductive amination. This methodology is based on a comprehensive understanding of the underlying reaction mechanism, which is attained by validating the reaction pathway and identifying the primary reaction intermediates. These mechanistic insights are then used to scrutinize the influence of various control handles on individual reaction steps and the dynamic interactions between competing steps. Ultimately, product-tailored selectivity control strategies are formulated that incorporate the most effective control handles.

In the state of the art, five main control handles have been investigated: (i) the catalytic system (*i.e.*, catalyst and co-catalyst selection), (ii) process design (*i.e.*, one-step or two-step processes), (iii) reaction temperature, (iv) amine-to-substrate (ATS) molar ratio, and (v) solvent choice. While the first three handles are also pivotal in the selectivity challenge of (hemi)cellulose valorization, the latter two are specific to the selectivity challenge in catalytic reductive amination. To date, this bottom-up methodology has been applied to the reductive amination of GA and acetol. In other words, cross-pollination of information between the two first parts of the holistic value chain remains limited to these two substrates, indicating a substantial opportunity to broaden the substrate scope.

5.2.2. Potential future research directions. Most state-of-the-art research on catalytic reductive amination has focused on polyol substrates such as EG, 1,2PG and glycerol, with minimal use of a bottom-up approach. Contrary, almost all research efforts have been devoted to developing active heterogeneous dehydrogenation–hydrogenation catalysts, often disregarding other aspects of the reaction mechanism. This rather ''black box'' approach has led to the development of generally active, yet unselective, catalytic systems. Future research should be inspired by the established approach in (hemi)cellulose valorization and aim to integrate this bottom-up methodology more extensively to a wider range of substrates, including (i) less reactive (*i.e.*, polyols), and more complex substrates (*i.e.*, larger oxygenates such as glucose, sorbitol or even cellulose).

Another notable future research direction relates to further expanding the aliphatic amine product scope. Of the three types of aliphatic amines, only aliphatic heterocyclic amines, such as piperazine and its derivatives, have not been systematically studied. From an academic standpoint, their selective synthesis would contribute to an even more profound understanding of the reaction pathway, while from an industrial standpoint, these compounds are indispensable in various applicative domains.

A final future research direction, which is also valid for lignocellulose valorization, involves the evolution from lab-scale reactions to industrialization by upscaling the process. This transition is accompanied by a set of new priorities and research topics. Some potential topics include the use of highly concentrated industrial feedstock solutions, catalyst development with emphasis on catalyst recycling and stability, reactor configuration (*e.g.*, batch, fed-batch, or a continuous set-up), downstream processing, *etc.* Furthermore, the development of an industrial process introduces new perspectives and evaluation criteria. In addition to selectivity and productivity, a potentially viable industrial process will be assessed using a multitude of criteria, including economics, sustainability, health and safety, work-up requirements, *etc.* underscoring the importance of a techno-economic analysis and life cycle assessment as decision-making tools when upscaling the process.

5.3. Applicative domains of (bio-based) aliphatic amines

Selectively produced bio-based aliphatic amines are indispensable compounds in a range of applications, the final part of the holistic bio-based aliphatic amine value chain. The pivotal role of aliphatic amines is exemplified by three diverse applicative domains that all require distinct characteristics of the employed (bio-based) aliphatic amine: (i) CO_2-reactive applications, (ii) polymerization and (iii) quaternary ammonium compounds.

5.3.1. CO_2-reactive applications. In CO_2-reactive applications, the amine's nucleophilicity and/or basicity are employed to react with CO_2. Primary and simple secondary amines rapidly react with CO_2 forming stable carbamate species *via* their labile proton. Conversely, sterically hindered secondary and tertiary amines catalyze the easily reversible, slow hydration of CO_2 into bicarbonate salts.

5.3.1.1. Carbon capture. On the one hand, these characteristic interactions can be exploited in carbon capture, in which anthropogenic CO_2 is removed from industrial flue gas streams using amine-based absorption. Traditional capturing systems demonstrate either fast absorption kinetics or favorable desorption. Consequently, research efforts have centered around the design of novel amine systems that integrate rapid absorption with facile desorption, while considering additional criteria such as resistance to degradation and low volatility.

5.3.1.2. Carbon capture: structural requirements. The most promising amine capture systems, both water-rich and water-lean, contain at least one sterically hindered primary or secondary amino group, as these amines generally combine fast absorption and favorable desorption thermodynamics.

5.3.1.3. Switchable solvents. On the other hand, the reactivity of aliphatic amines toward CO_2 can be exploited in switchable solvents, in which the presence of CO_2 either alters the ionic strength (*i.e.*, switchable water, SW) or interchanges the hydrophilic–hydrophobic nature of the amine solvent (*i.e.*, switchable hydrophilicity solvents, SHSs). Compared to traditional systems, switchable solvents are regarded as energy-efficient separation methods suitable for extraction, product purification and catalyst recovery.

5.3.1.4. Switchable solvents: structural requirements. Tertiary and sterically hindered secondary polyamines are preferentially used as switchable solvents due to their facile reversibility. Furthermore, each amino group of the polyamine can interact with CO_2 resulting in a more pronounced switchable effect. As SW and SHS require a hydrophilic and hydrophobic aliphatic amine, respectively, the water-miscibility of the amine can be modulated through its C/N ratio and the incorporation of alkyl substituents.

5.3.2. Polymerization. In the second domain, a versatile set of aliphatic amines is used as a, potentially reactive, polymerization catalyst in the synthesis of polymers such as (i) epoxies, (ii) polyurethanes (PUR), and (iii) atom transfer radical polymerization (ATRP)-derived polymers.

5.3.2.1. Epoxy resins. Epoxy resins are irreversibly transformed into a three-dimensional epoxy polymer by using curing agents such as aliphatic amines. Primary and secondary polyamines act as co-reactive curing agents by reacting with the epoxide functionalities of the resins, accelerating both polymerization and crosslinking. These co-reactive curing agents are incorporated into the polymer network and, hence, strongly influence the physicochemical properties of the resulting epoxy polymer.

5.3.2.2. Epoxy resins: structural requirements. Commercial ethylene polyamines have been extensively used as co-reactive curing agents, but they suffer from health- and safety-related drawbacks. In this regard, ethanolpolyamines seem to be promising alternatives since preliminary research indicates that they mitigate these shortcomings while remaining highly reactive.

5.3.2.3. Polyurethanes (PUR). PUR chemistry is characterized by a multitude of possible polymerization and crosslinking reactions. Therefore, catalysis is essential to consciously control each of these reactions. In this way, the choice of catalyst strongly affects the final properties of the polymer product. Tertiary aliphatic amines are an important class of PUR catalysts that affect the polymerization reactions *via* their Lewis basicity.

5.3.2.4. PUR: structural requirements. Over the past years, the high vapor pressure and susceptibility to oxidative degradation of traditional tertiary amines have decreased their use and stimulated the development of non-emissive, reactive tertiary amines. These reactive catalysts are functionalized with an additional hydroxyl or primary/secondary amino group that chemically binds into the polymer network.

5.3.2.5. Atom transfer radical polymerization (ATRP). ATRP is a robust reversible-deactivation radical polymerization method yielding well-defined and uniform polymers by the activation and deactivation of radicals regulated by a homogeneous catalytic complex. This catalytic complex consists of a transition metal, generally Cu, supported by a linear or branched tertiary alkyl polyamine ligand.

5.3.2.6. ATRP: structural requirements. To date, the most active and selective ATRP catalysts contain a polyamine ligand with three to four tertiary amino groups separated by two carbon atom linkers.

5.3.3. Quaternary ammonium compounds. In the final domain, QACs encompass a fourth distinct functional amino group, characterized by their substituted cationic nitrogen center. QACs are used in a variety of applications including antibacterial agents. Antibacterial QACs are amphiphile structures comprising a polar, charged head and long, non-polar alkyl substituents. With their cationic head, QACs target the negatively charged cell membrane of bacteria and subsequently cause cellular lysis by penetrating the intramembrane region with their non-polar side chains. Their effectiveness and simplicity have resulted in the omnipresent use of antibacterial QACs in multiple formulations and settings. The development of novel antibacterial QACs is urgent as the current commercial QACs accumulate in the environment and, hence, facilitate the development of bacterial resistance.

5.3.3.1. QACs: structural requirements. Recently, aliphatic multiQACs (*i.e.*, linear and branched alkyl polyamines with at least two charged nitrogen atoms) have emerged as promising next-generation antibacterial agents. Compared with current antibacterial QACs, these multiQACs are more active, less susceptible to resistance development and sometimes even possess promising biofilm-eradicating properties. Moreover, preliminary results indicate that the biodegradability of these multiQACs can be enhanced by incorporating cleavable ester or amide side chains.

5.3.4. Future challenges in the applicative domains. Despite their apparent disparity, these three domains do share some common objectives and challenges.

The growing significance of sustainability within the chemical industry has led to increased awareness regarding health and safety requirements. For example, (eco)toxicity has become an important evaluation criterion that should be considered in the development of novel aliphatic amines in various domains since it is a genuine concern for certain prevailing commercial amines. Furthermore, the development of bio-based monomers has gained profound research interest in recent years. However, a polymer can only be labeled fully bio-based if every component originates from biomass, including (reactive) aliphatic amine catalysts.

In this part of the holistic value chain, cross-pollination of information between different domains could also be valuable. Challenges of a certain domain could already be well-established structure–activity principles in another domain. For example, while amine blush, oxidative degradation and volatility of aliphatic amines are emerging and unresolved topics in PUR chemistry, they have been extensively investigated as fundamental principles in carbon capture.

5.4. Closing note

From a holistic perspective, bio-based aliphatic amines represent a versatile and valuable group of chemicals. Through

catalytic reductive amination, a variety of non-toxic, safe-to-handle, carbohydrate-derived substrates can be transformed into numerous alkyl polyamines, alkanolamines and aliphatic heterocyclic amines. The disparate structural properties of these three aliphatic amines make them fundamental components across a broad spectrum of applicative domains.

Abbreviations

1,2DA3P	1,2-Diamino-3-propanol
1,2PDA	1,2-Propylenediamine
1,2PG	1,2-Propylene glycol
1,2TMPDA	*N*,*N*,*N*′,*N*′-Tetramethyl-1,2-propylenediamine
1,3PG	1,3-Propylene glycol
1,3TEPDA	*N*,*N*,*N*′,*N*′-Tetraethyl-,1,3-propylenediamine
1,3TMPDA	*N*,*N*,*N*′,*N*′-Tetramethyl-1,3-propylenediamine
1A2P	1-Amino-2-propanol
1DMA2P	*N*,*N*-Dimethyl-1-amino-2-propanol
2A1,3PG	2-Amino-1,3-propylene glycol
2A1P	2-Amino-1-propanol
2EEDiPEDA	*N*-(2-Ethoxyethyl)-*N*′,*N*′-diisopropylethylenediamine
2EEMPA	*N*-(2-Ethoxyethyl)-3-morpholinopropyleneamine
2iPA1P	*N*-Isopropyl-2-amino-1-propanol
3(DMAE)A	Tris(2-dimethylaminoethyl)amine
3(DMAP)A	Trsi(2-dimethylaminopropyl)amine
3A1,2PG	3-Amino-1,2-propylene glycol
3DEA1,2PG	*N*,*N*-Diethyl-3-amino-1,2-propylene glycol
3DEA1P	*N*,*N*-Diethyl-3-amino-1-propanol
3DMA1P	*N*,*N*-Dimethyl-3-amino-1-propanol
AMP	2-Amino-2-methyl-1-propanol
AMT	Ammonium metatungstate
ATRP	Atom transfer radical polymerization
ATS molar ratio	Amine-to-substrate molar ratio
BAC	Benzalkonium chloride
BHEDMEDA	*N*,*N*′-Bis(2-hydroxyethyl)-*N*,*N*′-dimethylethylenediamine
CCUS	Carbon capture utilization and/or storage
CPC	Cetylpyridinium chloride
CTAB	Cetyltrimethylammonium bromide
DBEA	*N*,*N*-Dibutylethanolamine
DDAC	Dimethyldodecylammonium chloride
DEA	Diethanolamine
DEEA	*N*,*N*-Diethylethanolamine
DEGA	*N*,*N*-Diethylglucamine
DETriA	Diethylenetriamine
DHA	Dihydroxyacetone
DMA	Dimethylamine
DMAMP	*N*,*N*-Dimethyl-2-amino-2-methyl-1-propanol
DMCHA	*N*,*N*-Dimethylcyclohexylamine
DMEA	*N*,*N*-Dimethylethanolamine
DMPZ	*N*,*N*′-Dimethylpiperazine
DMSO	Dimethyl sulfoxide
EDA	Ethylenediamine
EDC	Ethylene dichloride
EG	Ethylene glycerol
EO	Ethylene oxide
EPOL	1-Ethyl-3-pyrrolidinol
GA	Glycolaldehyde
HMF	5-Hydroxymethylfurfural
HMTriETA	*N*,*N*,*N*′,*N*″,*N*‴,*N*‴′-Hexamethyltriethylenetetramine
HMTriPTA	*N*,*N*,*N*′,*N*″,*N*‴,*N*‴′-Hexamethyltripropylenetetramine
MBEA	*N*-Monobutylethanolamine
MBEC	Minimum biofilm elimination concentration
MDEA	*N*-Methyldiethanolamine
MEA	Monoethanolamine
MEEA	*N*-Monoethylethanolamine
MeOH	Methanol
MHEDETriA	*N*-(2-Monohydroxyethyl)-diethylenetriamine
MIC	Minimum inhibitory concentration
MiPEA	*N*-Monoisopropylethanolamine
MMA	Monomethylamine
MMEA	*N*-Monomethylethanolamine
MRSA	Methicillin-resistant *Staphylococcus aureus*
PA	*Pseudomonas aeruginosa*
PMDETriA	*N*,*N*,*N*′,*N*″,*N*″-Pentamethyldiethylenetriamine
PTriA	1,2,3-Propylenetriamine
PUR	Polyurethane
PZ	Piperazine
QAC	Quaternary ammonium compound
RDRP	Reversible-deactivation radical polymerization
SA	*Staphylococcus aureus*
SHS	Switchable hydrophilicity solvent
SW	Switchable water
THF	Tetrahydrofuran
TMA	Trimethylamine
TMEDA	*N*,*N*,*N*′,*N*′-Tetramethylethylenediamine
TriEA	Triethanolamine
TriEDA	Triethylenediamine
TriEPA	Triethylenepentamine
TriETA	Triethylenetetramine
TriMAEEA	*N*,*N*,*N*′-Trimethylaminoethylethanolamine
TriMEDA	*N*,*N*,*N*′-Trimethylethylenediamine

Data availability

All data is obtained from peer-reviewed articles, books, and patents as reported in the References list. No other datasets have been used.

Conflicts of interest

There are no conflicts to declare.

Acknowledgements

B. V. and B. F. S. acknowledge the C2 project of KU Leuven on bio-based amines. S. V. P. and B. F. S. acknowledge the Flemish government for their financial support in the A^3 and Mimosa 2.0 project (Vlaio). W. A. and B. F. S. thank internal funding from KU Leuven (IDN-FFASSD). T. N. acknowledges the BioApp C3/20/120 – Industrial Research Fund (IOF) KU Leuven for the doctoral fellowship. C. Z. thanks the Chinese Scholarship Council (no. 201906310137) for financial support.

References

1 S. A. Lawrence, *Amines: synthesis, properties, and applications*, Cambridge University Press, 2004.
2 P. Roose, K. Eller, E. Henkes, R. Rossbacher and H. Höke, *Ullmann's Encyclopedia of Industrial Chemistry*, Wiley-VCH, 2015, pp. 1–55.
3 V. Pattabathula, *Kirk-Othmer Encyclopedia of Chemical Technology*, John Wiley & Sons, 2019, pp. 1–33.
4 M. Appl, *Ullmann's Encyclopedia of Industrial Chemistry*, Wiley-VCH, 2011, pp. 107–137.
5 M. Appl, *Ullmann's Encyclopedia of Industrial Chemistry*, Wiley-VCH, 2011, vol. 3, pp. 139–225.
6 G. J. Leigh, in *Catalysts for Nitrogen Fixation*, ed. B. E. Smith, R. L. Richards and W. E. Newton, Springer, 2004, pp. 33–54.
7 P. Roose, *Ullmann's Encyclopedia of Industrial Chemistry*, Wiley-VCH, 2015, pp. 1–10.
8 D. R. Corbin, S. Schwarz and G. C. Sonnichsen, *Catal. Today*, 1997, **37**, 71–102.
9 K. S. Hayes, *Appl. Catal., A*, 2001, **221**, 187–195.
10 K. Weissermel and H.-J. Arpe, *Industrial Organic Chemistry*, Wiley-VCH, 4th edn, 2003, pp. 51–52.
11 H. Zimmermann and R. Walzl, *Ullmann's Encyclopedia of Industrial Chemistry*, Wiley-VCH, 2009, pp. 465–529.
12 K. Weissermel and H.-J. Arpe, *Industrial Organic Chemistry*, Wiley-VCH, 4th edn, 2003, pp. 63–66.
13 Y. Gao, L. Neal, D. Ding, W. Wu, C. Baroi, A. M. Gaffney and F. Li, *ACS Catal.*, 2019, **9**, 8592–8621.
14 K. Weissermel and H.-J. Arpe, *Industrial Organic Chemistry*, Wiley-VCH, 4th edn, 2003, pp. 145–152.
15 S. Rebsdat and D. Mayer, *Ullmann's Encyclopedia of Industrial Chemistry*, Wiley-VCH, 2001, pp. 547–572.
16 E.-L. Dreher, K. K. Beutel, J. D. Myers, T. Lübbe, S. Krieger and L. H. Pottenger, *Ullmann's Encyclopedia of Industrial Chemistry*, Wiley-VCH, 2014, pp. 1–81.
17 M. Frauenkron, J.-P. Melder, G. Ruider, R. Rossbacher and H. Höke, *Ullmann's Encyclopedia of Industrial Chemistry*, Wiley-VCH, 2001, pp. 405–431.
18 K. Weissermel and H.-J. Arpe, *Industrial Organic Chemistry*, Wiley-VCH, 4th edn, 2003, pp. 159–162.
19 C. Jones, M. R. Edens and J. F. Lochary, *Kirk-Othmer Encyclopedia of Chemical Technology*, Wiley-VCH, 2004, pp. 122–147.
20 S. Sridhar and R. G. Carter, *Kirk-Othmer Encyclopedia of Chemical Technology*, Wiley-VCH, 2001, vol. 8, pp. 485–519.
21 E. E. Sergeev, L. L. Gogin, T. B. Khlebnikova, E. G. Zhizhina and Z. P. Pai, *Catal. Ind.*, 2022, **14**, 218–230.
22 Maximize Market Research, Aliphatic Amines Market – Global Industry Analysis and Forecast (2024–2030), **https://www.maximizemarketresearch.com/market-report/global-aliphatic-amines-market/69637/**, (accessed 17 July 2024).
23 S&P Global, Ethanolamines, **https://www.spglobal.com/commodityinsights/en/ci/products/ethanolamines-chemical-economics-handbook.html**, (accessed 17 July 2024).
24 S&P Global, Ethyleneamines, **https://www.spglobal.com/commodityinsights/en/ci/products/ethyleneamines-chemical-economics-handbook.html**, (accessed 17 July 2024).
25 Organization of the Petroleum Exporting Countries (OPEC), 2022 World Oil Outlook 2045, 2022.
26 International Energy Agency, The future of petrochemicals – Towards more sustainable plastics and fertilizers, 2018.
27 E. De Jong, H. Stichnothe, G. Bell and H. Jorgensen, *Bio-Based Chemicals: A 2020 Update*, 2020.
28 J. Harnisch, C. Jubb, A. Nakhutin, V. C. S. Cianci, R. Lanza, T. Martinsen, A. K. W. Mohammad, M. M. O. Santos, A. McCulloch and B. T. Mader, in 2006 IPCC Guidelines for National Greenhouse Gas Inventories. V, Intergovernmental Panel on Climate Change, 2006, p. chapter 3.
29 A. Boulamanti and J. A. Moya, *Energy efficiency and GHG emissions: Prospective scenarios for the Chemical and Petrochemical Industry*, 2017.
30 W. H. Faveere, S. Van Praet, B. Vermeeren, K. N. R. Dumoleijn, K. Moonen, E. Taarning and B. F. Sels, *Angew. Chem.*, 2021, **133**, 12312–12331.
31 European Chemicals Agency, Ethylene oxide: substance infocard, **https://echa.europa.eu/substance-information/-/substanceinfo/100.000.773**.
32 European Chemicals Agency, 1,2-dichloroethane: substance infocard, **https://echa.europa.eu/substance-information/-/substanceinfo/100.003.145**.
33 M. Pera-Titus and F. Shi, *ChemSusChem*, 2014, **7**, 720–722.
34 V. Froidevaux, C. Negrell, S. Caillol, J. P. Pascault and B. Boutevin, *Chem. Rev.*, 2016, **116**, 14181–14224.
35 M. Pelckmans, T. Renders, S. Van De Vyver and B. F. Sels, *Green Chem.*, 2017, **19**, 5303–5331.
36 S. Hameury, H. Bensalem and K. D. O. Vigier, *Catalysts*, 2022, **12**, 1–35.
37 N. K. Gupta, P. Reif, P. Palenicek and M. Rose, *ACS Catal.*, 2022, **12**, 10400–10440.
38 L. Krietsch Boerner, Industrial ammonia production emits more CO2 than any other chemical-making reaction. Chemists want to change that, **https://cen.acs.org/environment/green-chemistry/Industrial-ammonia-production-emits-CO2/97/i24**.
39 S. Ghavam, M. Vahdati, I. A. G. Wilson and P. Styring, *Front. Energy Res.*, 2021, **9**, 1–19.
40 X. Cui, C. Tang and Q. Zhang, *Adv. Energy Mater.*, 2018, **8**, 1–25.

41 K. H. R. Rouwenhorst, P. M. Krzywda, N. E. Benes, G. Mul and L. Lefferts, *Ullmann's Encyclopedia of Industrial Chemistry*, 2020, pp. 1–20.
42 A. Corma, S. Iborra and A. Velty, *Chem. Rev.*, 2007, **107**, 2411–2502.
43 M. J. Biddy, C. J. Scarlata and C. M. Kinchin, *Chemicals from biomass: A market assessment of bioproducts with near-term potential*, 2016.
44 A. Shrotri, H. Kobayashi and A. Fukuoka, *Advances in Catalysis*, Elsevier, 2017, vol. 60, pp. 59–123.
45 G. Hayes, M. Laurel, D. Mackinnon, T. Zhao, H. A. Houck and C. R. Becer, *Chem. Rev.*, 2023, **123**, 2609–2734.
46 M. Christou and E. Alexopoulou, in *Biorefinery: From Biomass to Chemicals and Fuels*, ed. M. Aresta, A. Dibenedetto and F. Dumeignil, De Gruyter, 2012, pp. 49–80.
47 Y. Liao, S.-F. Koelewijn, G. Van den Bossche, J. Van Aelst, S. Van den Bosch, T. Renders, K. Navare, T. Nicolaï, K. Van Aelst, M. Maesen, H. Matsushima, J. Thevelein, K. Van Acker, B. Lagrain, D. Verboekend and B. F. Sels, *Science*, 2020, **367**, 1385–1390.
48 W. Deng, Y. Feng, J. Fu, H. Guo, Y. Guo, B. Han, Z. Jiang, L. Kong, C. Li, H. Liu, P. T. T. Nguyen, P. Ren, F. Wang, S. Wang, Y. Wang, Y. Wang, S. S. Wong, K. Yan, N. Yan, X. Yang, Y. Zhang, Z. Zhang, X. Zeng and H. Zhou, *Green Energy Environ.*, 2023, **8**, 10–114.
49 N. Yan and X. Chen, *Nature*, 2015, **524**, 155–157.
50 X. Chen, H. Yang and N. Yan, *Chem. – Eur. J.*, 2016, **22**, 13402–13421.
51 M. J. Hülsey, *Green Energy Environ.*, 2018, **3**, 318–327.
52 M. Kaisler, L. A. M. van den Broeck and C. Boeriu, *Chitin and chitosan: properties an applications*, Elsevier, 1st edn, 2020, pp. 229–244.
53 T. T. Pham, X. Chen, T. Söhnel, N. Yan and J. Sperry, *Green Chem.*, 2020, **22**, 1978–1984.
54 W. Schutyser, T. Renders, S. Van Den Bosch, S. F. Koelewijn, G. T. Beckham and B. F. Sels, *Chem. Soc. Rev.*, 2018, **47**, 852–908.
55 A. M. Raspolli Galletti and C. Antonetti, in *Biorefinery: From Biomass to Chemicals and Fuels*, ed. M. Aresta, A. Dibenedetto and F. Dumeignil, De Gruyter, 2012, pp. 101–121.
56 Z. Sun and K. Barta, *Chem. Commun.*, 2018, **54**, 7725–7745.
57 X. Shen and R. Sun, *Carbohydr. Polym.*, 2021, **261**, 117884.
58 M. Ragnar, G. Henriksson, M. E. Lindström, M. Wimby, J. Blechschmidt and S. Heinemann, *Ullmann's Encyclopedia of Industrial Chemistry*, Wiley-VCH, 2014, pp. 1–92.
59 T. Renders, S. Van Den Bosch, S. F. Koelewijn, W. Schutyser and B. F. Sels, *Energy Environ. Sci.*, 2017, **10**, 1551–1557.
60 T. Renders, G. Van den Bossche, T. Vangeel, K. Van Aelst and B. Sels, *Curr. Opin. Biotechnol.*, 2019, **56**, 193–201.
61 M. V. Galkin and J. S. M. Samec, *ChemSusChem*, 2016, **9**, 1544–1558.
62 Z. Sun, A. De Santi, S. Elangovan and K. Barta, *Chem. Rev.*, 2018, **118**, 614–678.
63 M. M. Abu-Omar, K. Barta, G. T. Beckham, J. S. Luterbacher, J. Ralph, R. Rinaldi, Y. Román-Leshkov, J. S. M. Samec, B. F. Sels and F. Wang, *Energy Environ. Sci.*, 2021, **14**, 262–292.
64 D. M. Alonso, J. Q. Bond and J. A. Dumesic, *Green Chem.*, 2010, **12**, 1493–1513.
65 A. A. Ahmad, N. A. Zawawi, F. H. Kasim, A. Inayat and A. Khasri, *Renewable Sustainable Energy Rev.*, 2016, **53**, 1333–1347.
66 A. V. Bridgwater, *Biomass Bioenergy*, 2012, **38**, 68–94.
67 C. B. Schandel, M. Høj, C. M. Osmundsen, A. D. Jensen and E. Taarning, *ChemSusChem*, 2020, **13**, 688–692.
68 A. J. J. Straathof, *Chem. Rev.*, 2014, **114**, 1871–1908.
69 R. A. Sheldon, *Green Chem.*, 2014, **16**, 950–963.
70 S. Van de Vyver, J. Geboers, P. A. Jacobs and B. F. Sels, *ChemCatChem*, 2011, **3**, 82–94.
71 J. A. Geboers, S. Van De Vyver, R. Ooms, B. Op De Beeck, P. A. Jacobs and B. F. Sels, *Catal. Sci. Technol.*, 2011, **1**, 714–726.
72 I. Delidovich and R. Palkovits, *ChemSusChem*, 2016, **9**, 547–561.
73 I. Delidovich, *ACS Catal.*, 2023, **13**, 2250–2267.
74 H. Li, S. Yang, S. Saravanamurugan and A. Riisager, *ACS Catal.*, 2017, **7**, 3010–3029.
75 M. Moliner, Y. Román-Leshkov and M. E. Davis, *Proc. Natl. Acad. Sci. U. S. A.*, 2010, **107**, 6164–6168.
76 J. M. de Bruijn, A. P. G. Kieboom and H. van Bekkum, *Starch/Stärke*, 1987, vol. 39, pp. 23–28.
77 C. Liu, J. M. Carraher, J. L. Swedberg, C. R. Herndon, C. N. Fleitman and J.-P. Tessonnier, *ACS Catal.*, 2014, **4**, 4295–4298.
78 C. Moreau, R. Durand, A. Roux and D. Tichit, *Appl. Catal., A*, 2000, **193**, 257–264.
79 P. Zhu, H. Li and A. Riisager, *Catalysts*, 2022, **12**, 1–19.
80 E. Peeters, S. Calderon-Ardila, I. Hermans, M. Dusselier and B. F. Sels, *ACS Catal.*, 2022, **12**, 9559–9569.
81 P. Sun, C. Liu, H. Wang, Y. Liao, X. Li, Q. Liu, B. F. Sels and C. Wang, *Angew. Chem., Int. Ed.*, 2023, **62**, e202215737.
82 L. Petruš, M. Petrušova and Z. Hricovíniová, in *Glycoscience*, ed. A. E. Stütz, Springer, Berlin, 2001, vol. 215, pp. 15–41.
83 F. Ju, D. Vander Velde and E. Nikolla, *ACS Catal.*, 2014, **4**, 1358–1364.
84 M. Zheng, J. Pang, R. Sun, A. Wang and T. Zhang, *ACS Catal.*, 2017, **7**, 1939–1954.
85 C. B. Schandel, M. Høj, C. M. Osmundsen, M. J. Beier, E. Taarning and A. D. Jensen, *ACS Sustainable Chem. Eng.*, 2021, **9**, 305–311.
86 J. Zhang, B. Hou, A. Wang, Z. Li, H. Wang and T. Zhang, *Am. Inst. Chem. Eng.*, 2014, **60**, 3804–3813.
87 M. S. Holm, S. Saravanamurugan and E. Taarning, *Science*, 2010, **328**, 602–606.
88 A. Bayu, A. Abudula and G. Guan, *Fuel Process. Technol.*, 2019, **196**, 106162.
89 H. Baniamerian, H. Martin, M. Josef and A. D. Jensen, *Appl. Catal., B*, 2023, **330**, 122650.
90 Y. Liu, C. Luo and H. Liu, *Angew. Chem., Int. Ed.*, 2012, **51**, 3249–3253.

91 Y. Liu, W. Zhang, C. Hao, S. Wang and H. Liu, *Proc. Natl. Acad. Sci. U. S. A.*, 2022, **119**, 1–12.
92 C. Dussenne, T. Delaunay, V. Wiatz, H. Wyart, I. Suisse and M. Sauthier, *Green Chem.*, 2017, **19**, 5332–5344.
93 F. Delbecq, M. R. Khodadadi, D. Rodriguez Padron, R. Varma and C. Len, *Mol. Catal.*, 2020, **482**, 110648.
94 E. Cousin, K. Namhaed, Y. Pérès, P. Cognet, M. Delmas, H. Hermansyah, M. Gozan, P. A. Alaba and M. K. Aroua, *Sci. Total Environ.*, 2022, **847**, 157599.
95 S. P. Teong, G. Yi and Y. Zhang, *Green Chem.*, 2014, **16**, 2015–2026.
96 B. R. Caes, R. E. Teixeira, K. G. Knapp and R. T. Raines, *ACS Sustainable Chem. Eng.*, 2015, **3**, 2591–2605.
97 C. Chatterjee, F. Pong and A. Sen, *Green Chem.*, 2015, 40–71.
98 M. J. Ahmed and B. H. Hameed, *J. Taiwan Inst. Chem. Eng.*, 2019, **96**, 341–352.
99 S. Nishimura, *Handbook of heterogeneous catalytic hydrogenation for organic synthesis*, John Wiley & Sons, 2001.
100 T. W. van Deelen, C. Hernández Mejía and K. P. de Jong, *Nat. Catal.*, 2019, **2**, 955–970.
101 N. H. R. Annuar, Z. A. Alexzman, A. R. M. Daud, A. F. N. Alias, H. M. Hairi and H. D. Setiabudi, *J. Environ. Chem. Eng.*, 2022, **10**, 107229.
102 Y. Huang, B. Wang, H. Yuan, Y. Sun, D. Yang, X. Cui and F. Shi, *Catal. Sci. Technol.*, 2021, **11**, 1652–1664.
103 G. Liang, L. He, H. Cheng, W. Li, X. Li, C. Zhang, Y. Yu and F. Zhao, *J. Catal.*, 2014, **309**, 468–476.
104 A. M. Ruppert, K. Weinberg and R. Palkovits, *Angew. Chem., Int. Ed.*, 2012, **51**, 2564–2601.
105 H. N. Anchan, N. S. Bhat, N. Vinod, P. S. Prabhakar and S. Dutta, *Biomass Convers. Biorefin.*, 2024, **14**, 9915–9948.
106 H. Zhao, J. E. Holladay, Y. Wang, J. M. White and Z. C. Zhang, *J. Biobased Mater. Bioenergy*, 2017, **1**, 210–215.
107 Q. Xiang, Y. Y. Lee, P. O. Pettersson and R. W. Torget, *Appl. Biochem. Biotechnol.*, 2003, **105–108**, 505–514.
108 L. Hu, L. Lin, Z. Wu, S. Zhou and S. Liu, *Appl. Catal., B*, 2015, **174–175**, 225–243.
109 R. Zhong and B. F. Sels, *Appl. Catal., B*, 2018, **236**, 518–545.
110 J. Zhong, J. Pérez-Ramírez and N. Yan, *Green Chem.*, 2021, **23**, 18–36.
111 L. Shuai and X. Pan, *Energy Environ. Sci.*, 2012, **5**, 6889–6894.
112 N. S. Kapu and H. L. Trajano, *Biofuels, Bioprod. Biorefin.*, 2014, **8**, 857–870.
113 H. Kobayashi, H. Kaiki, A. Shrotri, K. Techikawara and A. Fukuoka, *Chem. Sci.*, 2016, **7**, 692–696.
114 V. I. Sharkov, *Angew. Chem., Int. Ed. Engl.*, 1963, **2**, 405–492.
115 J. M. Robinson, C. E. Burgess, M. A. Bently, C. D. Brasher, B. O. Horne, D. M. Lillard, J. M. Macias, H. D. Mandal, S. C. Mills, K. D. O'Hara, J. T. Pon, A. F. Raigoza, E. H. Sanchez and J. S. Villarreal, *Biomass Bioenergy*, 2004, **26**, 473–483.
116 R. Palkovits, K. Tajvidi, M. Ruppert and J. Procelewska, *Chem. Commun.*, 2011, **47**, 576–578.
117 A. Fukuoka and P. L. Dhepe, *Angew. Chem., Int. Ed.*, 2006, **45**, 5161–5163.
118 W. Deng, X. Tan, W. Fang, Q. Zhang and Y. Wang, *Catal. Lett.*, 2009, **133**, 167–174.
119 J. Geboers, S. Van De Vyver, K. Carpentier, P. Jacobs and B. Sels, *Chem. Commun.*, 2011, **47**, 5590–5592.
120 A. Negoi, K. Triantafyllidis, V. I. Parvulescu and S. M. Coman, *Catal. Today*, 2014, **223**, 122–128.
121 L. S. Ribeiro, J. J. de, M. Órfão and M. F. R. Pereira, *Bioresour. Technol.*, 2017, **244**, 1173–1177.
122 A. Shrotri, H. Kobayashi and A. Fukuoka, *Acc. Chem. Res.*, 2018, **51**, 761–768.
123 Y. Zhou, R. L. Smith and X. Qi, *Green Chem.*, 2024, **26**, 202–243.
124 S. Saravanamurugan and A. Riisager, *Catal. Sci. Technol.*, 2014, **4**, 3186–3190.
125 F. Carly and P. Fickers, *Yeast*, 2018, **35**, 455–463.
126 D. A. Rzechonek, A. Dobrowolski, W. Rymowicz and A. M. Mirończuk, *Crit. Rev. Biotechnol.*, 2018, **38**, 620–633.
127 S. Tolborg, S. Meier, S. Saravanamurugan, P. Fristrup, E. Taarning and I. Sádaba, *ChemSusChem*, 2016, **9**, 3054–3061.
128 E. Santacesaria, G. M. Vicente, M. Di Serio and R. Tesser, *Catal. Today*, 2012, **195**, 2–13.
129 M. Checa, S. Nogales-Delgado, V. Montes and J. M. Encinar, *Catalysts*, 2020, **10**, 1–41.
130 P. F. F. Amaral, T. F. Ferreira, G. C. Fontes and M. A. Z. Coelho, *Food Bioprod. Process.*, 2009, **87**, 179–186.
131 B. Katryniok, H. Kimura, E. Skrzyńska, J. S. Girardon, P. Fongarland, M. Capron, R. Ducoulombier, N. Mimura, S. Paul and F. Dumeignil, *Green Chem.*, 2011, **13**, 1960–1979.
132 J. Sun and H. Liu, *Green Chem.*, 2011, **13**, 135–142.
133 C. Heisig, C. Glotzbach, S. Schirrmeister and T. Turek, *Chem. Eng. Technol.*, 2021, **44**, 761–772.
134 Y. Wang, J. Zhou and X. Guo, *RSC Adv.*, 2015, **5**, 74611–74628.
135 Avantium Knowledge Centre, US10131600 B2, 2018.
136 G. Zhao, M. Zheng, R. Sun, Z. Tai, J. Pang, A. Wang, X. Wang and T. Zhang, *AIChE J.*, 2016, **63**, 2072–2080.
137 R. Ooms, M. Dusselier, J. A. Geboers, B. Op De Beeck, R. Verhaeven, E. Gobechiya, J. A. Martens, A. Redl and B. F. Sels, *Green Chem.*, 2014, **16**, 695–707.
138 Y. Li, Y. Liao, X. Cao, T. Wang, L. Ma, J. Long, Q. Liu and Y. Xua, *Biomass Bioenergy*, 2015, **74**, 148–161.
139 M. K. Wong, S. S. M. Lock, Y. H. Chan, S. J. Yeoh and I. S. Tan, *Chem. Eng. J.*, 2023, **468**, 143699.
140 A. N. Marchesan, M. P. Oncken, R. Maciel Filho and M. R. Wolf Maciel, *Green Chem.*, 2019, **21**, 5168–5194.
141 M. Główka and T. Krawczyk, *ACS Sustainable Chem. Eng.*, 2023, **11**, 7274–7287.
142 Y. Hirano, K. Sagata and Y. Kita, *Appl. Catal., A*, 2015, **502**, 1–7.
143 Z. Xiao, S. Jin, G. Sha, C. T. Williams and C. Liang, *Ind. Eng. Chem. Res.*, 2014, **53**, 8735–8743.
144 C. Liu, C. Zhang, S. Hao, S. Sun, K. Liu, J. Xu, Y. Zhu and Y. Li, *Catal. Today*, 2016, **261**, 116–127.

145 C. Liu, Z. Zhang, X. Zhai, X. Wang, J. Gui, C. Zhang, Y. Zhu and Y. Li, *New J. Chem.*, 2019, **43**, 3733–3742.
146 A. A. B. Kirali, S. Sreekantan and B. Marimuthu, *Catal. Commun.*, 2022, **165**, 106447.
147 T. Deng and H. Liu, *J. Mol. Catal. A: Chem.*, 2014, **388–389**, 66–73.
148 S. Basu and A. K. Sen, *ChemBioEng Rev.*, 2021, **8**, 633–653.
149 T. Rajkhowa, G. B. Marin and J. W. Thybaut, *Appl. Catal., B*, 2017, **205**, 469–480.
150 R. A. Sheldon, D. Brady and M. L. Bode, *Chem. Sci.*, 2020, **11**, 2587–2605.
151 S. Wu, R. Snajdrova, J. C. Moore, K. Baldenius and U. T. Bornscheuer, *Angew. Chem., Int. Ed.*, 2021, **60**, 88–119.
152 F. G. Mutti, T. Knaus, N. S. Scrutton, M. Breuer and N. J. Turner, *Science*, 2015, **349**, 1525–1529.
153 T. Knaus, W. Böhmer and F. G. Mutti, *Green Chem.*, 2017, **19**, 453–463.
154 S. D. Mürtz, N. Kurig, F. J. Holzhäuser and R. Palkovits, *Green Chem.*, 2021, **23**, 8428–8433.
155 T. Kim, D. Il Park, S. Kim, D. Yadav, S. Hong, S. H. Kim, H. J. Yoon and K. Jin, *Chem. Commun.*, 2023, **59**, 4818–4821.
156 S. Gomez, J. A. Peters and T. Maschmeyer, *Adv. Synth. Catal.*, 2002, **344**, 1037–1057.
157 K. Murugesan, T. Senthamarai, V. G. Chandrashekhar, K. Natte, P. C. J. Kamer, M. Beller and R. V. Jagadeesh, *Chem. Soc. Rev.*, 2020, **49**, 6273–6328.
158 E. Podyacheva, O. Afanasyev, A. Tsygankov, M. Makarova and D. Chusov, *Synthesis*, 2019, 2667–2677.
159 E. W. Baxter and A. B. Reitz, *Organic Reactions*, Wiley-VCH, 2004, pp. 1–57.
160 M. L. Moore, *Organic Reactions*, Wiley-VCH, 1949, vol. 5, pp. 301–324.
161 M. Kitamura, D. Lee, S. Hayashi, S. Tanaka and M. Yoshimura, *J. Org. Chem.*, 2002, **67**, 8685–8687.
162 A. De, N. C. Ghosal, S. Mahato, S. Santra, G. V. Zyryanov and A. Majee, *ChemistrySelect*, 2018, **3**, 4058–4066.
163 D. Chusov and B. List, *Angew. Chem., Int. Ed.*, 2014, **53**, 5199–5201.
164 A. A. Tsygankov, M. Makarova and D. Chusov, *Mendeleev Commun.*, 2018, **28**, 113–122.
165 Y. Wang, S. Furukawa, X. Fu and N. Yan, *ACS Catal.*, 2020, **10**, 311–335.
166 T. Irrgang and R. Kempe, *Chem. Rev.*, 2020, **120**, 9583–9674.
167 J. P. Adams, C. M. Alder, I. Andrews, A. M. Bullion, M. Campbell-Crawford, M. G. Darcy, J. D. Hayler, R. K. Henderson, C. A. Oare, I. Pendrak, A. M. Redman, L. E. Shuster, H. F. Sneddon and M. D. Walker, *Green Chem.*, 2013, **15**, 1542–1549.
168 A. Corma, J. Navas and M. J. Sabater, *Chem. Rev.*, 2018, **118**, 1410–1459.
169 A. Baiker, *Stud. Surf. Sci. Catal.*, 1988, **41**, 283–290.
170 G. Guillena, D. J. Ramón and M. Yus, *Chem. Rev.*, 2010, **110**, 1611–1641.
171 K. I. Shimizu, *Catal. Sci. Technol.*, 2015, **5**, 1412–1427.
172 T. Irrgang and R. Kempe, *Chem. Rev.*, 2019, **119**, 2524–2549.
173 B. Girisuta, L. P. B. M. Janssen and H. J. Heeres, *Ind. Eng. Chem. Res.*, 2007, **46**, 1696–1708.
174 J. M. Carraher, C. N. Fleitman and J.-P. Tessonnier, *ACS Catal.*, 2015, **5**, 3162–3173.
175 C. Li, Y. Wang, Y. Zhang, M. Wang, X. Sun, H. Cui and Y. Xie, *ChemistrySelect*, 2020, **5**, 270–279.
176 J. Tang, X. Guo, L. Zhu and C. Hu, *ACS Catal.*, 2015, **5**, 5097–5103.
177 Z. Zhou, X. Li, T. Zeng, W. Hong, Z. Cheng and W. Yuan, *Chin. J. Chem. Eng.*, 2010, **18**, 384–390.
178 J. E. Hodge, *Agricultural and Food Chemistry*, 1953, vol. 1, pp. 928–943.
179 H. Nursten, *The Maillard Reaction: Chemistry, biochemistry and implications*, Royal Society of Chemistry, 2005, pp. 5–30.
180 D. M. Roundhill, *Chem. Rev.*, 1992, **92**, 1–27.
181 J. He, L. Chen, S. Liu, K. Song, S. Yang and A. Riisager, *Green Chem.*, 2020, **22**, 6714–6747.
182 D. Ruijten, T. Narmon, H. De Weer and R. Van Der Zweep, *ChemSusChem*, 2022, **15**, e202200868.
183 D. Ruijten, T. Narmon, K. Van Aelst, H. De Weer, R. Van Der Zweep, T. Hendrickx, C. Poleunis, L. Li, K. M. Van Geem, D. P. Debecker and B. F. Sels, *ACS Sustainable Chem. Eng.*, 2023, **11**, 4776–4788.
184 X. Wu, M. V. Galkin and K. Barta, *Chem Catal.*, 2021, **1**, 1466–1479.
185 X. Wu, M. De Bruyn and K. Barta, *ChemSusChem*, 2022, **15**, e202200914.
186 J. Ma, D. Le and N. Yan, *Chem*, 2023, **9**, 1–12.
187 H. Li, H. Guo, Z. Fang, R. L. Smith and M. Aida, *Green Chem.*, 2020, **22**, 582–611.
188 A. C. Fernandes, *Methodologies in Amine Synthesis: Challenges and Applications*, Wiley-VCH, 2021, pp. 341–376.
189 W. Deng, Y. Wang, S. Zhang, K. M. Gupta, M. J. Hülsey, H. Asakura, L. Liu, Y. Han, E. M. Karp, G. T. Beckham, P. J. Dyson, J. Jiang, T. Tanaka, Y. Wang and N. Yan, *Proc. Natl. Acad. Sci. U. S. A.*, 2018, **115**, 5093–5098.
190 R. Coeck and D. E. De Vos, *Green Chem.*, 2020, **22**, 5105–5114.
191 A. Garcia-Ortiz, J. D. Vidal, M. J. Climent, P. Concepcion, A. Corma and S. Iborra, *ACS Sustainable Chem. Eng.*, 2019, 6243–6250.
192 J. Sha, B. T. Kusema, W. Zhou, Z. Yan, S. Strei and M. Peratitus, *Green Chem.*, 2021, **23**, 7093–7099.
193 T. A. Gokhale and B. M. Bhanage, in *Production of N-containing Chemicals and Materials from Biomass*, ed. Z. Fang, R. L. Smith and L. Xu, Springer, 2023, pp. 21–71.
194 J. F. Lin, C. C. Wu and M. H. Lien, *J. Phys. Chem.*, 1995, **99**, 16903–16908.
195 P. Pérez and A. Toro-Labbé, *Theor. Chem. Acc.*, 2001, **105**, 422–430.
196 V. A. Yaylayan, A. H. Despointes and M. S. Feather, *Crit. Rev. Food Sci. Nutr.*, 1994, **34**, 321–369.

197 T. M. Wrodnigg and B. Eder, *Glycoscience*, Springer, 2001, pp. 115–152.
198 K. U. Leuven, WO2019/193117 A1, 2019.
199 W. Faveere, T. Mihaylov, M. Pelckmans, K. Moonen, F. Gillis-D'Hamers, R. Bosschaerts, K. Pierloot and B. F. Sels, *ACS Catal.*, 2020, **10**, 391–404.
200 S. Van Praet, G. Preegel, F. Rammal and B. F. Sels, *ACS Sustainable Chem. Eng.*, 2022, **10**, 6503–6508.
201 Rhodia Operations, WO2021/114166 A1, 2021.
202 S. Van Praet, F. Rammal, B. Vermeeren, T. Nicolaï, K. Dumoleijn, T. Rottiers and B. F. Sels, *Chem. Eng. J.*, 2023, **475**, 146316.
203 G. Liang, A. Wang, L. Li, G. Xu, N. Yan and T. Zhang, *Angew. Chem., Int. Ed.*, 2017, **56**, 3050–3054.
204 BASF SE, US2012/0271068 A1, 2012.
205 BASF SE, US2009/0240084 A1, 2009.
206 BASF SE, US11208373 B2, 2018.
207 BASF SE, WO2020/178085A1, 2020, 1–42.
208 Z. Xie, H. An, X. Zhao and Y. Wang, *Mol. Catal.*, 2022, **528**, 112492.
209 H. An, J. Li, G. Zheng, G. Wang, X. Zhao and Y. Wang, *ChemistrySelect*, 2022, **7**, 1–11.
210 BASF SE, WO2020/249427 A1, 2020.
211 BASF SE, WO2020/249426 A1, 2020.
212 J. Runeberg, A. Baiker and J. Kijenski, *Appl. Catal.*, 1985, **17**, 309–319.
213 M. Pelckmans, T. Mihaylov, W. Faveere, J. Poissonnier, F. Van Waes, K. Moonen, G. B. Marin, J. W. Thybaut, K. Pierloot and B. F. Sels, *ACS Catal.*, 2018, **8**, 4201–4212.
214 M. Pelckmans, W. Vermandel, F. Van Waes, K. Moonen and B. F. Sels, *Angew. Chem., Int. Ed.*, 2017, **56**, 14540–14544.
215 B. Vermeeren, S. Van Praet, W. Arts and B. F. Sels, *Chem Catal.*, 2023, **3**, 100602.
216 T. Trégner, J. Trejbal, N. Ruhswurmová and M. Zapletal, *Chem. Biochem. Eng. Q.*, 2018, **31**, 455–470.
217 T. Takanashi, Y. Nakagawa and K. Tomishige, *Chem. Lett.*, 2014, **43**, 822–824.
218 C. Yue, K. Di, L.-P. Gu, Z.-W. Zhang and L.-L. Ding, *Mol. Catal.*, 2019, **477**, 110539.
219 Wanhua Chemical Group, CN112125814A, 2020.
220 B. Vermeeren, S. Van Praet, A. De Ridder and B. F. Sels, *ACS Sustainable Chem. Eng.*, 2024, **12**, 10209–10220.
221 Jefferson Chemical Company, US3448153, 1969.
222 J. Boulos, F. Goc, T. Vandenbrouck, N. Perret, J. Dhainaut, S. Royer and F. Rataboul, *ChemSusChem*, 2024, **17**, e202400540.
223 Procter & Gamble Company, US2007/0287865 A1, 2007.
224 Merck, US5023379, 1991.
225 Penn A Kem LLC, US8653306 B1, 2014.
226 BASF SE, US2010/0240894A1, 2010.
227 W. Wayne and H. Adkins, *J. Am. Chem. Soc.*, 1940, **62**, 3314–3316.
228 T. Seddig, T. Naundorf, H. Kipphardt and W. Maison, *Mater. Corros.*, 2023, **74**, 394–402.
229 BASF SE, US2010/0311973 A1, 2010.
230 M. Safariamin, S. Paul, K. Moonen, D. Ulrichts, F. Dumeignil and B. Katryniok, *Catal. Sci. Technol.*, 2016, **6**, 2129–2135.
231 J. Ding, M. Cui, T. Ma, R. Shao, W. Xu and P. Wang, *Mol. Catal.*, 2018, **457**, 51–58.
232 Dalian Institute, CN107011194 B, 2019.
233 G. Drake and Y. Roman-Leshkov, *Chem Catal.*, 2023, **3**, 1–3.
234 A. Fischer, T. Mallat and A. Baiker, *Catal. Today*, 1997, **37**, 167–189.
235 Jefferson Chemical Company, US 3151115, 1964.
236 BASF SE, US 3270059, 1966.
237 V. A. Yaylayan, S. Harty-Majors and A. A. Ismail, *J. Agric. Food Chem.*, 1999, **47**, 2335–2340.
238 J. Sun, S. So and G. da Silva, *Int. J. Quantum Chem.*, 2017, **117**, 1–5.
239 J. Niemeier, R. V. Engel and M. Rose, *Green Chem.*, 2017, **19**, 2839–2845.
240 F. Du, X. Jin, W. Yan, M. Zhao, P. S. Thapa and R. V. Chaudhari, *Catal. Today*, 2018, **302**, 227–232.
241 X. Dai, J. Rabeah, H. Yuan, A. Brückner, X. Cui and F. Shi, *ChemSusChem*, 2016, **9**, 3133–3138.
242 DuPont de Nemours & Company, US 2016962, 1935.
243 Cerestar Holding BV, EP0536939A1, 1993.
244 J. Poissonnier, M. Pelckmans, F. Van Waes, K. Moonen, B. F. Sels, J. W. Thybaut and G. B. Marin, *Appl. Catal., B*, 2018, **227**, 161–169.
245 Taminco bvba, EP3290401 A1, 2018.
246 W. Gao, S. Liang, R. Wang, Q. Jiang, Y. Zhang, Q. Zheng, B. Xie, C. Y. Toe, X. Zhu, J. Wang, L. Huang, Y. Gao, Z. Wang, C. Jo, Q. Wang, L. Wang, Y. Liu, B. Louis, J. Scott, A. C. Roger, R. Amal, H. He and S. E. Park, *Chem. Soc. Rev.*, 2020, **49**, 8584–8686.
247 J. C. M. Pires, F. G. Martins, M. C. M. Alvim-Ferraz and M. Simões, *Chem. Eng. Res. Des.*, 2011, **89**, 1446–1460.
248 T. Wilberforce, A. G. Olabi, E. T. Sayed, K. Elsaid and M. A. Abdelkareem, *Sci. Total Environ.*, 2021, **761**, 143203.
249 M. Bui, C. S. Adjiman, E. J. Anthony, A. Boston, S. Brown, P. S. Fennell, S. Fuss, A. Galindo, L. A. Hackett, J. P. Hallett, H. J. Herzog, G. Jackson, J. Kemper, S. Krevor, G. C. Maitland, M. Matuszewski, I. S. Metcalfe, C. Petit, G. Puxty, J. Reimer, D. M. Reiner, E. S. Rubin, S. A. Scott, N. Shah, B. Smit, J. P. M. Trusler, P. Webley, J. Wilcox and N. Mac Dowell, *Energy Environ. Sci.*, 2018, **11**, 1062–1176.
250 F. de Meyer and S. Jouenne, *Curr. Opin. Chem. Eng.*, 2022, **38**, 1–7.
251 I. M. Bernhardsen and H. K. Knuutila, *Int. J. Greenhouse Gas Control*, 2017, **61**, 27–48.
252 G. T. Rochelle, *Science*, 2009, **325**, 1652–1654.
253 E. Kayahan, U. Di Caprio, A. Van den Bogaert, M. N. Khan, M. Bulut, L. Braeken, T. Van Gerven and M. E. Leblebici, *Chem. Eng. Process.*, 2023, **184**, 109285.
254 C. Zhou, I. Khalil, F. Rammal, M. Dusselier, P. Kumar, M. Lacroix, E. Makshina, Y. Liao and B. F. Sels, *ACS Catal.*, 2022, **12**, 11485–11493.
255 F. de Meyer and C. Bignaud, *Chem. Eng. J.*, 2022, **428**, 1–12.

256 F. Bougie and M. C. Iliuta, *J. Chem. Eng. Data*, 2012, **57**, 635–669.
257 F. A. Chowdhury, H. Okabe, H. Yamada, M. Onoda and Y. Fujioka, *Energy Procedia*, 2011, **4**, 201–208.
258 N. El Hadri, D. V. Quang, E. L. V. Goetheer and M. R. M. Abu Zahra, *Appl. Energy*, 2017, **185**, 1433–1449.
259 S. Martin, H. Lepaumier, D. Picq, J. Kittel, T. De Bruin, A. Faraj and P. L. Carrette, *Ind. Eng. Chem. Res.*, 2012, **51**, 6283–6289.
260 F. Vega, A. Sanna, B. Navarrete, M. M. Maroto-Valer and V. Cortés, *Greenhouse Gases: Sci. Technol.*, 2014, **4**, 707–733.
261 P. Singh and G. F. Versteeg, *Process Saf. Environ. Prot.*, 2008, **86**, 347–359.
262 P. Singh, J. P. M. Niederer and G. F. Versteeg, *Chem. Eng. Res. Des.*, 2009, **87**, 135–144.
263 G. Rochelle, E. Chen, S. Freeman, D. Van Wagener, Q. Xu and A. Voice, *Chem. Eng. J.*, 2011, **171**, 725–733.
264 F. A. Chowdhury, H. Yamada, T. Higashii, K. Goto and M. Onoda, *Ind. Eng. Chem. Res.*, 2013, **52**, 8323–8331.
265 M. Xiao, H. Liu, H. Gao and Z. Liang, *J. Chem. Thermodyn.*, 2018, **122**, 170–182.
266 Q. Yang, G. Puxty, S. James, M. Bown, P. Feron and W. Conway, *Energy Fuels*, 2016, **30**, 7503–7510.
267 G. Puxty, R. Rowland, A. Allport, Q. Yang, M. Bown, R. Burns, M. Maeder and M. Attalla, *Environ. Sci. Technol.*, 2009, **43**, 6427–6433.
268 E. F. da Silva and H. F. Svendsen, *Int. J. Greenhouse Gas Control*, 2007, **1**, 151–157.
269 X. Rozanska, E. Wimmer and F. de Meyer, *J. Chem. Inf. Model.*, 2021, **61**, 1814–1824.
270 A. A. Orlov, A. Valtz, C. Coquelet, X. Rozanska, E. Wimmer, G. Marcou, D. Horvath, B. Poulain, A. Varnek and F. de Meyer, *Commun. Chem.*, 2022, **5**, 1–7.
271 F. Vega, F. M. Baena-Moreno, L. M. Gallego Fernández, E. Portillo, B. Navarrete and Z. Zhang, *Appl. Energy*, 2020, **260**, 114313.
272 P. Muchan, C. Saiwan, J. Narku-Tetteh, R. Idem, T. Supap and P. Tontiwachwuthikul, *Chem. Eng. Sci.*, 2017, **170**, 574–582.
273 N. Mirza and D. Kearns, State of the Art: CCS Technologies 2022, 2022.
274 R. R. Wanderley, D. D. D. Pinto and H. K. Knuutila, *Sep. Purif. Technol.*, 2021, **260**, 118193.
275 J. Leclaire and D. J. Heldebrant, *Green Chem.*, 2018, **20**, 5058–5081.
276 D. J. Heldebrant, P. K. Koech, V. Glezakou, R. Rousseau, D. Malhotra and D. C. Cantu, *Chem. Rev.*, 2017, **117**, 9594–9624.
277 F. Barzagli, F. Mani and M. Peruzzini, *Environ. Sci. Technol.*, 2016, **50**, 7239–7246.
278 D. C. Cantu, D. Malhotra, M. T. Nguyen, P. K. Koech, D. Zhang, V. A. Glezakou, R. Rousseau, J. Page, R. Zheng, R. J. Perry and D. J. Heldebrant, *ChemSusChem*, 2020, **13**, 3429–3438.
279 R. F. Zheng, D. Barpaga, P. M. Mathias, D. Malhotra, P. K. Koech, Y. Jiang, M. Bhakta, M. Lail, A. Rayer, G. A. Whyatt, C. J. Freeman, A. J. Zwoster, K. K. Weitz and D. J. Heldebrant, *Energy Environ. Sci.*, 2020, **13**, 4106–4113.
280 D. Barpaga, Y. Jiang, R. F. Zheng, D. Malhotra, P. K. Koech, A. Zwoster, P. M. Mathias and D. J. Heldebrant, *ACS Sustainable Chem. Eng.*, 2022, **10**, 4522–4528.
281 C. J. Clarke, W. Tu, O. Levers, A. Bröhl and J. P. Hallett, *Chem. Rev.*, 2018, **118**, 747–800.
282 P. G. Jessop, D. J. Heldebrant, X. Li, C. A. Eckert and C. L. Liotta, *Nature*, 2005, **436**, 1102.
283 P. G. Jessop and M. F. Cunningham, *CO2-switchable materials: solvents, surfactants, solutes and solids*, Royal Society of Chemistry, 2020.
284 P. G. Jessop, *Aldrichimica Acta*, 2015, **48**, 18–21.
285 J. R. Vanderveen, S. Burra, J. Geng, A. Goyon, A. Jardine, H. E. Shin, T. Andrea, P. J. Dyson and P. G. Jessop, *ChemPhysChem*, 2018, **19**, 2093–2100.
286 S. M. Mercer and P. G. Jessop, *ChemSusChem*, 2010, **3**, 467–470.
287 S. M. Mercer, T. Robert, D. V. Dixon, C. S. Chen, Z. Ghoshouni, J. R. Harjani, S. Jahangiri, G. H. Peslherbe and P. G. Jessop, *Green Chem.*, 2012, **14**, 832–839.
288 A. K. Alshamrani, J. R. Vanderveen and P. G. Jessop, *Phys. Chem. Chem. Phys.*, 2016, **18**, 19276–19288.
289 S. Püschel, J. Sadowski, T. Rösler, K. R. Ehmann, A. J. Vorholt and W. Leitner, *ACS Sustainable Chem. Eng.*, 2022, **10**, 3749–3756.
290 Y. Bazel, M. Rečlo and Y. Chubirka, *Microchem. J.*, 2020, **157**, 105115.
291 P. G. Jessop, L. Kozycz, Z. G. Rahami, D. Schoenmakers, A. R. Boyd, D. Wechsler and A. M. Holland, *Green Chem.*, 2011, **13**, 619–623.
292 J. R. Vanderveen, J. Durelle and P. G. Jessop, *Green Chem.*, 2014, **16**, 1187–1197.
293 C. Samorì, D. López Barreiro, R. Vet, L. Pezzolesi, D. W. F. Brilman, P. Galletti and E. Tagliavini, *Green Chem.*, 2013, **15**, 353–356.
294 C. Russell and C. Rodriguez, *Energy*, 2023, **278**, 127983.
295 S. Cheng, K. Rathnakumar and S. I. Martínez-Monteagudo, *Foods*, 2019, **8**, 265.
296 V. Sapone, A. Iannone, A. Alivernini, A. Cicci, P. G. Jessop and M. Bravi, *Sep. Purif. Technol.*, 2023, **308**, 122843.
297 C. Samorì, D. Cespi, P. Blair, P. Galletti, D. Malferrari, F. Passarini, I. Vassura and E. Tagliavini, *Green Chem.*, 2017, **19**, 1714–1720.
298 J. R. Vanderveen, J. Geng, S. Zhang and P. G. Jessop, *RSC Adv.*, 2018, **8**, 27318–27325.
299 J. Cheng, H. Guo, Y. Qiu, Z. Zhang, Y. Mao, L. Qian, W. Yang and J. Y. Park, *Bioresour. Technol.*, 2020, **312**, 123607.
300 X. Li, Z. Yang, H. Sui, A. Jain and L. He, *Fuel*, 2018, **221**, 303–310.
301 K. J. Viner, H. M. Roy, R. Lee, O. He, P. Champagne and P. G. Jessop, *Green Chem.*, 2019, **21**, 4786–4791.
302 H. Q. Pham and M. J. Marks, *Ullmann's Encyclopedia of Industrial Chemistry*, Wiley-VCH, 2005, pp. 156–244.

303 W. Brostow, S. H. Goodman and J. Wahrmund, *Handbook of Thermoset Plastics*, Elsevier, 3rd edn, 2014, pp. 191–252.
304 G. Gibson, *Brydson's Plastics Materials*, 8th edn, 2017, pp. 773–797.
305 F. L. Jin, X. Li and S. J. Park, *J. Ind. Eng. Chem.*, 2015, **29**, 1–11.
306 R. Auvergne, S. Caillol, G. David, B. Boutevin and J. P. Pascault, *Chem. Rev.*, 2014, **114**, 1082–1115.
307 E. A. Baroncini, S. Kumar Yadav, G. R. Palmese and J. F. Stanzione, *J. Appl. Polym. Sci.*, 2016, **133**, 44103.
308 J. Liu, S. Wang, Y. Peng, J. Zhu, W. Zhao and X. Liu, *Prog. Polym. Sci.*, 2021, **113**, 101353.
309 K. Van Aelst, E. Van Sinay, T. Vangeel, Y. Zhang, T. Renders, S. Van den Bosch, J. Van Aelst and B. F. Sels, *Chem. Commun.*, 2021, **57**, 5642–5645.
310 C. Pappa, E. Feghali, K. Vanbroekhoven and K. S. Triantafyllidis, *Curr. Opin. Green Sustainable Chem.*, 2022, **38**, 100687.
311 Y. Zhang, S. Stepanova, K. Van Aelst and B. F. Sels, *Curr. Opin. Green Sustainable Chem.*, 2023, **40**, 100750.
312 ThreeBond, Curing agents for epoxy resin, 1990.
313 B. L. Burton, *Epoxy Resin Formulators' Meeting*, 2006, pp. 1–17.
314 A. S. Mora, R. Tayouo, B. Boutevin, G. David and S. Caillol, *Eur. Polym. J.*, 2020, **123**, 1–14.
315 A. S. Mora, R. Tayouo, B. Boutevin, G. David and S. Caillol, *Green Chem.*, 2018, **20**, 4075–4084.
316 A. K. Ingberman, R. K. Walton, C. F. Pitt and M. N. Paul, *Ind. Eng. Chem.*, 1957, **49**, 1105.
317 M. F. Sonnenschein, *Polyurethanes: Science, Technology, Markets, and Trends*, John Wiley & Sons, 2nd edn, 2021.
318 G. Wegener, M. Brandt, L. Duda, J. Hofmann, B. Klesczewski, D. Koch, R. J. Kumpf, H. Orzesek, H. G. Pirkl, C. Six, C. Steinlein and M. Weisbeck, *Appl. Catal., A*, 2001, **221**, 303–335.
319 B. Nohra, L. Candy, C. Guerin and Y. Raoul, *Macromolecules*, 2013, **46**, 3771–3792.
320 P. Furtwengler and L. Avérous, *Polym. Chem.*, 2018, **9**, 4258–4287.
321 A. Tenorio-Alfonso, M. C. Sánchez and J. M. Franco, *J. Polym. Environ.*, 2020, **28**, 749–774.
322 G. Brereton, R. M. Emanuel, R. Lomax, K. Pennington, T. Ryan, H. Tebbe, M. Timm, P. Ware, K. Winkler, T. Yuan, Z. Zhu, N. Adam, G. Avar, H. Blankenheim, W. Friederichs, M. Giersig, E. Weigand, M. Halfmann, F.-W. Wittbecker, D.-R. Larimer, U. Maier, S. Meyer-Ahrens, K.-L. Noble and H.-G. Wussow, *Ullmann's Encyclopedia of Industrial Chemistry*, Wiley-VCH, 2019, pp. 1–76.
323 J. O. Akindoyo, M. D. H. Beg, S. Ghazali, M. R. Islam, N. Jeyaratnam and A. R. Yuvaraj, *RSC Adv.*, 2016, **6**, 114453–114482.
324 A. L. Silva and J. C. Bordado, *Catal. Rev.: Sci. Eng.*, 2004, **46**, 31–51.
325 S. Dworakowska, D. Bogdał, F. Zaccheria and N. Ravasio, *Catal. Today*, 2014, **223**, 148–156.
326 N. Malwitz, S. W. Wong, K. C. Frisch and P. A. Manis, *J. Cell. Plast.*, 1987, **23**, 461–502.
327 R. Van Maris, Y. Tamano, H. Yoshimura and K. M. Gay, *J. Cell. Plast.*, 2005, **41**, 305–322.
328 M. Muuronen, P. Deglmann and Ž. Tomović, *J. Org. Chem.*, 2019, **84**, 8202–8209.
329 B. Eling, Ž. Tomović and V. Schädler, *Macromol. Chem. Phys.*, 2020, **221**, 1–11.
330 Huntsman Corporation, Performance Products JEFFCAT catalysts, 2012.
331 BASF, Intermediates for the PUR Industry, 2015.
332 Evonik, Additives for spray polyurethane foam (SPF) applications, 2017.
333 A. Strachota, B. Strachotová and M. Špírková, *Mater. Manuf. Processes*, 2008, **23**, 566–570.
334 Dow Global Technologies Inc, WO03/016372 A1, 2004.
335 N. Corrigan, K. Jung, G. Moad, C. J. Hawker, K. Matyjaszewski and C. Boyer, *Prog. Polym. Sci.*, 2020, **111**, 101311.
336 F. Gomollón-Bel, *Chem. Int.*, 2019, **41**, 12–17.
337 J. Wang and K. Matyjaszewski, *J. Am. Chem. Soc.*, 1995, **117**, 5614–5615.
338 M. Kato, M. Kamigaito, M. Sawamoto and T. Higashimuras, *Macromolecules*, 1995, **28**, 1721–1723.
339 M. Destarac, *Polym. Chem.*, 2018, **9**, 4947–4967.
340 K. Matyjaszewski and J. Xia, *Chem. Rev.*, 2001, **101**, 2921–2990.
341 S. Dworakowska, F. Lorandi, A. Gorczyński and K. Matyjaszewski, *Adv. Sci.*, 2022, **9**, 2106076.
342 J. Xia and K. Matyjaszewski, *Macromolecules*, 1997, **30**, 7697–7700.
343 W. Tang, Y. Kwak, W. Braunecker, N. V. Tsarevsky, M. L. Coote and K. Matyjaszewski, *J. Am. Chem. Soc.*, 2008, **130**, 10702–10713.
344 T. G. Ribelli, F. Lorandi, M. Fantin and K. Matyjaszewski, *Macromol. Rapid Commun.*, 2019, **40**, 1–44.
345 E. B. Walker, in *Handbook of Topical Antimicrobials*, ed. D. S. Paulson, CRC Press, 2002.
346 F. Bureš, *Top. Curr. Chem.*, 2019, **377**, 14.
347 A. Brändström, *Adv. Phys. Org. Chem.*, 1977, **15**, 267–330.
348 M. Dusselier and M. E. Davis, *Chem. Rev.*, 2018, **118**, 5265–5329.
349 S. Mishra and V. K. Tyagi, *J. Oleo Sci.*, 2007, **56**, 269–276.
350 A. N. Vereshchagin, N. A. Frolov, K. S. Egorova, M. M. Seitkalieva and V. P. Ananikov, *Int. J. Mol. Sci.*, 2021, **22**, 6793.
351 C. P. Gerba, *Appl. Environ. Microbiol.*, 2015, **81**, 464–469.
352 M. C. Jennings, K. P. C. Minbiole and W. M. Wuest, *ACS Infect. Dis.*, 2015, **1**, 288–303.
353 K. P. C. Minbiole, M. C. Jennings, L. E. Ator, J. W. Black, M. C. Grenier, J. E. LaDow, K. L. Caran, K. Seifert and W. M. Wuest, *Tetrahedron*, 2016, **72**, 3559–3566.
354 K. R. Morrison, R. A. Allen, K. P. C. Minbiole and W. M. Wuest, *Tetrahedron Lett.*, 2019, **60**, 1–13.
355 T. J. Paniak, M. C. Jennings, P. C. Shanahan, M. D. Joyce, C. N. Santiago, W. M. Wuest and K. P. C. Minbiole, *Bioorg. Med. Chem. Lett.*, 2014, **24**, 5824–5828.

356 M. E. Forman, M. C. Jennings, W. M. Wuest and K. P. C. Minbiole, *ChemMedChem*, 2016, **11**, 1401–1405.
357 M. A. Mitchell, A. A. Iannetta, M. C. Jennings, M. H. Fletcher, W. M. Wuest and K. P. C. Minbiole, *ChemBioChem*, 2015, **16**, 2299–2303.
358 M. C. Jennings, M. E. Forman, S. M. Duggan, K. P. C. Minbiole and W. M. Wuest, *ChemBioChem*, 2017, **18**, 1573–1577.
359 M. C. Jennings, B. A. Buttaro, K. P. C. Minbiole and W. M. Wuest, *ACS Infect. Dis.*, 2015, **1**, 304–309.
360 R. A. Allen, M. C. Jennings, M. A. Mitchell, S. E. Al-Khalifa, W. M. Wuest and K. P. C. Minbiole, *Bioorg. Med. Chem. Lett.*, 2017, **27**, 2107–2112.
361 M. C. Jennings, L. E. Ator, T. J. Paniak, K. P. C. Minbiole and W. M. Wuest, *ChemBioChem*, 2014, **15**, 2211–2215.
362 A. D. Verderosa, M. Totsika and K. E. Fairfull-Smith, *Front. Chem.*, 2019, **7**, 1–17.
363 J. W. Black, M. C. Jennings, J. Azarewicz, T. J. Paniak, M. C. Grenier, W. M. Wuest and K. P. C. Minbiole, *Bioorg. Med. Chem. Lett.*, 2013, **24**, 99–102.